THE EFFECT OF WIND PATTERN CHANGE ON THE
ENVIRONMENTAL/CLIMATIC CONDITIONS WITHIN CITIES

by

Bahadır Baykal

B.S., Civil Engineering, Sakarya University, 2014

Submitted to the Institute for Graduate Studies in

Science and Engineering in partial fulfillment of

the requirements for the degree of

Master of Science

Graduate Program in Computational Science and Engineering

Boğaziçi University

2019

THE EFFECT OF WIND PATTERN CHANGE ON THE
ENVIRONMENTAL/CLIMATIC CONDITIONS WITHIN CITIES

APPROVED BY:

Prof. M. Levent Kurnaz   . . . .
(Thesis Supervisor)

Assoc. Prof. Ali Ecder   . . . .

Assist. Prof. Tuğba Öztürk   . . . .

DATE OF APPROVAL: 30.05.2019

ACKNOWLEDGEMENTS

First and foremost, I would like to thank my thesis supervisor, Prof. M. Levent Kurnaz. I still remember the first conversation we had when I met him, his attitude to me even he was not my advisor was a sign of how much any student is precious to him. After I have become his thesis student, he has generously guided my crude ideas about this study. No word can describe how much I am grateful to him.

I thank my friends, who have supported me and shared their knowledge through the years at my master's degree. Their companionship helped me a lot.

I also would like to genuinely thank my dear Esra. When I get frustrated after working overtime and missed weekends and holidays, she was very tolerant and supportive of me.

Finally, I would like to give the most special thanks to my family. I am grateful to my mother Gülsen Baykal and my father Ali Baykal for their unconditional support through my life. I would not have accomplished this thesis without their continuous encouragement. I sincerely love them.

ABSTRACT

THE EFFECT OF WIND PATTERN CHANGE ON THE ENVIRONMENTAL/CLIMATIC CONDITIONS WITHIN CITIES

The labor force demand by the Industrial Revolution has led to an increase in the population of cities. This situation was followed by rapid development of urban areas with starting of nineteenth century to accommodate labor force around the industry.

This situation has ended up with altering more land surfaces to buildings, car parks, roads or other structure types. However, it cannot be said that all the urbanization steps are taken properly. Thus, these anthropogenic developments have affected wind flow in urban. Arbitrary built urban areas restrict the wind flow in street canyons and make it slower than the flow above the building blocks, hence reduce the cooling effect of wind at near-ground levels. However, increasing the wind speed in streets can improve thermal comfort of people by the means of convective heat transfer through the skin.

Thermal comfort and wind flow patterns are important environmental issues when designing new urban areas. Starting from this point, this thesis focuses on computational fluid dynamics (CFD) models to observe wind flow and thermal comfort of arbitrary built urban areas in Mecidiyeköy, Istanbul. Mecidiyeköy is an arbitrarily urbanized and one of the most crowded hubs of Istanbul, which is modelled as it is and compared with alternative design scenarios in wind flow and thermal comfort results. In general, this thesis analyzes the impact of buildings on wind flow, hence thermal comfort in cities.

ÖZET

RÜZGAR YÖNLERİNDEKİ DEĞİŞİKLİKLERİN ŞEHİRLERDEKİ ÇEVRE/İKLİM ŞARTLARINA ETKİSİ

Endüstri Devrimi'nin beraberinde getirdiği iş gücü ihtiyacı şehirlerin nüfüsunun artmasına neden olmuştur. Bunu takiben, artan iş gücünü sanayi bölgelerinin çevresinde barındırabilmek için kentsel alanlar on dokuzuncu yüzyıldan itibaren ani bir şekilde gelişmeye başlamıştır.

Kentsel alanların gelişmesi arazi ve arsaların yerlerini binalara, otoparklara, yollara ya da diğer yapılara bırakmasına neden oldu. Bununla birlikte, bütün bu kentleşme adımlarının düzgün bir şekilde atıldığı da söylenemez. İnsan eliyle yapılmış bu değişiklikler kentsel alanlardaki rüzgar akımı etkilemiştir. Gelişigüzel inşa edilmiş kentsel alanlar, sokaklardaki rüzgar akımını kısıtlamış ve yavaş bir hale getirmiştir. Böylece, sokak seviyesinde rüzgarın serinletici etkisi azalmıştır. Buna rağmen, sokaklardaki rüzgar hızı arttırılarak insanların termal konforu konvektif ısı transferi yoluyla iyileştirilebilir.

Yeni kentsel alanların dizayn sürecinde, termal konfor ve rüzgar akımı yönleri önemli birer sorundur. Bu noktadan hareketle, bu tezde; hesaplamalı akışkanlar dinamiği modelleri ile Mecidiyeköy'deki gelişigüzel inşa edilmiş kentsel alanlarda termal konfor ve rüzgar akımı incelenmiştir. İstanbul'un en kalabalık merkezlerinden biri olan Mecidiyeköy, gerçeğine uygun olarak modellenmiş ve alternatif dizayn senaryoları ile rüzgar akımı ve termal konfor sonuçlarına göre karşılaştırılmıştır. Genel olarak bu tezde, binaların şehirlerdeki rüzgar akımı ve dolayısıyla termal konfor üzerindeki etkisi analiz edilmiştir.

TABLE OF CONTENTS

LIST OF FIGURES

LIST OF TABLES

LIST OF SYMBOLS

H	Building Height
L	Street Length
m	Meter
s	Second
T	Air Temperature
V	Wind Speed
W	Street Width

LIST OF ACRONYMS/ABBREVIATIONS

2D	Two Dimensional
3D	Three Dimensional
C	Celsius
CAD	Computer Aided Design
CFD	Computational Fluid Dynamics
DWG	Drawing File
E	East
F	Fahrenheit
kph	Kilometers per Hour
mph	Miles per Hour
N	North
NE	North East
NW	North West
pde	Partial Differential Equation
RANS	Reynolds-averaged Navier-Stokes Equations
RNG	Renormalization Group
S	South
SAT	Standard ACIS Text
SC	Steadman Celsius
SE	South East
SST	Menter's Shear Stress Transport
SW	South West
TED	Turbulent Energy Dissipation
TKE	Turbulent Kinetic Energy
W	West

1. INTRODUCTION

People need shelters since the beginning of history. At the beginning caves, tents and huts were used as shelter. When the populations decided to become settlers, people have started to build lasting structures for living and providing services to community, hence the first cities occurred.

However, when looking at today's world, cities are far beyond their initial predecessors. Nowadays, cities consist of numerous multistorey buildings such as, apartments, schools, hospitals, skyscrapers and public buildings on one hand and car parks, shopping malls, entertainment places, paved surfaces, roads and public gardens on the other. Moreover, populations of today's cities are incomparable to their predecessors. From this point of view, it is obvious that the urbanism idea has covered a well distance from shelters to another point.

While urbanism idea has been developing, agricultural lands, lowlands, lakes, gardens and even hills are replaced by structures. These structures have hosted more people in considerably small places compared to rural areas. As an outcome of living together of many people, urban areas have become economic, social, trade and entertainment hubs in their surroundings. Thus, urban areas have created opportunities that motivate more and more people to migrate to cities.

Furthermore, increasing land prices, limited construction areas and rising populations create a dilemma for cities. To accommodate more people in these restrictions, either urban areas have become taller and denser or cities have sprawled to their vicinities. Unfortunately, as a result of being economic locomotive and the most populated city of Turkey, Istanbul has been experiencing both processes. Because of the industrialization wave after the 1950s, city has sprawled and urbanized arbitrarily [1, 2].

The study area, Mecidiyeköy is a great example of dense urban parts of Istanbul. Mecidiyeköy is a neighborhood of Şişli in the European side of Istanbul. After 1950s, the neighborhood urbanized rapidly and through the years has become one of the most important metropolitan areas of the city. Today Mecidiyeköy, is stuck between dense urbanization of housing, commercial and transportation structures.

Wind flow in urban areas is under effect of urban design and density. Densely urbanized parts of the city hinder or shift direction of wind flow. Altered wind flow also changes the thermal comfort of people especially in hot weather conditions. From this point of view, in this thesis, first, current urbanization of Mecidiyeköy is modelled as three dimensional (3D) in computer aided design (CAD) softwares without any modification. Then, urban wind flow in Mecidiyeköy's current urbanization is analyzed by the way of numerical simulation with Computational Fluid Dynamics software (CFD). Next, five design alternatives are 3D modelled in CAD softwares for the same land size with Mecidiyeköy and wind flow for these alternatives are analyzed in same way. Last, thermal comfort analysis for Mecidiyeköy and other five alternatives due to urban wind flow is conducted.

2. URBAN DEVELOPMENT

2.1. Urbanization

Urbanization can be defined as "the process by which large numbers of people become permanently concentrated in relatively small areas, forming cities" [3]. Urbanization process first started as a result of Industrial Revolution in United Kingdom in 1900s [4]. After 50 years, in the year of 1950 around 30% of the population of world was living in urban areas. However, this ratio had increased to 47% by the year 2000. For today, 55% of the world's population is living in urban areas. According to the estimations, more than 68% of population of the world will be living in urban areas in 2050 [5]. Figure 2.1 illustrates the changes on world's urban and rural populations since 1950 and provide projections about next decades until the year of 2050. In the year of 2007, urban population surpassed the rural population and the trend has never changed since then. Furthermore, it is obvious that the urban population has a bigger growing rate than rural population. Also, rural population has reached a stagnation after the beginning of 2000s and will experience a drop after the year of 2040 [6]. When looking to the projections and population increases in the urban areas, rapid urbanization process that has been going on for the last 70 years should not be found strange.

For the year of 2018, North America, Latin America and Caribbean, Europe and the Oceania are the most urbanized regions of world, with respectively 82%, 81%, 74% and 68% of their population are living in urban areas. Urban population of the world was 751 million in 1950 and increased to 4.2 billion in the year of 2018 [5]. Between same years, Turkey's urban population have risen from 5.3 million to 61.56 million and it is projected to be 82.19 million by the 2050 [7].

When the fact is considered at city level, Tokyo is the most crowded city with its 37 million residents and followed by Delhi and Shanghai with 29 and 26 million
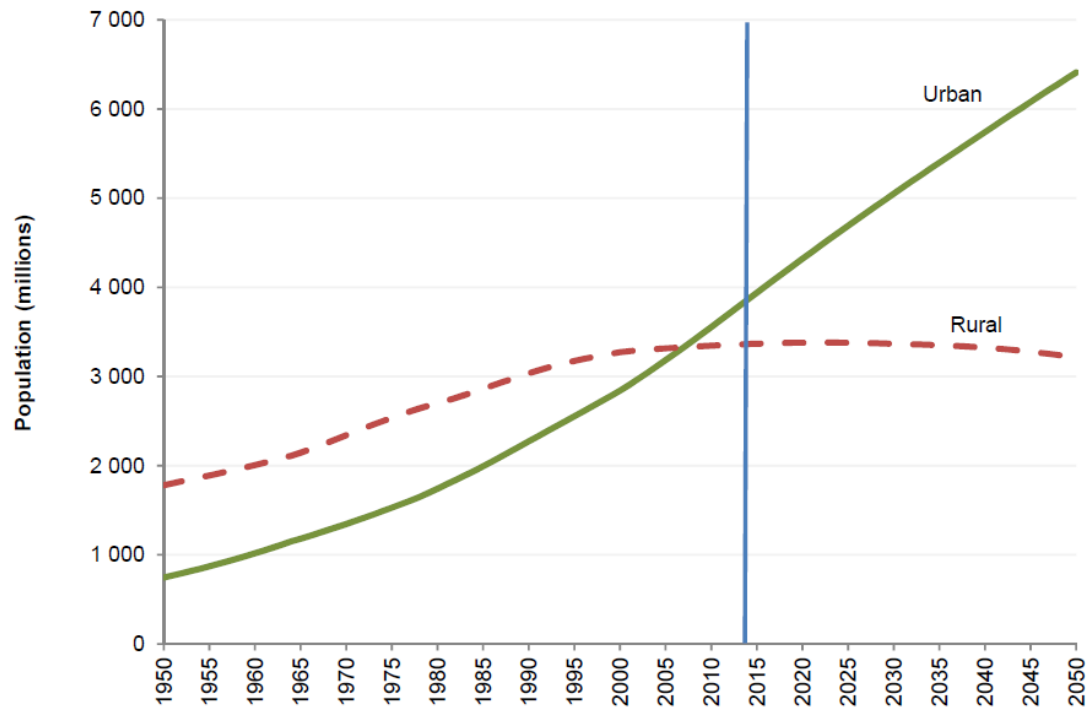
Figure 2.1. Urban and rural populations of world with 2050 projections [6].

residents respectively in 2018 [5]. Cities like these, which have more than 10 million residents are named as megacity. There were 31 megacities globally in the year of 2016, according to projections there would be 41 megacities in the world in the year of 2030 [8].

On the other hand, Turkey's most crowded and only megacity, Istanbul's population was more than 15 million inhabitants by the year of 2017 and it is projected to be 16.7 million inhabitants in the year of 2025 [9]. Moreover, Istanbul constitutes 18.5% of Turkey's total population and 25.1% of country's urban population, alone [8].

2.2. Urban Sprawl

Urban sprawl is arbitrary development of urban areas. Urban sprawl also known as suburbanization and described as "the physical pattern of low-density expansion of large urban areas, under market conditions, mainly into the surrounding agricultural areas" by The European Environment Agency [10]. Sprawl of urban areas threatens the cities in economic, environmental and social ways and also prevents fights against climate change. Major problems due to the sprawl of cities are increasing energy requirements and land use change. These problems do not only affect the urban areas but also threaten the rural parts by the way of increasing green house gas emissions, air and noise pollution.

The phenomenon has arisen at United States in beginning of the twentieth century. Increasing private mobility by the way of private cars and new public transportation systems among community boosted the desire about gardened detached houses. In this case urban sprawl initially took place at the developed regions of North America. The high income groups, who live in metropolitan areas, wanted to move the places, where can provide healthier and uncongested lifestyle without giving up on urban services has preferred suburbans to rural areas. Contrarily, urban sprawl has also been propelled by population growth and socioeconomic factors such as, land and house prices, cultural preferences and individual housing needs in some regions like Europe and Asia [11].

While, urban sprawl makes automobiles a vital need for everyday in regions like North America, automobile travel has shaped the progress of urban sprawl through the growth of highway and freeway networks [12]. Figure 2.2 illustrates car dependency with a highway, which has 18 lines, in Toronto, Canada and suburbanization in the background.

Levittown is a popular example for urban sprawl from the United States. The project is started in the year of 1947 in the Long Island, New York for hosting the

Figure 2.2. Highway 401 in Toronto, Canada [13].

veterans of World War Two. Thus, it describes the prototype lifestyle after war in the United States. Levittown is consisted of more than 17000 houses based on six different models and built between the years of 1946 and 1951. The name Levittown became a symbol after the suburb was built. When the construction sector boomed after the war, many suburbans are inspired by the project [14]. Figure 2.3 is a section from Levittown in Long Island, New York.

On the other hand, cities are more compact in Europe, when they are compared to cities of United States. The reason is that the cities in Europe are founded much before the common use of transportation systems, hence the core of the cites are generally historical. However, since being more compact than the cities from United States even today, sprawl of the European cities are emerged after 1950s. Today, urban sprawl is also a common phenomenon in the old continent [10].

For instance, Dublin is a small city when it is compared to other European capitals and it shapes the urban pattern of Ireland by economic and demographic
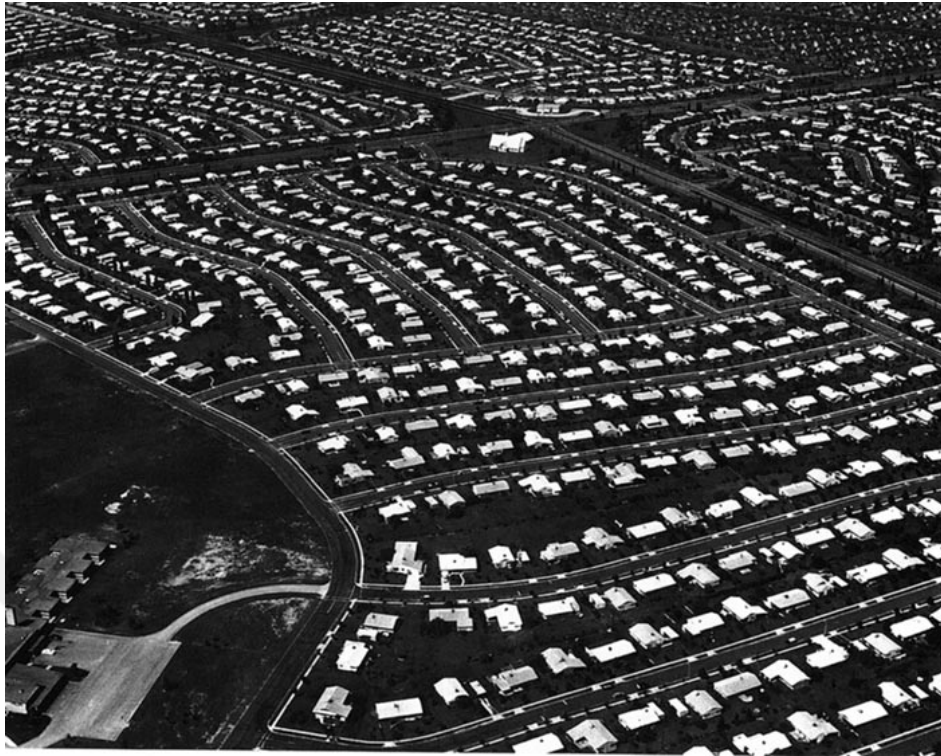
Figure 2.3. Levittown suburb, New York [15].

ways. Population of the Dublin was 1.5 million in the year of 2002, which was the 40% of the Ireland's total population. According to The National Spatial Strategy, population of the Dublin will be around 2.2 million people by the year of 2020, which means city will have to host half a million more residents [16].

Rise of house prices, economic development and population growth are considered as the main reasons of the sprawl of Dublin. Increase of house prices and old building stock and small size of flats in the city centre direct people to rural areas close to the city, where it is easier to buy or build houses in economic ways. Thus, people who need more space choose to live in suburbs rather than city center. These situations end up with expansion of villages and rural parts of Dublin. Moreover, due to transportation flaws of city, it can be easier to commute from villages to city centre than commuting with public transport in city [17].

Through the simulations, suburbanization of Dublin in the near future is calculated. When looking to the 2025 scenario, expansion of the Dublin will be increased 110% compared to situation in the year of 1990 [10]. Figure 2.4 shows the comparison of the urban sprawl between the year of 1990 and the projections about the year of 2025.
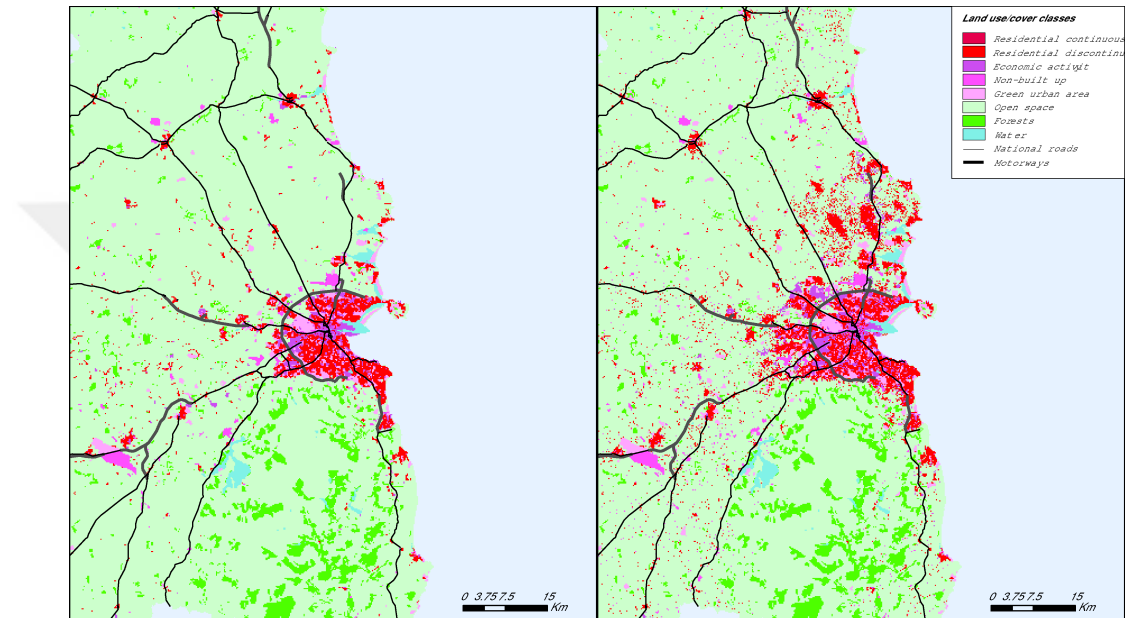
Figure 2.4. Urban sprawl comparison of Dublin between 1990 on the left and projections about 2025 on the right [18].

In general, it is governments' obligation to prevent economic, social and environmental effects of the phenomenon. Thus, governments must step up to the fight in reversing urban sprawl.

2.3. Urbanization of Istanbul

Istanbul is the largest city of Turkey with a long history at the intersection point of Asia and Europe. Istanbul has always been the locomotive of Turkey's economy, yet after the 1950s, Istanbul has grown enormously. The city has more than 15 million

residents today and gets continuous migration from countryside. Urban population of Istanbul was almost 1.8 million in the year 1965, which is a very small number when compared to today's situation [19]. Also, the built up area has sprawled nearly 600% with migration waves [10].

Up to the year of 1950, Turkey's main economic activity was based on agriculture, which is followed by little industrial activities. In this year by the way of first multiparty elections the government passed into new hands. New government opened Turkish economy to global market through new liberal reforms. This situation was followed by a boom in industry which was propelled by global partners and credits [20].

The boom in the industry made Istanbul the primary place, where needs many labor force for new industrial areas in the surroundings of the city, hence migration from countryside to urban areas increased the population of Istanbul. Following that, squatter settlements sprang up as an answer to migrants' accommodation requirements and has shaped Istanbul's demography and urban areas in later years [21].

Early settlements were arisen in the public lands, which were occupied by the squatters. Initial buildings in these areas were makeshift shanty houses, yet they were substituted by masonry buildings or multistorey reinforced concrete structures in very short time. Zeytinburnu and Gültepe are two examples of first settlements, which experienced the transformation from shanty houses to reinforced concrete structures or masonry buildings. Through the years squatter settlements have been legalized by the way of granting the lands to squatters. Thus, first settlements are still parts of Istanbul [20].

However, these areas have strong problems today. First, most of the building stock is old and they are not built respect to building codes, hence these areas can be considered as danger zones in a city which is entrenched on fault lines. Second, squatter settlements were not built in core of the city, yet the city has grown and these

settlements became arbitrary built neighbours of relatively more planned metropolitan parts. Figure 2.5 illustrates the current situation of these areas. In short, squatter settlements were uncontrolled and rough solutions, which treated enormous housing problem of Istanbul due to industrialization in 1950s in a very bad way.

Figure 2.5. Squatter settlements and their new neighbours in Istanbul [22].

When the early 1980s came, a new industrial move took place in Turkey because of globalization and neo liberal policies. Successive privatizations about government enterprises were implemented. As an outcome of these applications, economic mobility nearly doubled the urban population of Istanbul between the years of 1980 and 1985 from 2.9 million to 5.56 million inhabitants [23]. Moreover, involvement to customs union with European Union in 1996, increased the foreign investments in the city [20].

Through the years, from early 1980s to late 1990s, affordable housing necessity in Istanbul was handled by private sector. Instead of occupation of public lands by squatters, owners of agricultural areas in the surroundings of the city allocated their lands and sold them to squatters. These allocated lands on the market were legal,

when compared to old accommodation attempts of migrants, yet these areas were also very small. Thus, mostly multi storey structures built on these ares to accommodate more and more people, with very narrow gaps between the buildings. Consequently, very dense urban areas were arisen in these parts of the city. Figure 2.6 shows the extent of situation. Again, through the years these areas were legalized too [20, 24].

Figure 2.6. A photo from dense urban areas of Istanbul [25].

In 1999, Izmit earthquake in the Marmara region was a milestone for the urbanization process of Istanbul. After the earthquake, reconstruction or structural strengthening of building stock has become the main objective of urban planning [24]. In addition, new regulations were implemented too, such as, modification of the the existing building codes and limiting the number of storeys of new buildings in respect to the earthquake forces.

Improving economic situation and regulations for European Union membership have raised the living standards of the country to some extend in 2000s. Thus, housing preferences has been changed in last years from city center to suburbia [26]. Moving

out from the city center to suburbia generally ends up at detached houses or gated communities. Detached houses with their own gardens, pools and garages are mostly preferred by families. On the other hand, gated communities with guards, shopping centers, schools, clinics and entertainment areas within are not unfamiliar parts of the Istanbul's suburbia. There is not any current source to get exact number of gated communities in the city, yet there were around 300 in the year of 2005 [10].

Furthermore in 2000s, urban regeneration projects have also become parts of everyday life in Istanbul. Rejuvenating the building stock and replacing squatter settlements with planned residential areas are the main aims of regeneration move. This new aspect about urbanization strengthened the construction industry and skyrocketed the number of contractors at the city in late years. Such that, construction industry has become the locomotive of Turkish economy.

Since the 1950s, population growth in Istanbul has brought along many problems too. Air and water pollution, traffic congestion, arbitrary built areas, very dense urbanization, squatter settlements, lack of infrastructure, environmental degradation, unemployment and social problems are some of them [10,27]. Nevertheless, predictions about the future do not have any slowing signal about the increase of city's population. Figure 2.7 illustrates the future growing trend of Istanbul's population.

It seems that, population increase will also be the main factor that shapes Istanbul in the future. Figure 2.8 below illustrates the Istanbul's future sprawl for the year of 2020. When looking to the results, it can be said that, urbanization far from the metropolitan areas of the city can summarize the issue. This situation is outcomes of new housing preference of residents and relatively cheap land prices in surrounding areas of Istanbul. In addition to that, there are different trends of urbanization as can be seen from the results. To begin with, there will be new buildings in the available lands among the present structures. Next, the growth along the west and east coastal line can be seen at a glance. The coastal growth is more apparent at the European side

The chart shows Population vs Year with equation $y = 2E-204x^{63.851}$ and $R^2 = 1$.
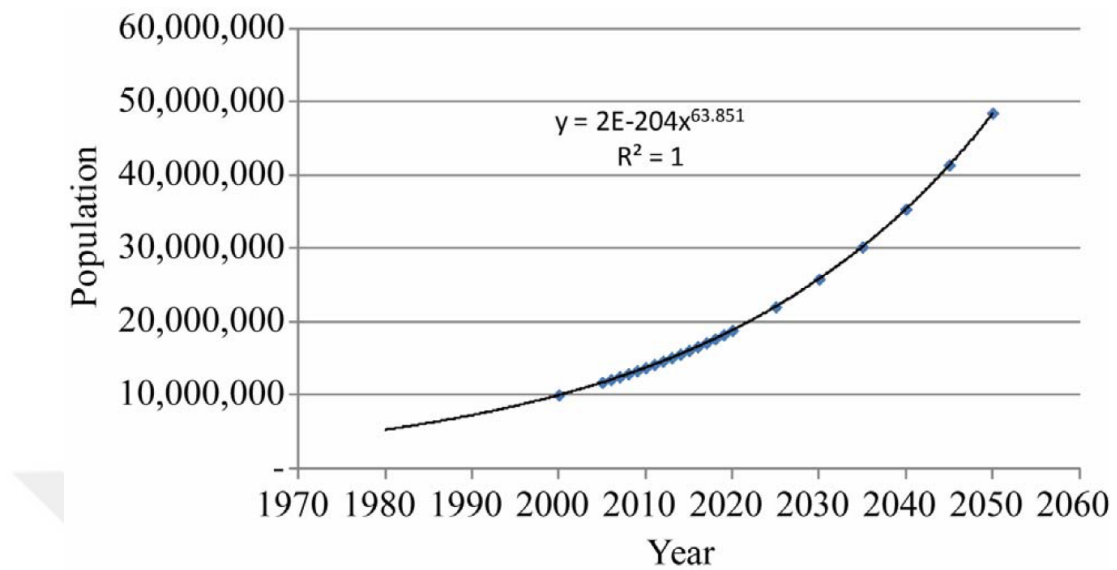
Figure 2.7. Istanbul's future population presumption [28].

of the city. Lastly, decrease of forest area at the northern side of the city also draws the attention because of new building areas [10]. To sum up, it is obvious that Istanbul will continue to experience urban sprawl in near future due to population growth.

On the other hand, trade centers and industrial zones are parts of cities like housing areas. By the way of increasing population, expansion of these kind of city parts also inevitable. Thus, urbanization and sprawl of the city is not an one way phenomena. As long as, Istanbul is the economic capital of Turkey, trade areas and industrial zones in surroundings of the city will prefer the closest available lands to metropolitan areas for reducing costs [27].

Moreover, connecting sides of Istanbul to each other have always been a problem. Traffic congestion and malfunction of transportation systems are chronic illnesses of the city. To handle these matters several steps has taken in the 2000s. For instance, Marmaray project has linked the Asian and European sides of Istanbul under the Sea of Marmara with integration into railway and subway networks. Furthermore, also a

2000

Simulated 2020

Land use classes

- Continuous urban fabric
- Discontinuous urban fabric
- Industrial and commercial areas
- Transport areas
- Green urban areas
- Agricultural areas
- Natural areas
- Other land uses
- Mineral extraction sites
- Water
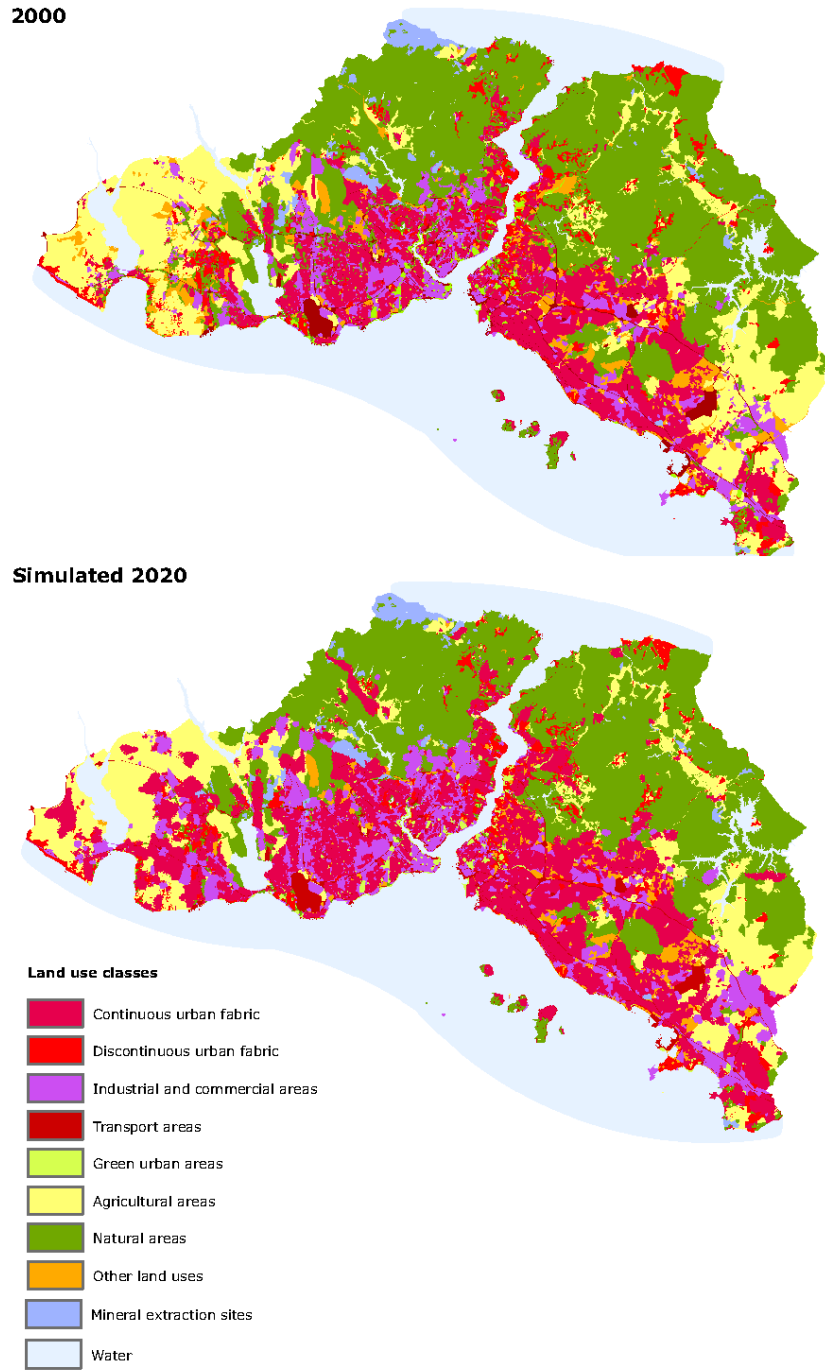
Figure 2.8. Urban Sprawl of Istanbul in the year of 2020 due to population [29].

third bridge built on Bosphorus at the north of the other two bridges as a solution to same problems.

The zone plans that were prepared in 1960s, suggested an east - west growth pattern for Istanbul, yet the city has sprawled through the north because of the bridges built on Bosphorus. Hence, drastic effects of massive transportation projects on urban sprawl cannot be ignored. Figure 2.9 below shows the expected sprawl of Istanbul in the year of 2030 due to third Bosporus bridge. The forest areas at the northern parts of the city in both Asian and European sides will be confronted with urbanization [30].
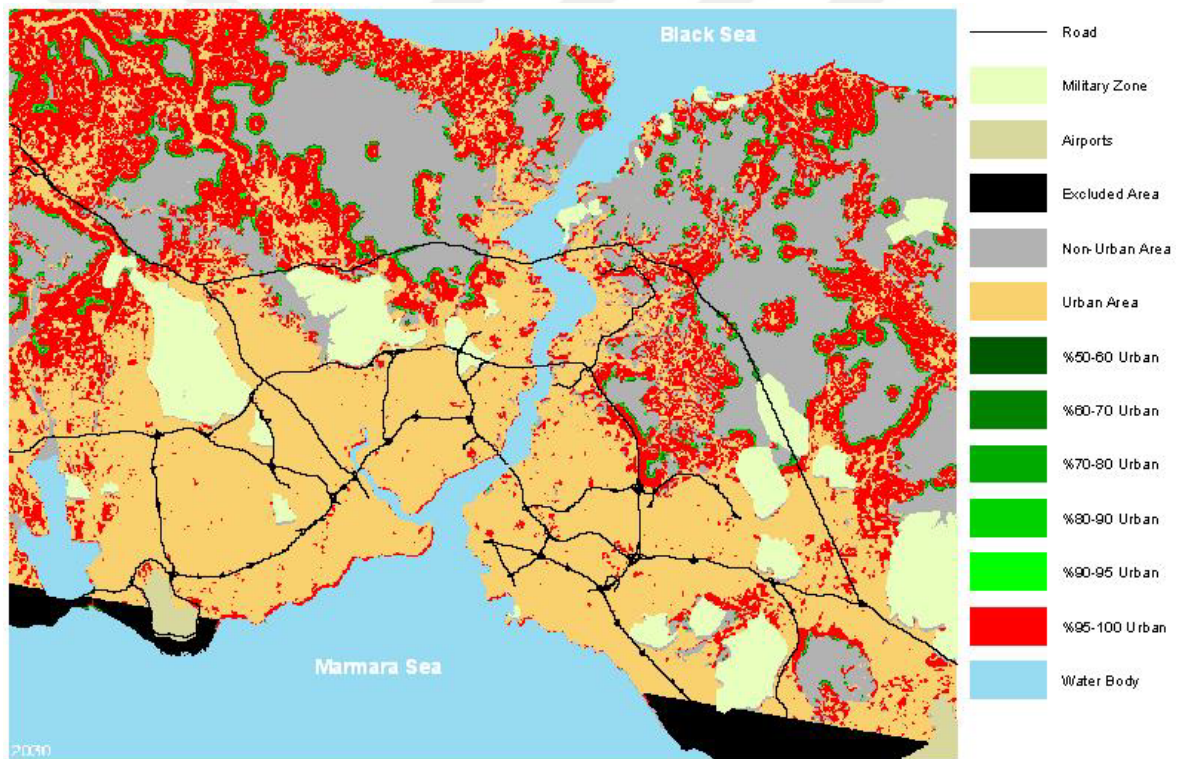
Figure 2.9. Effect of third Bosporus bridge on Istanbul's sprawl in the year of 2030 [30].

3. EFFECTS OF URBANIZATION ON WIND FLOW, HENCE THERMAL COMFORT

Through the urbanization process, lands are covered with building materials. Natural surfaces such as, agricultural lands, lowlands, lakes or forests are altered to buildings, parking lots, roads or other structure types, which has ended up with differentiating aerodynamic characteristics of areas. At this point, expecting impacts of these alterations on wind flow in urban areas, hence thermal comfort would not be wrong.

First attention about the phenomenon was drawn by Kremser in the year of 1909. For testing the decrease of wind speed in the urban areas, an anemometer was placed on the top of a school in one of the closer suburban areas of Berlin, Germany. The anemometer was at the height of 32 meters above the ground, showed 5.1 m/s as mean wind speed. A decade later, landscape changed around the school and the previous open terrain turned into apartment housing. This time, the anemometer was just 7 meters above the average roof height, hence the mean wind speed was dropped to 3.9 m/s, which reflects a reduction of 24% in a decade [31].

In the year of 1979, another study published by Rubinshtein about the same issue. At this study Rubinshtein recorded the changes on wind speed as a result of urbanization process between the years of 1945 and 1971 in Gantsevitchi, which is a growing town of Belarus at these years. Through the long study period, Gantsevitchi's annual mean wind speed decreased from 3.9 m/s in 1945 to 2.5 m/s in 1971, which is a drop of 36% as can be seen at the Figure 3.1 in detail [31].

Many years have passed after these studies, yet the effect of urban modifications on wind flow in the cities is still a major problem. While the years were passing, many new cities has been built and most of the old cities have sprawled or become denser, hence realizing the decreasing trends of wind speed in urban areas do not take long
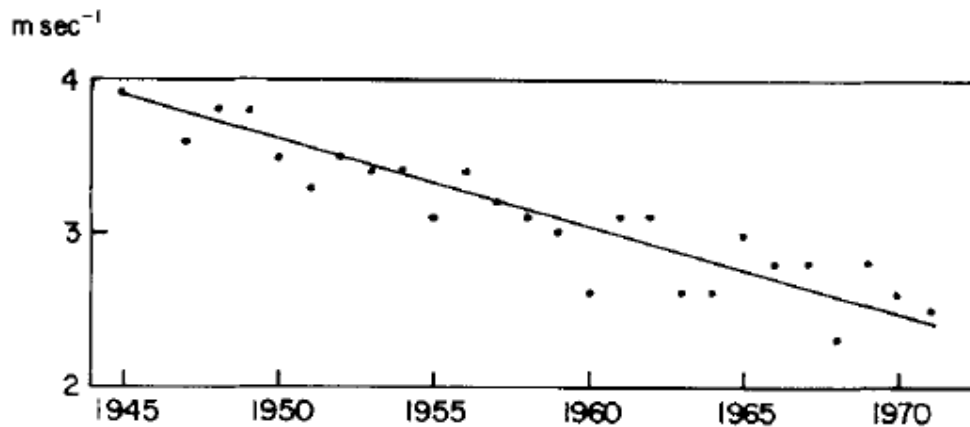
Figure 3.1. Annual mean wind speed trend of Gantsevitchi, Belarus [31].

time like Rubinshtein's study. For instance, Hong Kong's mean wind velocity decreased almost 40% at a decade because of dense urbanization. The graph at Figure 3.2 shows the records of urban anemometer stations in Hong Kong between the years of 1994 and 2004 [32].

On the other hand, in today's world, buildings have become taller and bulkier because of high land prices or limited construction areas. These tall and bulky buildings with less gaps between them make urban areas less permeable places for wind flow by the means of natural ventilation at pedestrian level [33]. Also vortexes are arisen in urban canyons owing to high rise buildings [34]. Moreover, wind flow comes to a stopping point at near ground levels in especially arbitrary built dense urban areas [35].

When the wind flow in urban areas is affected by several deficiencies in urban design, correspondingly climatic conditions of urban areas are altered too. Slower wind speed at near ground levels or in other words at pedestrian levels, worsens the thermal comfort of people in urban. Cooling effect of wind by the way of convective heat transfer by the skin has become weaker with slower flow speed [35, 36].
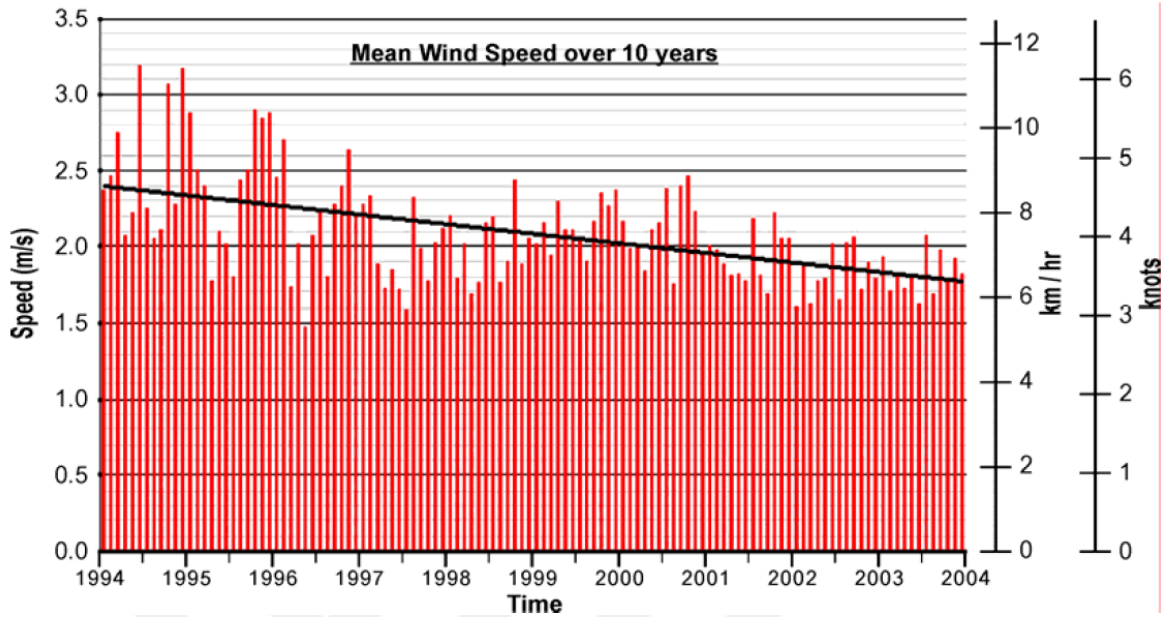
Figure 3.2. Mean wind speed change of Hong Kong because of urbanization [32].

Moreover, heat waves are becoming more common and take longer times due to climate change. This increases the adverse effects of urban areas on human thermal comfort. High temperature in urban areas with lack of proper ventilation also increases mortality rates. For example, the heat wave in Europe in the summer of 2003 ended up with more than 70000 deaths. People with diseases and elder ones are more vulnerable to this kind of phenomena in congested urban environments. In addition, in European Union, mortality rates are estimated to increase up to 4% for one degree rise in temperatures above the local cut off point [37].

When the increasing emissions and pollution in cities are taken account, proper wind flow in urban areas become important again from a different perspective. Wind flow in urban areas carries chemicals, fumes, dust, pollutants, exhaust and greenhouse gases. However, stagnant air in streets limits the dispersion of these carried materials. Thus, these particles, pollutants and gases are not dispersed randomly by flow in urban areas. Consequently, carried materials accumulate in some parts of urban areas or around some buildings which creates contaminated hot spots in urban environment [38].

If the urban area can ventilate itself by the way of wind flow, air quality within streets would be increased and emission gases sent away without need for anything else [39].

Lastly, thermal comfort in urban areas directly affect the energy consumption. Demand for cooling in hot weather conditions increases. However, energy use for cooling would be less for a city with natural ventilation was considered at design stage. At the light of this, designing an urban environment with considering wind flow, hence thermal comfort is a key to have energy efficient urban areas too.

4. STUDY AREA

The study is conducted in Mecidiyeköy, which is a neighborhood of Şişli in Istanbul. Mecidiyeköy is located around 41° 4′ 0″ North and 29° 0′ 0″ East coordinates in European side of the city. The neighborhood is constituted on the area of approximately 460000 square meters and had 19960 residents in 2014 [40]. The Figure 4.1 shows Mecidiyeköy in its boundaries with lines marked in red, and its location on the map.
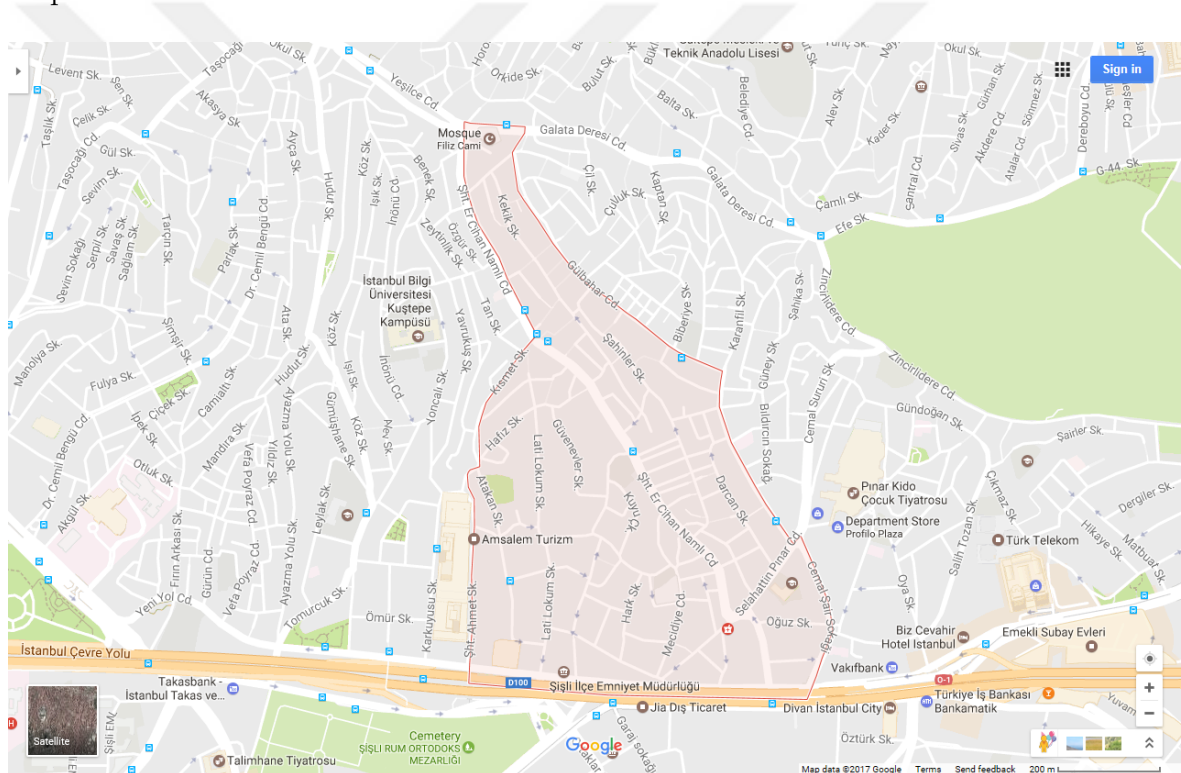
Figure 4.1. Mecidiyeköy neighborhood between its boundaries on a map [41].

Mecidiyeköy preserved its rural status until the 1950s. Afterwards, the neighborhood has become a development area and experienced rapid urbanization. In following decades, Mecidiyeköy has been one of the densest housing and commercial urban areas of the city. Through these years, green areas have melted away against buildings and infrastructure.

With construction of Büyükdere main street and hosting the D100 beltway of Bosporus Bridge since beginning of 1970s, transformed Mecidiyeköy into one of the most important and intense transfer centers of urban transportation in Istanbul. Furthermore, Mecidyeköy is also playing a large role at the public transportation of Istanbul with metro and metrobus lines. The Figure 4.2 below, shows the extent of intensity via public transportation queue on one hand and traffic congestion on the other.

Figure 4.2. Mecidiyeköy's intensive queues [42].

Today, Mecidiyeköy has been suffering from dense and unplanned urbanization. The building stock consists of various types of structure, from squatter settlements to high rise buildings, gated communities and business centers. The Figure 4.3 illustrates the level of dense urbanization in the neighborhood. On the other hand, traffic congestion and infrastructure problems are parts of daily life in the neighborhood. Moreover, Mecidiyeköy is under effect of very loud traffic noise at all hours of the day because of D100 beltway and traffic congestion [43].

Figure 4.3. Multistorey buildings in Mecidiyeköy with very small gap between them [44].

5. METHODOLOGY

5.1. Modelling

To begin with, the central part of Mecidiyeköy, where the major business and housing activities take place is modelled as 3D. The modelled part of Mecidiyeköy is approximately 181403 square meters. Shaded region on the Figure 5.1 below shows the modelled area and the yellow region belongs to the Mecidiyeköy neighborhood on the map that taken from Urban Information System of Şişli municipality.
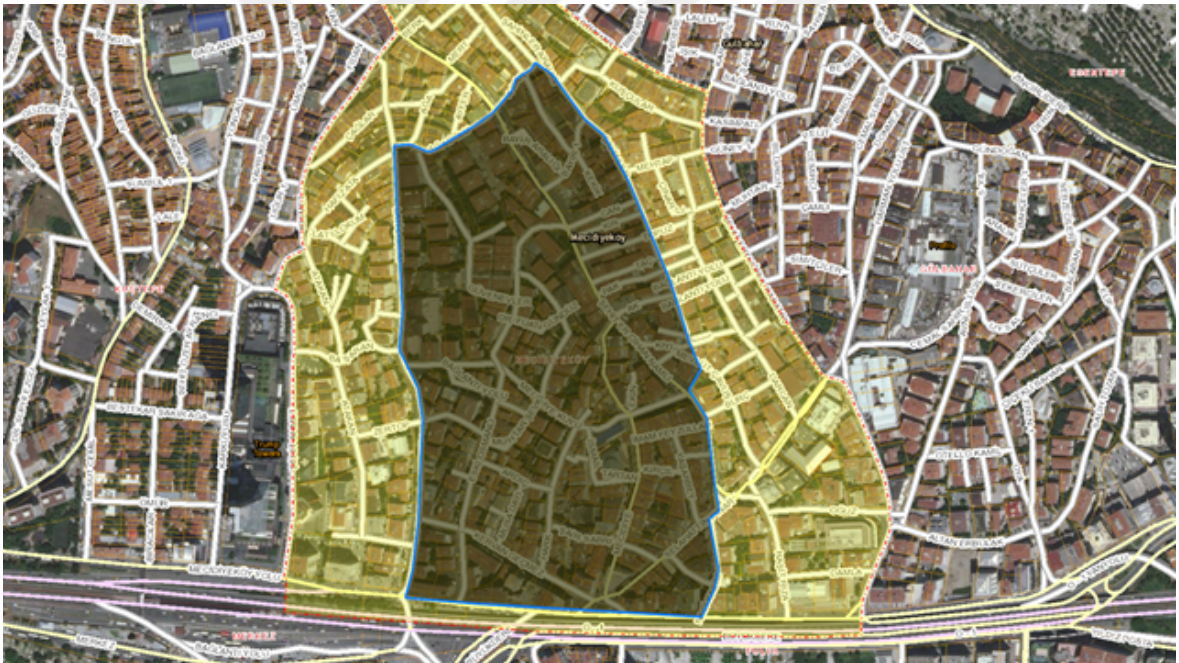
Figure 5.1. Modelled part of Mecidiyeköy [45].

The modelled area consists of various types of buildings from single storey to multistorey structures such as, apartments, gated communities, schools, squatter settlements, trade centers and a mosque. Alleys, dead end streets and parking lots are placed irregularly among these buildings as an example of Istanbul's urbanization.

Nevertheless, the modelled area also shares a complete lack of green areas like its surroundings.

The 3D model of the selected part of Mecidiyeköy was taken shape on 2D base map of Şişli municipality. A view from DWG file of the 2D base map of Mecidiyeköy can be seen at the Figure 5.2.
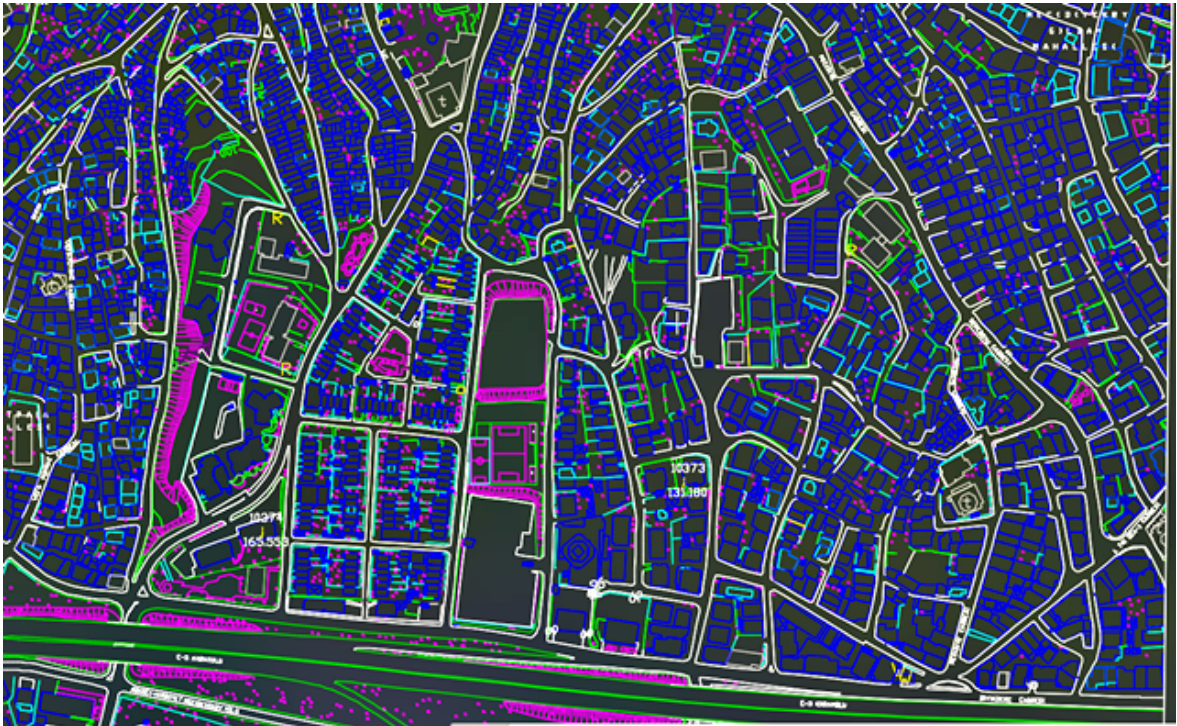
Figure 5.2. Example from 2D base map of Mecidiyeköy.

Modelling of the area is carried out in SketchUP. SketchUP is a 3D modelling computer program. The program can be used for drawing applications from architectural to engineering or film and video game design [46].

For modelling in the program, first the 2D base map of Mecidiyeköy is imported, then the buildings are drawn in third dimension. At this step, number of storeys of all the modeled buildings are obtained from the urban information system of Şişli

municipality. Number of storeys of the buildings change from one to 12. However, due to lack of information about storey heights of buildings the storey height is considered as 3.2 meters for all buildings, which is one of the most common storey heights at built structures in Istanbul. Figure 5.3 shows the storey height at design stage in detail.
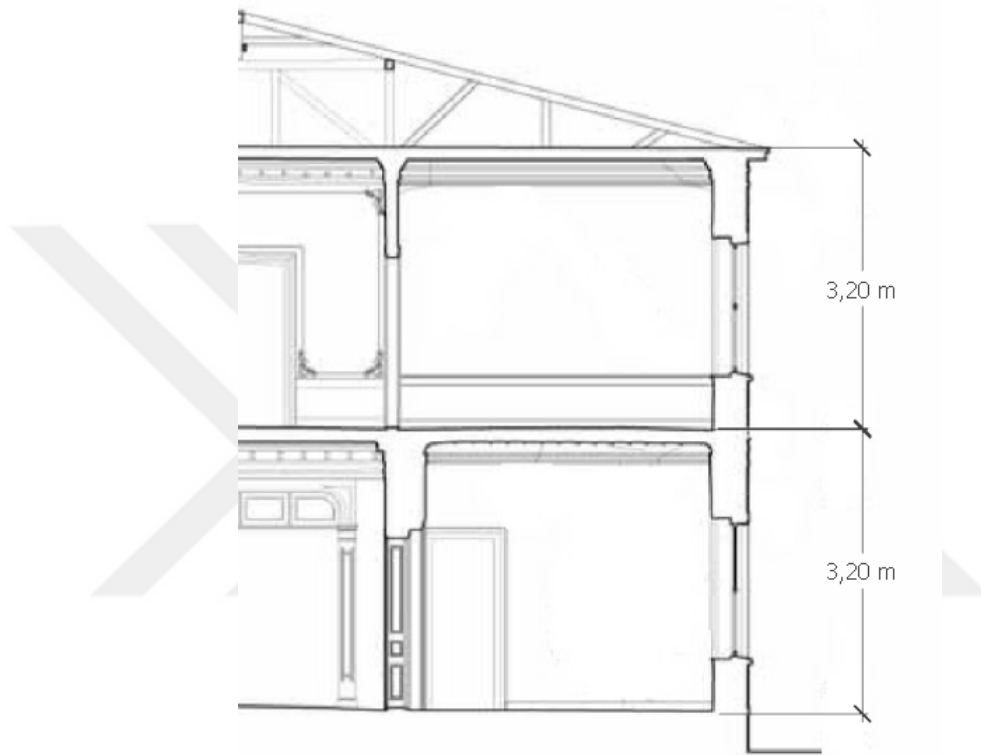
Figure 5.3. Decided storey height for modelled buildings.

At the end, more than 500 buildings are modelled realistically as 3D in the SketchUp modelling program. However, the terrain features are neglected. The model dimensions are 365.14 meters at the width and 640.13 meters on the length. Also model height changes from 3.2 meters at the lower point to 38.4 meters at the top point due to building heights. All of the model can be seen at the Figure 5.4 below.
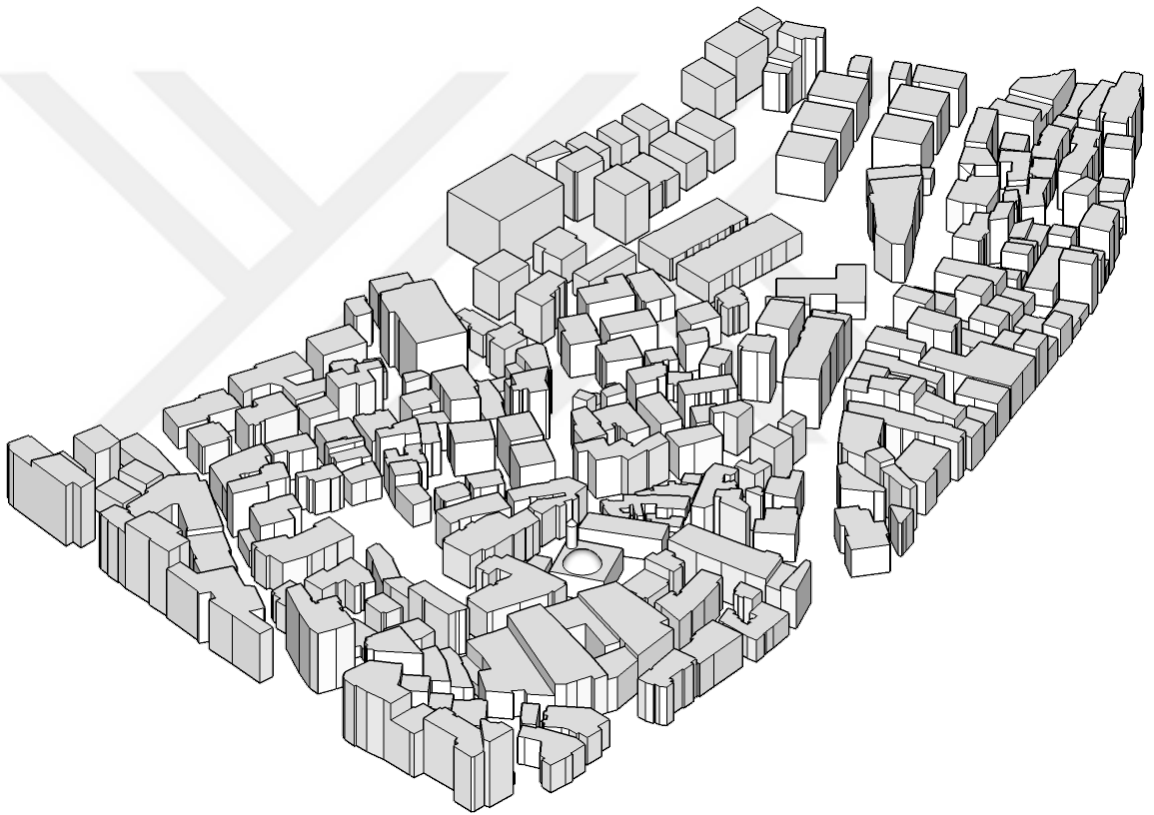
Figure 5.4. An isometric view of the model.

After modelling Mecidiyeköy, five different alternatives are designed for comparing by the means of wind velocity and apparent temperature. There are several criteria considered while designing these alternatives. First, the area of Mecidiyeköy is taken and used as a $425m \times 425m$ square. The alternatives are built on this square. Next, the total volume 1690557 m^3 of the buildings in the Mecidiyeköy is preserved for alternatives to provide same services to community as available buildings. Third, the 25 meters gap between the building blocks are same for all the alternatives except last two.

The first alternative is consisted of relatively large square buildings with $50m \times 50m$ and $16.67m \times 16.67m$ courtyards in the middle of each building with the height of 38.04 meters. Also, the building blocks are placed to enclose a large park with the dimensions of $325m \times 325m$. The alternative can be seen at the following figure.
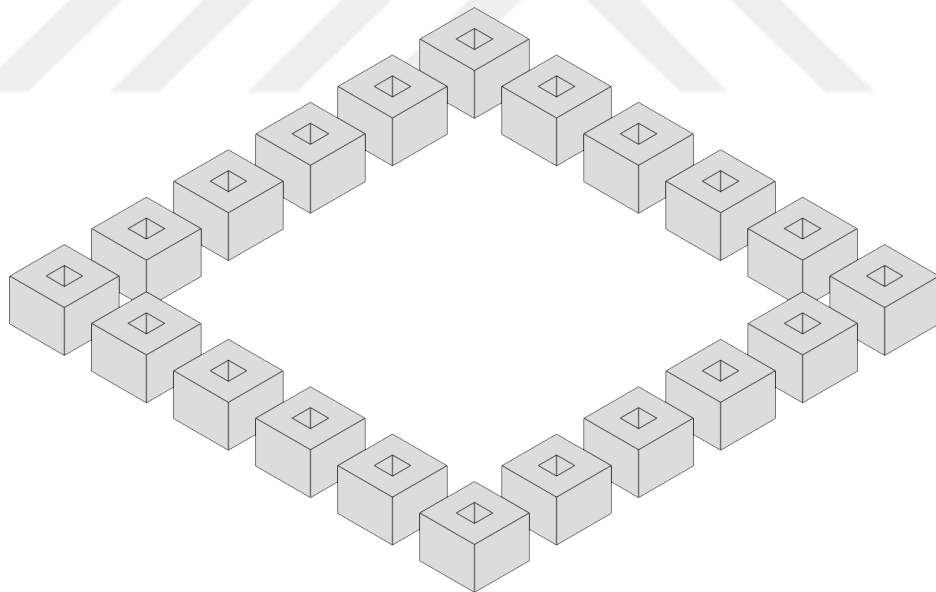
Figure 5.5. An isometric view of the first alternative.

The second alternative have 48 identical buildings. The base area of the buildings are $31.25m \times 31.25m$ and the height of them is 36.07 meters. Again the the building blocks are placed to enclose a park with the dimensions of $250m \times 250m$. The alternative can be seen at the next figure.
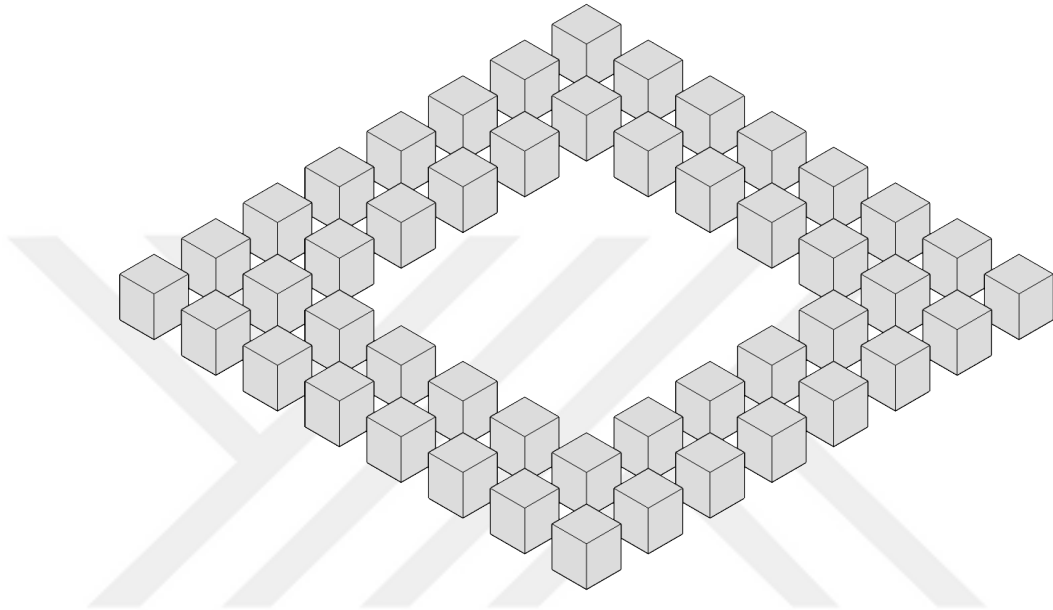
Figure 5.6. An isometric view of the second alternative.

The third alternative shares the identical buildings with the second alternative. However, this time the buildings are placed on all of the model area without a park, hence the number of the buildings is increased to 64 and the height is decreased to 27.05 meters. The alternative can be seen at the next figure.
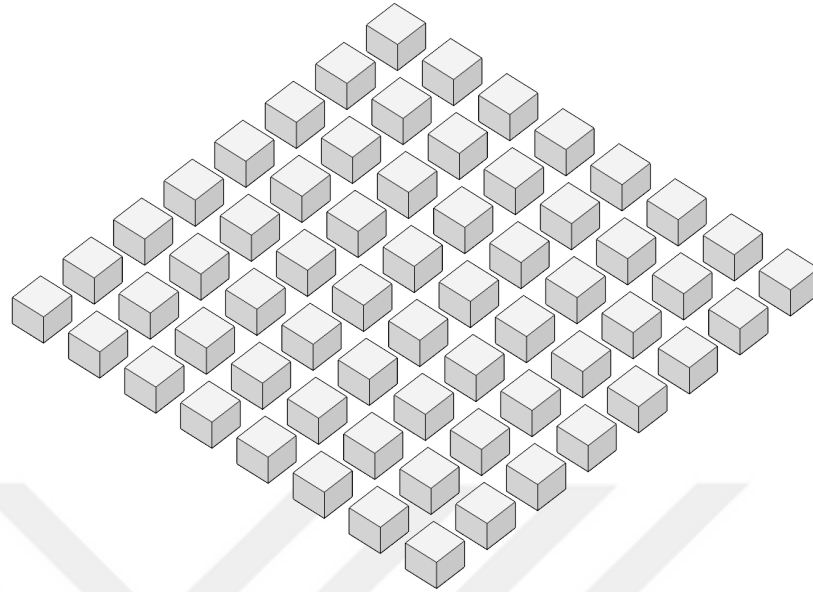
Figure 5.7. An isometric view of the third alternative.

At the fourth alternative, 37 buildings are randomly distributed on the modelling area. The buildings are identical with the second and third alternatives', yet the height of the buildings at this alternative is increased to 46.8 meters due to the building number. The alternative can be seen at the Figure 5.8.

The fifth alternative is same as the fourth alternative in every aspect except the building height. In this alternative, also the building height varies randomly from 34.80 to 55.20 meters. The alternative can be seen at the Figure 5.9.
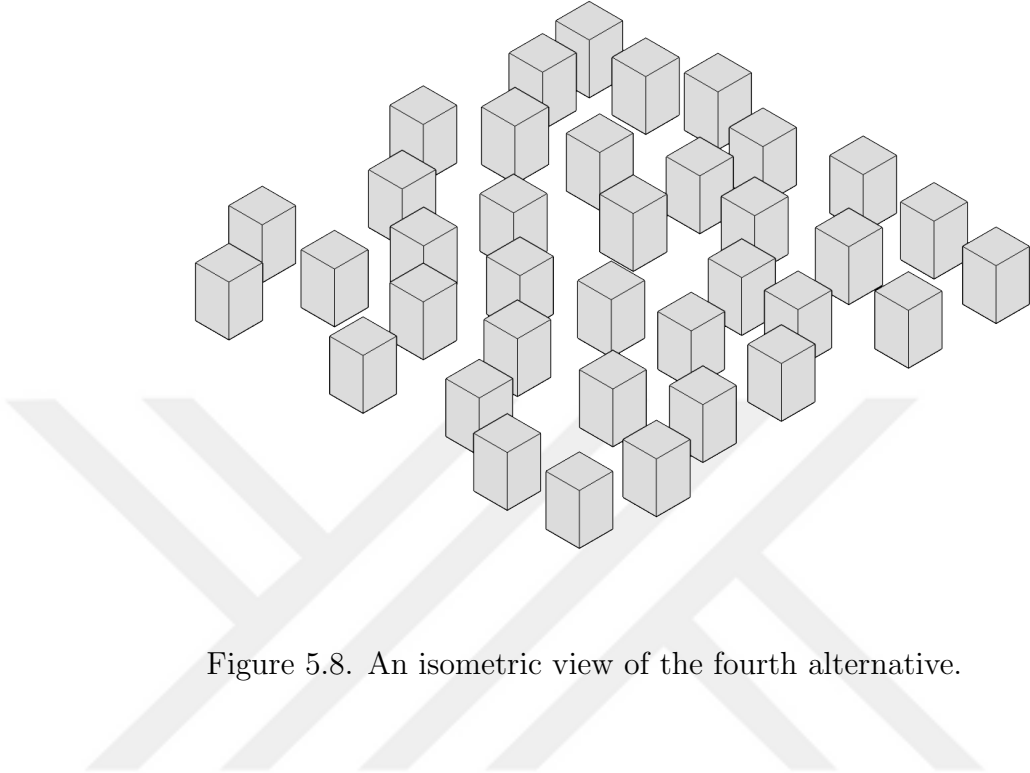
Figure 5.8. An isometric view of the fourth alternative.
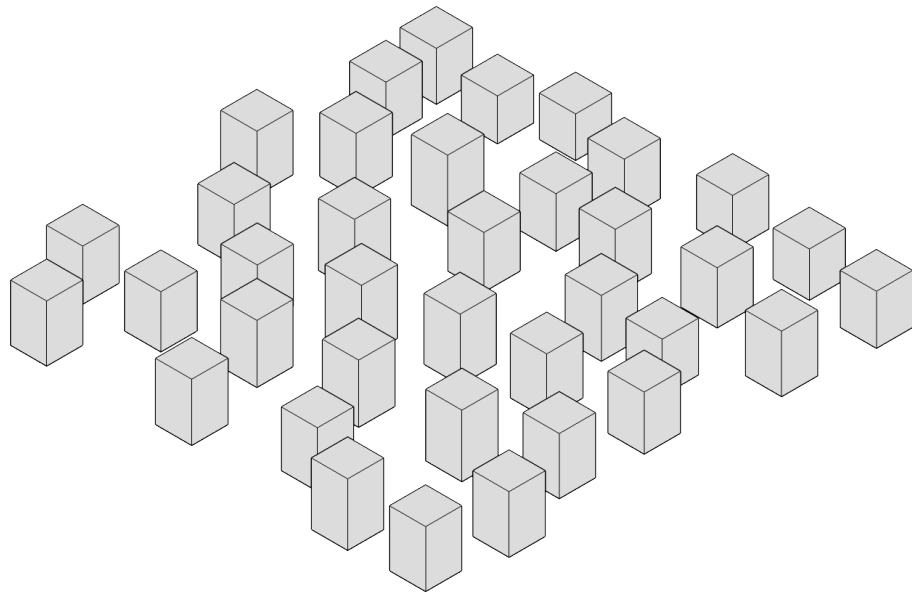
Figure 5.9. An isometric view of the fifth alternative.

5.2. Wind Flow in Urban

5.2.1. Flow Around a Building

Buildings create an aerodynamic modification on the landscapes, hence the wind flow around the buildings has to differ from the landscapes. Wind flow pattern around a flat roofed building with its windward facade is placed at the normal of flow is illustrated in the following Figure 5.10. Also the flow patterns around the building are described with numbers.

When the wind flow is approaching to the building, it shifts from its direction. Some of the air is deflected over top of the building and some of the air flows around the building, flow patterns 1 and 2 at the figure. Also a stagnation point occurs at the windward facade of the building. The wind flow creates maximum pressure at the upper middle part of the facade, where is approximately 70% of the height of the building, hence the air becomes still at this point and the pressure decreases to outwards such as, upwards, sideways and downwards, flow patterns 3,4 and 5 at the figure. Significant amount of the air at the lower levels produce a vortex, which is called as standing vortex, frontal vortex or horseshoe vortex, flow pattern 6 at the figure, yet the direction of the vortex is in contrast with the wind. When the wind and flows of the vortex meet, another stagnation point also occurs, 7 at the figure. The standing vortex also stretches to sides of the building, hence flow pattern 8 occurs at high speed. Afterwards, these flows join to the main wind around the building, pattern 9. On the other hand, underpressure zone occurs at the leeward side of the building because of back flow and recirculation, patterns 10 and 13 at the figure. A third stagnation point emerges due to opposite directions of flow patterns and low wind speed at the end of recirculation. The point is at ground level, 11 in the figure. After the third stagnation point main wind flow returns to its original direction, yet the wind speed continues to be slow at for a quite distance, 12 in the figure. The backflow also creates, slow vortexes at the leeward facade of the building, flow pattern 13 at the figure. Between

flow patterns 13 and 9, high velocity vortexes occur at the separation of flow, 14 in the figure which is named as shear layer [47].
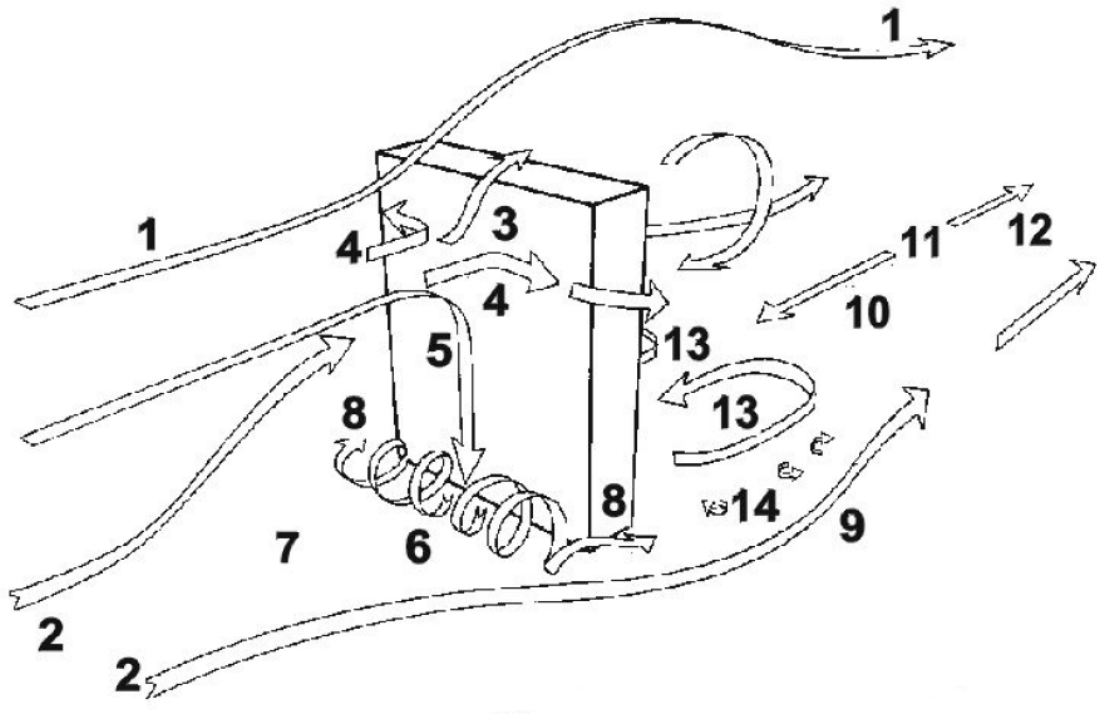
Figure 5.10. Wind flow patterns around a building [47].

After this detailed description about the flow patterns around a building, a general approach with 2D illustrations could be better for understanding the concept. When the wind flow encounters with a sharp edged and flat roofed building, four different flow zones occur at the side section of the building. The zones can be seen at the Figure 5.11. The flow zones are named as, A; undisturbed, B; displacement, C; cavity and D is wake.

While the flow accelerates over the top and sides of the building, it has become separated from the surfaces. Thus, leeward facade, sides and roof of the building experience suction instead of pressure. By this way air pressure decreases and these suction areas are shaped by reverse flows, hence the circulation in C zone emerges.
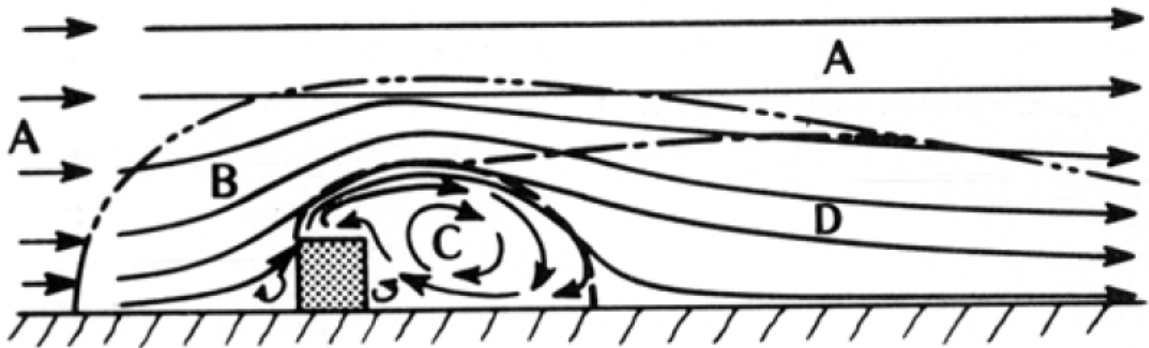
Figure 5.11. Side section of flow zones around a building [48].

This circulation affects to the suction area above the roof. Cavity zone C, which is created by eddy circulation and suction areas shown in the Figure 5.12.
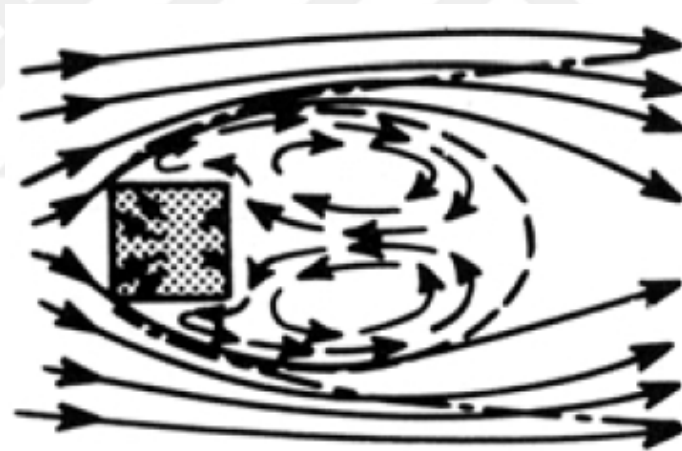
Figure 5.12. Plan view of wind flow around a building [48].

5.2.2. Flow Among Buildings

Urban geometry is one of the most important factors that affects wind in the streets. Thus, in an urban area wind flow pattern depends on spacing of buildings, street widths and building heights. Oke (1988) conducted the one of the first studies about the phenomenon, and specified three different flow pattern regimes by the way of building heights (H) and street widths along wind (W). The regimes are namely, isolated roughness flow, wake interference flow and skimming flow [49]. The flow regimes can be seen at the Figure 5.13.
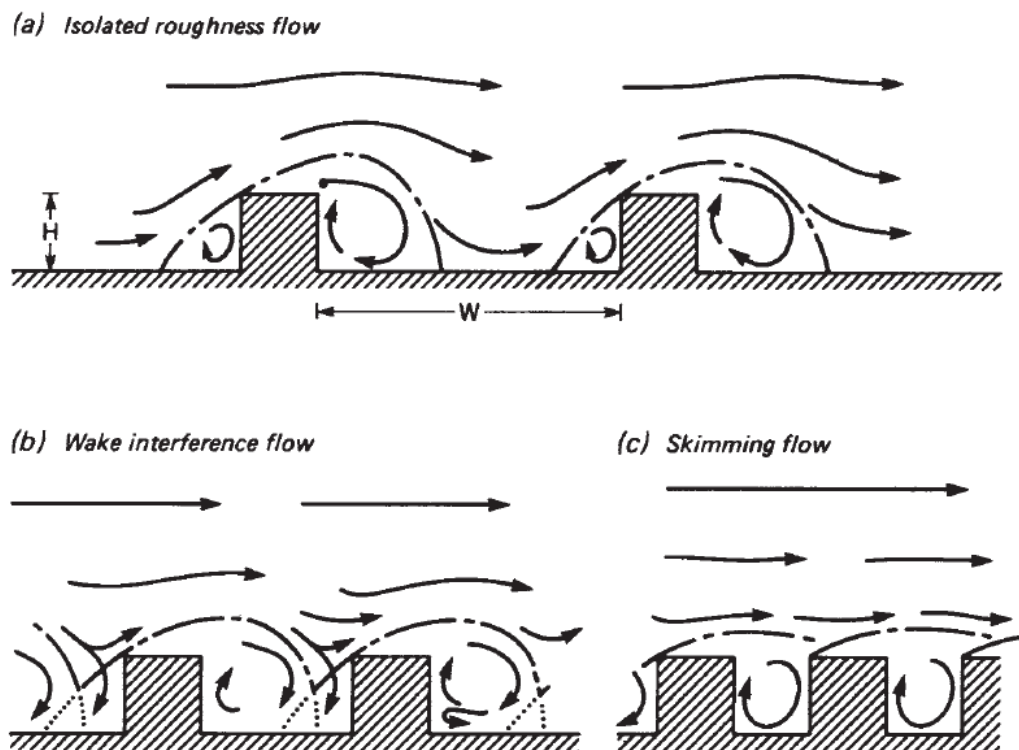
Figure 5.13. Three types of flow regimes [48].

If the spacing between the buildings are wide, in other words $H/W < 0.3$, flow behind the initial building do not affect the flow at the front of windward facade of the next building, hence the flow regime is termed as isolated roughness flow. In this regime, flow moves as the buildings are isolated obstacles.

When the street width has become narrower, wake zone behind the initial building affects the upward flow and stagnation point at the wind ward facade of the next building. This regime occurs at the $0.3 < H/W < 0.7$ conditions and named as wake interference flow.

At denser built areas, closely placed buildings exclude the main wind to flow through streets, hence large part of the wind cannot get into streets. This situation, creates a vortex in cavity zone between the successive buildings under the flow, hence the wind flow skims above the roof level. This type of flow regime is named as skimming flow and occurs while the $H/W > 0.7$.

Moreover, it can be thought that the street length (L) also has effects on the wind flow in the streets. However, length of street has a little effect on the flow regime types. The main driver on the transition between the flow regimes is the H/W ratio [49]. The effect of L/H and H/W ratios on the transition between flow regime types and thresholds of regime types are shown in the Figure 5.14.
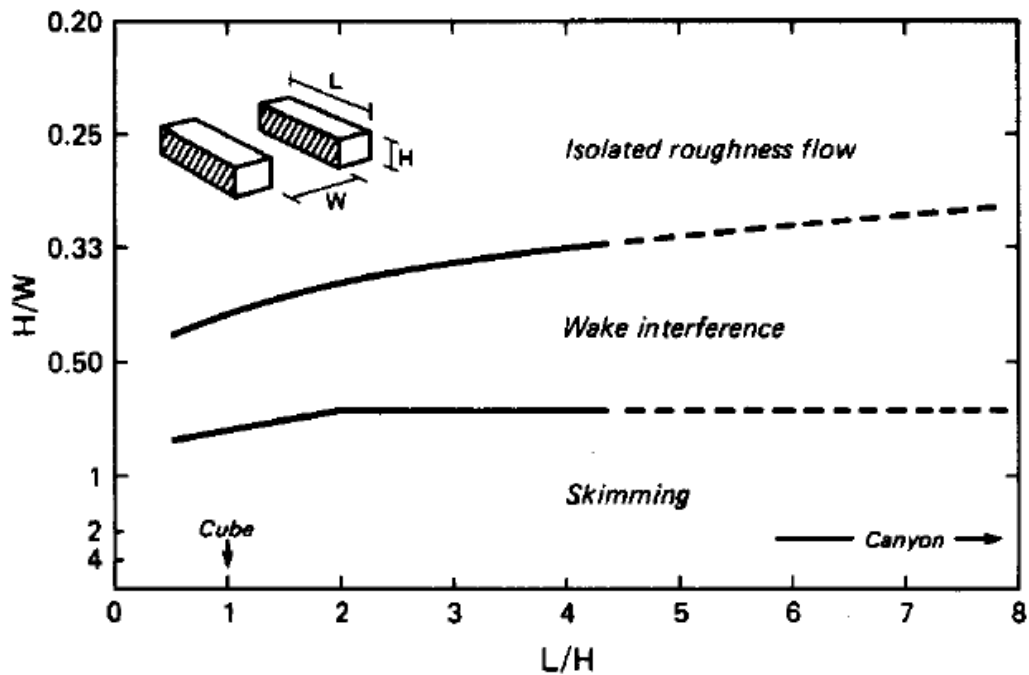
Figure 5.14. Treshold lines of flow regimes [49].

When the three flow regimes are considered, it can be said that the skimming flow is the worst scenario for streets by the means of natural ventilation. In the conditions of this flow regime, wind velocity in street is generally ten times lower than the main wind flow [50].

Nevertheless, urban areas are very complicated when they are compared to the described streets in the flow regime types. Also, the H/W ratios are not applicable to the real life in most of the cities. Wind flow at intersection of streets is another complex 3D issue that the 2D approach by the way of ratios would not be adequate [51].

5.3. Theoretical Background of Computational Fluid Dynamics Simulations

5.3.1. Governing Equations

Governing equations for fluid flow are Navier - Stokes or momentum equations and energy equation. The following equations are three dimensional mass, momentum and energy conservation equations for incompressible flows of Newtonian fluids in Cartesian coordinates. The governing partial differential equations can be written as below.

Continuity Equation:

$$\frac{\partial \rho}{\partial t} + \frac{\partial \rho u}{\partial x} + \frac{\partial \rho v}{\partial y} + \frac{\partial \rho w}{\partial z} = 0 \tag{5.1}$$

X-Momentum Equation:

$$\rho \frac{\partial u}{\partial t} + \rho u \frac{\partial u}{\partial x} + \rho v \frac{\partial u}{\partial y} + \rho w \frac{\partial u}{\partial z}$$

$$= \rho g_x - \frac{\partial p}{\partial x} + \frac{\partial}{\partial x}\left[2\mu \frac{\partial u}{\partial x}\right] + \frac{\partial}{\partial y}\left[\mu(\frac{\partial u}{\partial y} + \frac{\partial v}{\partial x})\right] + \frac{\partial}{\partial z}\left[\mu(\frac{\partial u}{\partial z} + \frac{\partial w}{\partial x})\right] + S_\omega + S_{DR} \tag{5.2}$$

Y-Momentum Equation:

$$\rho\frac{\partial v}{\partial t} + \rho u\frac{\partial v}{\partial x} + \rho v\frac{\partial v}{\partial y} + \rho w\frac{\partial v}{\partial z}$$

$$= \rho g_y - \frac{\partial p}{\partial y} + \frac{\partial}{\partial y}\left[2\mu\frac{\partial v}{\partial y}\right] + \frac{\partial}{\partial x}\left[\mu(\frac{\partial u}{\partial y} + \frac{\partial v}{\partial x})\right] + \frac{\partial}{\partial z}\left[\mu(\frac{\partial v}{\partial z} + \frac{\partial w}{\partial y})\right] + S_\omega + S_{DR}$$

$$(5.3)$$

Z-Momentum Equation:

$$\rho\frac{\partial w}{\partial t} + \rho u\frac{\partial w}{\partial x} + \rho v\frac{\partial w}{\partial y} + \rho w\frac{\partial w}{\partial z}$$

$$= \rho g_z - \frac{\partial p}{\partial z} + \frac{\partial}{\partial z}\left[2\mu\frac{\partial w}{\partial z}\right] + \frac{\partial}{\partial x}\left[\mu(\frac{\partial u}{\partial z} + \frac{\partial w}{\partial x})\right] + \frac{\partial}{\partial y}\left[\mu(\frac{\partial v}{\partial z} + \frac{\partial w}{\partial y})\right] + S_\omega + S_{DR}$$

$$(5.4)$$

Energy Equation at static temperature:

$$\rho C_p\frac{\partial T}{\partial t} + \rho C_p u\frac{\partial T}{\partial x} + \rho C_p v\frac{\partial T}{\partial y} + \rho C_p w\frac{\partial T}{\partial z}$$

$$= \frac{\partial}{\partial x}\left[k\frac{\partial T}{\partial x}\right] + \frac{\partial}{\partial y}\left[k\frac{\partial T}{\partial y}\right] + \frac{\partial}{\partial z}\left[k\frac{\partial T}{\partial z}\right] + q_V$$

$$(5.5)$$

In the equations, u is velocity component in x direction, v velocity component in y direction, and w velocity component in z direction. Also time is t, p is pressure, μ is viscosity, ρ is density and g_x, g_y and g_Z are gravitational acceleration in x, y, z directions in the partial differential equations. Last two terms in the momentum equations (5.2, 5.3 and 5.4) are, S_ω for rotating coordinates and S_{DR} for distributed resistances. At the energy equation, C_p is constant pressure for specific heat, k is thermal conductivity, q_V is volumetric heat source and T is temperature.

The momentum, continuity and energy equations represent following five terms, u, v, w, p and T as unknowns in five equations. Thus, they define fluid flow in steady-state conditions for Cartesian geometries [52].

5.3.2. Turbulent Flow

Turbulent flow is very important while simulating flow in urban areas with CFD. 3D time dependent continuity and Navier - Stokes equations can be applied to turbulent flow, yet because of the infinite number of time and length scales in turbulent flows, solution of these equations requires too many finite elements. Even solving a simple geometry creates finite elements on the order of 106 to 108, hence huge computer resources is needed. Thus, it would not be convenient to model turbulent flow of CFD simulations in this way.

To overcome this issue, governing partial differential equations (pde) are averaged over present scales. Thus, the most common approach for turbulent flow in CFD simulations, Reynolds - Averaged Navier - Stokes equations (RANS equations) are produced. In this thesis time averaged pdes are used by the way of Autodesk Simulation CFD program.

Time averaged equations are produced through presuming the dependent variables can be represented by superposition of a mean value and a fluctuating value, where the fluctuation is about the mean. By this way, x component of velocity can be produced as below.

$$u = U + u'$$

Where, U is mean velocity and u' is the fluctuation about the mean. Similarly governing equations are averaged over time. After that, capital letters represent the

mean values and lower case letters represent fluctuating values except temperature. Moreover, momentum equations also get new terms. The averaged governing pdes can be written as below.

Continuity Equation:

$$\frac{\partial \rho}{\partial t} + \frac{\partial \rho U}{\partial x} + \frac{\partial \rho V}{\partial y} + \frac{\partial \rho W}{\partial z} = 0 \tag{5.1}$$

X-Momentum Equation:

$$\rho \frac{\partial U}{\partial t} + \rho U \frac{\partial U}{\partial x} + \rho V \frac{\partial U}{\partial y} + \rho W \frac{\partial U}{\partial z} = \rho g_x - \frac{\partial P}{\partial x} + S_{DR} + S_\omega +$$

$$\frac{\partial}{\partial x}\left[2\mu\frac{\partial U}{\partial x} - \rho uu\right] + \frac{\partial}{\partial y}\left[\mu(\frac{\partial U}{\partial y} + \frac{\partial V}{\partial x}) - \rho uv\right] + \frac{\partial}{\partial z}\left[\mu(\frac{\partial U}{\partial z} + \frac{\partial W}{\partial x}) - \rho uw\right]$$

$$\tag{5.6}$$

Y-Momentum Equation:

$$\rho \frac{\partial V}{\partial t} + \rho U \frac{\partial V}{\partial x} + \rho V \frac{\partial V}{\partial y} + \rho W \frac{\partial V}{\partial z} = \rho g_y - \frac{\partial P}{\partial y} + S_{DR} + S_\omega +$$

$$\frac{\partial}{\partial y}\left[2\mu\frac{\partial V}{\partial y} - \rho vv\right] + \frac{\partial}{\partial x}\left[\mu(\frac{\partial U}{\partial y} + \frac{\partial V}{\partial x}) - \rho uv\right] + \frac{\partial}{\partial z}\left[\mu(\frac{\partial V}{\partial z} + \frac{\partial W}{\partial y}) - \rho vw\right]$$

$$\tag{5.7}$$

Z-Momentum Equation:

$$\rho \frac{\partial W}{\partial t} + \rho U \frac{\partial W}{\partial x} + \rho V \frac{\partial W}{\partial y} + \rho W \frac{\partial W}{\partial z} = \rho g_z - \frac{\partial P}{\partial z} + S_{DR} + S_\omega +$$

$$\frac{\partial}{\partial z}\left[2\mu\frac{\partial W}{\partial z} - \rho ww\right] + \frac{\partial}{\partial x}\left[\mu(\frac{\partial U}{\partial x} + \frac{\partial W}{\partial x}) - \rho uw\right] + \frac{\partial}{\partial y}\left[\mu(\frac{\partial V}{\partial z} + \frac{\partial W}{\partial y}) - \rho vw\right]$$

$$\tag{5.8}$$

Energy Equation:

$$\rho C_p \frac{\partial T}{\partial t} + \rho C_p U \frac{\partial T}{\partial x} + \rho C_p V \frac{\partial T}{\partial y} + \rho C_p W \frac{\partial T}{\partial z}$$

$$= \frac{\partial}{\partial x}\left[k\frac{\partial T}{\partial x} - \rho C_p uT'\right] + \frac{\partial}{\partial y}\left[k\frac{\partial T}{\partial y} - \rho C_p vT'\right] + \frac{\partial}{\partial z}\left[k\frac{\partial T}{\partial z} - \rho C_p wT'\right] + q_V$$

(5.9)

The extra terms, ρuu, ρuv, ρuw, ρvv, ρvw, ρww, $\rho C_p uT'$, $\rho C_p vT'$, $\rho C_p wT'$ are produced in momentum and energy equations because of averaging. The extra terms in momentum pdes are called Reynold Stress Terms.

After the addition of extra terms, the situation has changed to five equations and 14 unknowns. At a point, this closure problem should be handled by relating these extra terms to previous unknowns. Thus, the closure problem is solved by turbulence models [53].

5.3.3. Standard $k - \varepsilon$ Turbulence Model

The $k - \varepsilon$ is the most common turbulence model in CFD for simulating characteristics of turbulent flows and also used in this thesis. This is a two equation turbulence model and provide description of the turbulence through two transport pdes, which give kinetic energy K and turbulent energy dissipation ε. Eddy viscosity and eddy conductivity for the pdes can be calculated by the following Equations 5.10 and 5.11.

Eddy Viscosity:

$$\mu_t = C_\mu \rho \frac{K^2}{\varepsilon}$$

(5.10)

Eddy Conductivity:

$$k_t = \frac{\mu_t C_p}{\sigma_t} \tag{5.11}$$

Where, σ_t represents turbulent Prandt number and generally taken as 1.0 and C_μ is an empirical constant and its value is 0.09. Transport equations for K and ε are derived by the using moments of momentum equations. The transport pdes for $k - \varepsilon$ turbulence model can be written as following equations.

Turbulent Kinetic Energy (TKE) Equation:

$$\rho\frac{\partial K}{\partial t} + \rho U\frac{\partial K}{\partial x} + \rho V\frac{\partial K}{\partial y} + \rho W\frac{\partial K}{\partial z}$$

$$= \frac{\partial}{\partial x}\left[(\frac{\mu_t}{\sigma_K})\frac{\partial K}{\partial x}\right] + \frac{\partial}{\partial y}\left[(\frac{\mu_t}{\sigma_K})\frac{\partial K}{\partial y}\right] + \frac{\partial}{\partial z}\left[(\frac{\mu_t}{\sigma_K})\frac{\partial K}{\partial z}\right] - \rho\varepsilon$$

$$+\mu_t\left[2(\frac{\partial U}{\partial x})^2 + 2(\frac{\partial V}{\partial y})^2 + 2(\frac{\partial W}{\partial z})^2 + (\frac{\partial U}{\partial y} + \frac{\partial V}{\partial x})^2 + (\frac{\partial U}{\partial z} + \frac{\partial W}{\partial x})^2 + (\frac{\partial V}{\partial z} + \frac{\partial W}{\partial y})^2\right]$$

$$\tag{5.12}$$

Turbulent Energy Dissipation (TED) Equation:

$$\rho\frac{\partial \varepsilon}{\partial t} + \rho U\frac{\partial \varepsilon}{\partial x} + \rho V\frac{\partial \varepsilon}{\partial y} + \rho W\frac{\partial \varepsilon}{\partial z}$$

$$= \frac{\partial}{\partial x}\left[(\frac{\mu_t}{\sigma_\varepsilon})\frac{\partial \varepsilon}{\partial x}\right] + \frac{\partial}{\partial y}\left[(\frac{\mu_t}{\sigma_\varepsilon})\frac{\partial \varepsilon}{\partial y}\right] + \frac{\partial}{\partial z}\left[(\frac{\mu_t}{\sigma_\varepsilon})\frac{\partial \varepsilon}{\partial z}\right] - C_2\rho\frac{\varepsilon^2}{K}$$

$$+C_1\mu_t\frac{\varepsilon}{K}\left[2(\frac{\partial U}{\partial x})^2 + 2(\frac{\partial V}{\partial y})^2 + 2(\frac{\partial W}{\partial z})^2\right]$$

$$+C_1\mu_t\frac{\varepsilon}{K}\left[(\frac{\partial U}{\partial y} + \frac{\partial V}{\partial x})^2 + (\frac{\partial U}{\partial z} + \frac{\partial W}{\partial x})^2 + (\frac{\partial V}{\partial z} + \frac{\partial W}{\partial y})^2\right]$$

$$\tag{5.13}$$

In the TKE and TED equations, σ_K and σ_ε are turbulent Schmidt numbers and their values are 1.0 and 1.3 respectively. C_1 and C_2 are empirical constants and their values are 1.44 and 1.92 respectively. With these last two equations, the closure problem is solved. There are nine unknowns; U, V, W, p, T, μ_t, k_t, K, ε and nine equations [54].

5.4. CFD Simulation

Autodesk CFD 2019, which is a software that provides computational fluid dynamics simulation tools, is used for the running CFD simulations in this thesis. Before stepping up to the simulation, the model drawings must be prepared for the software. For this issue, models are edited by the way of following Autodesk CFD 2019's guidelines.

First, a volume that surrounds the model must be built. The recommended dimensions which are related to the model dimensions can be seen at the following two figures below [55].
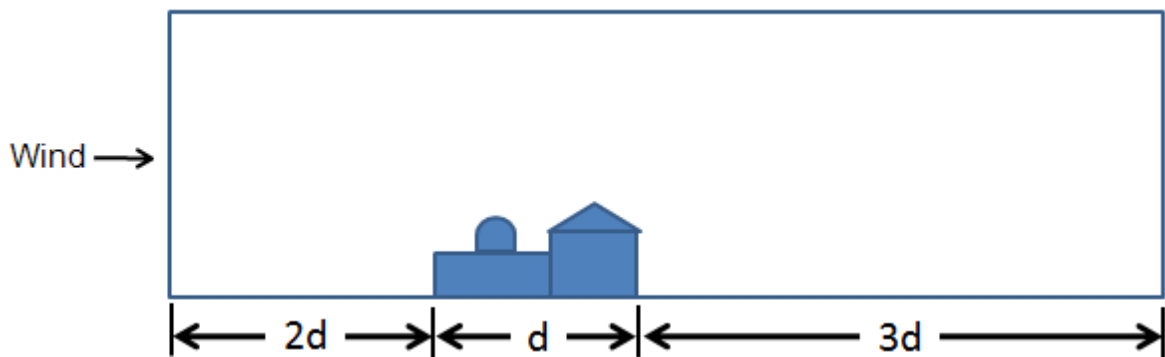
Figure 5.15. Surrounding volume, lateral section [55].
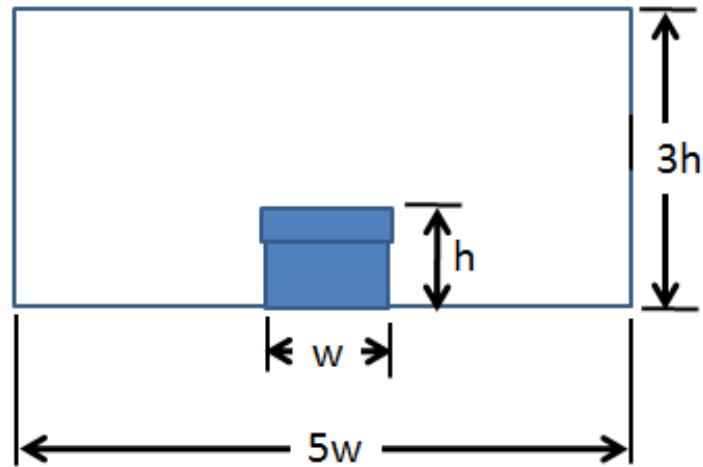
Figure 5.16. Surrounding volume, frontal section [55].

As illustrated in the Figure 5.15 and Figure 5.16, the surrounding volume should be six times of the original model at lateral section, five times at frontal section and the volume's height should be three times of the model. In addition, Autodesk CFD 2019 recommends that the creation of the volume in a CAD software, hence the surrounding volume and model's ground plane can be coplanar [55]. To meet these guidelines and recommendations, model drawings that are edited in AutoCAD, which is one of the most popular CAD softwares and widely used in industry.

For the beginning of model editing phase, the model drawings are imported to AutoCAD from SketchUP files. Models' surrounding volumes are constructed in this CAD software with reliance according to the guidelines. Following that, the edited models are exported as SAT file types for providing compatibility with the Autodesk CFD 2019. An example of the edited model within its surrounding volume in AutoCAD can be seen at the following Figure 5.17.

Next, the SAT file which consists the model's final state is imported to the Autodesk CFD 2019, hence the domain is generated. In the CFD simulation software, first
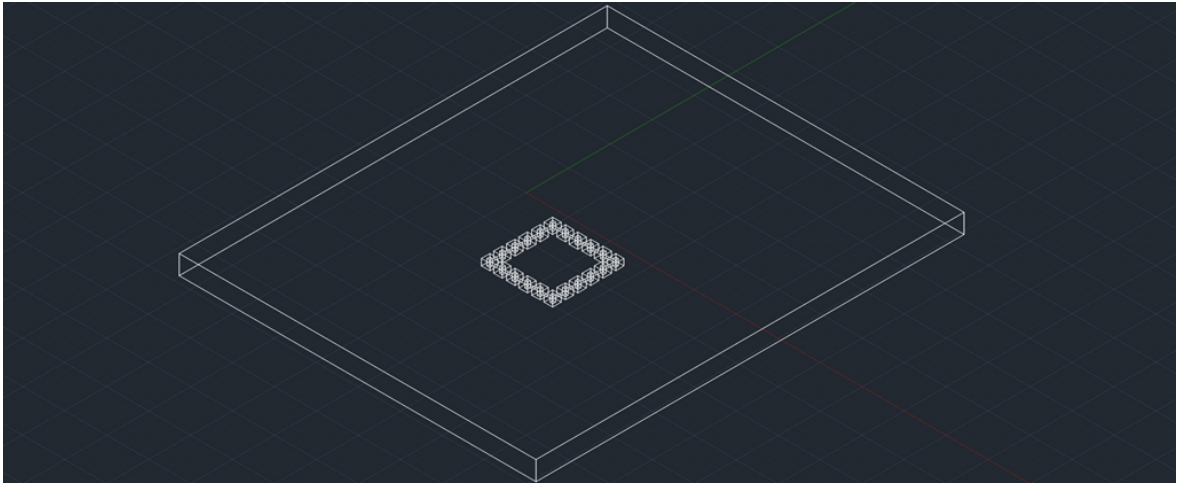
Figure 5.17. First alternative in its surrounding volume.

of all, materials are assigned to the parts of the model. Air is assigned to all regions of the surrounding volume and concrete is selected and assigned to the buildings due to the current building stock of study area. Figure 5.18 shows the situation of the model at this step.
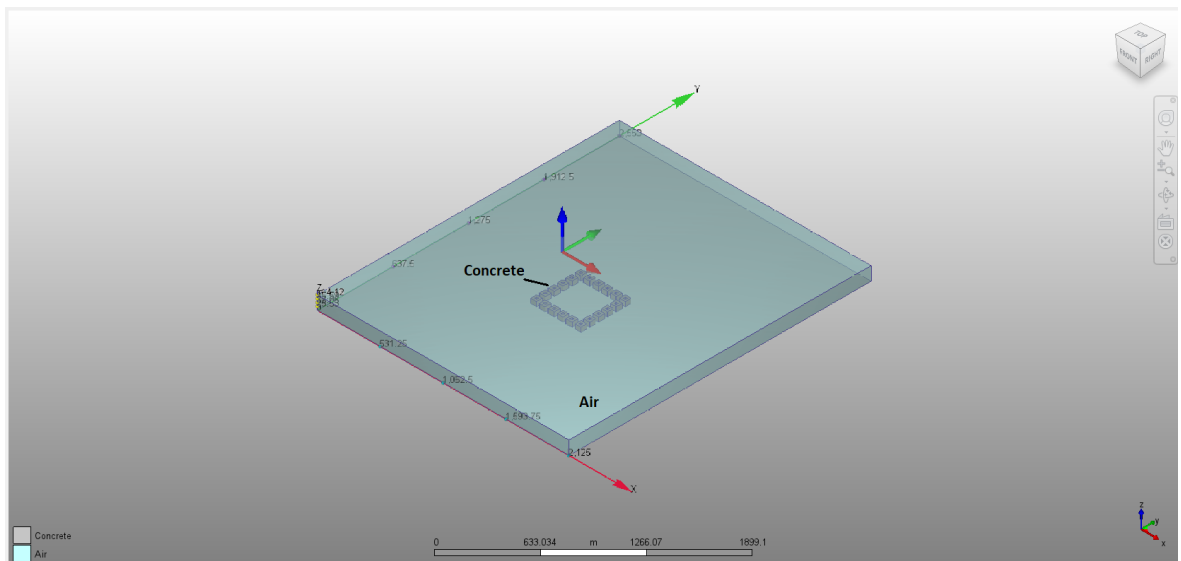
Figure 5.18. First alternative after assigning the materials.

After the materials, boundary conditions must be applied to the model. At this point, wind speed and wind direction become significant. For the study in this thesis, average wind speed and wind direction data of last 36 years for Istanbul is used. The average wind speed between January 1982 and December 2018 for Istanbul is 16.2 kph which equals to 4.5 m/s and can be seen at the Figure 5.19 with averaged annual wind speeds through the same years. Also, Istanbul experienced wind mostly from northeast and north directions with the rate of 30% and 28% respectively between the January 1982 and December 2018. The rate of wind directions that affect the Istanbul is illustrated at Figure 5.20 [56].

Wind-force per Day (January 1982 - December 2018)

Jan	Feb	Mar	Apr	May	Jun	
17.2	**17.2**	**16.1**	**14.4**	**14.3**	**14.5**	[kph]
95	97	97	97	97	97	Data availability[%]

Jul	Aug	Sep	Oct	Nov	Dec	
17.3	**18.2**	**15.8**	**15.8**	**15.7**	**17.8**	[kph]
97	97	99	99	99	99	Data availability[%]

Averaged Value (January 1982 - December 2018) : **16.2 kph**

Figure 5.19. Averaged wind speed for Istanbul [56].

Wind-direction (January 1982 - December 2018)

N	28 %
NE	30 %
E	8 %
SE	3 %
S	7 %
SW	14 %
W	5 %
NW	4 %
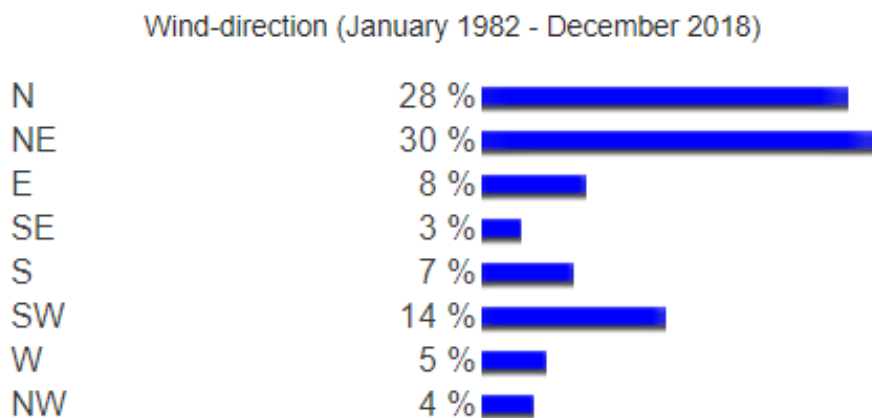
Figure 5.20. Wind directions for Istanbul [56].

At the light of these, CFD simulation of five alternatives' and Mecidiyeköy's models are conducted for the wind speed of 4.5 m/s in both north and northeast directions. For defining wind velocity in the simulations, wind speed is applied to the inlet side of the domain as velocity boundary condition. Also zero static gauge pressure is applied to the outlet side of the domain to make outlet pressure equal to atmospheric pressure. On the other hand, slip/symmetry boundary condition is applied to the top and sides of the domain. Slip/symmetry boundary condition lets the fluid to flow along the domain and prevents fluid to stop at walls of the domain. In addition, Autodesk CFD recommends to assign slip/symmetry boundary conditions when simulating a free space environment like the study in this thesis. Moreover, there is not any boundary condition applied to the ground of the domain due to the fact that the air does not move along the ground [55, 57]. Figure 5.21 illustrates the boundary conditions, also the model of first alternative after applying the boundary conditions can be seen at the Figure 5.22.
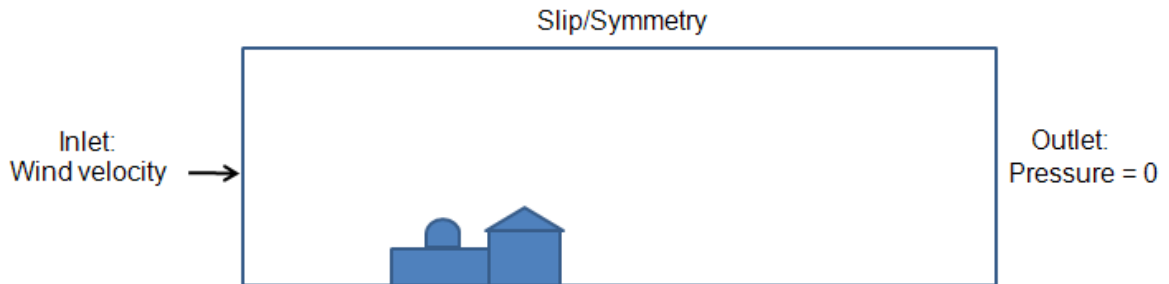
Figure 5.21. Applied boundary conditions to the domain [55].

Next step after assigning the boundary conditions is meshing of the domain. Meshing is an important phase in the CFD simulations, because it directly affects both convergence of solution and accuracy of the results. For providing these necessities, elements of the mesh must cover the model's geometry meticulously. Gaps or edges that occur in the meshing phase should be avoided.

For the study in this thesis, mesh of the model should be suitable to solve the wind flow. The regions of the domain where host the wakes, vortexes and separation
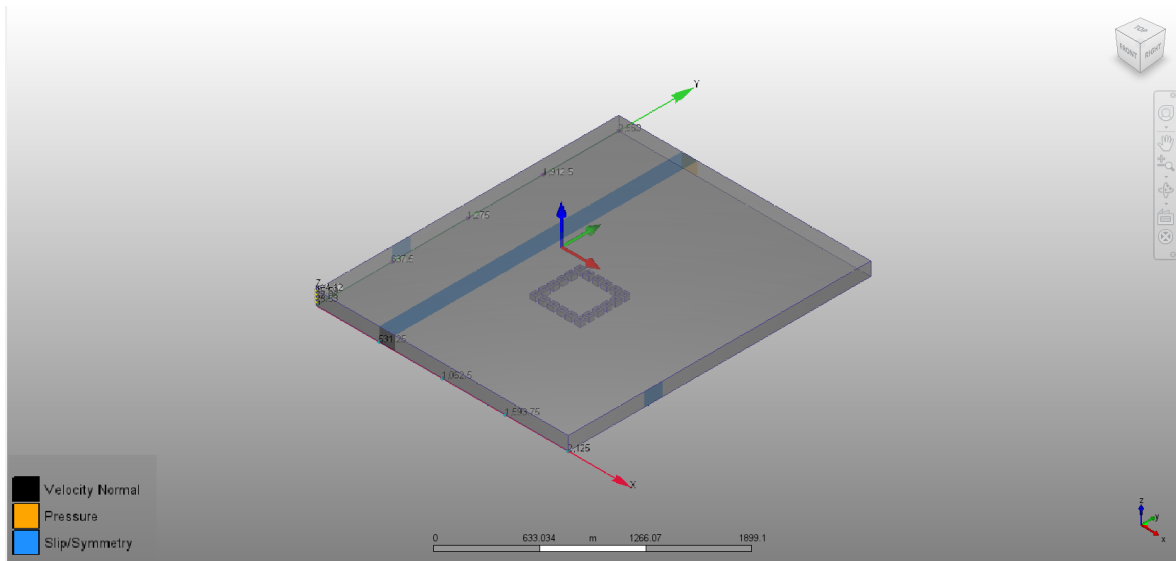
Figure 5.22. First alternative after assigning the boundary conditions.

regions of the flow requires fine mesh, hence coarse mesh elements in these regions of the domain may not be able to cover the model correctly or can create flaws in the mesh depending on the geometry. Owing to that, mesh distribution should be defined for peculiar needs of the regions in the domain. This kind of mesh distribution would also be efficient by the means of convergence time and accuracy of the results [55].

At the light of these, automatic meshing feature of Autodesk CFD 2019 is used for creating meshes of the models in this study. Automatic meshing feature of the simulation program has benefits as following. First, the mesh distribution is created more efficiently, the mesh is fine at required regions of the domain and coarse at where it can be. Second, solution accuracy increases as a result of better mesh quality and mesh transition. Third, proper mesh transition makes the solution more robust due to a well-posed mathematical model [58]. Defined mesh of the first alternative as an example to the outcome of automatic meshing can be seen at the Figure 5.23. At the end of meshing step, meshes that have elements up to 1.1 million are created for the models.
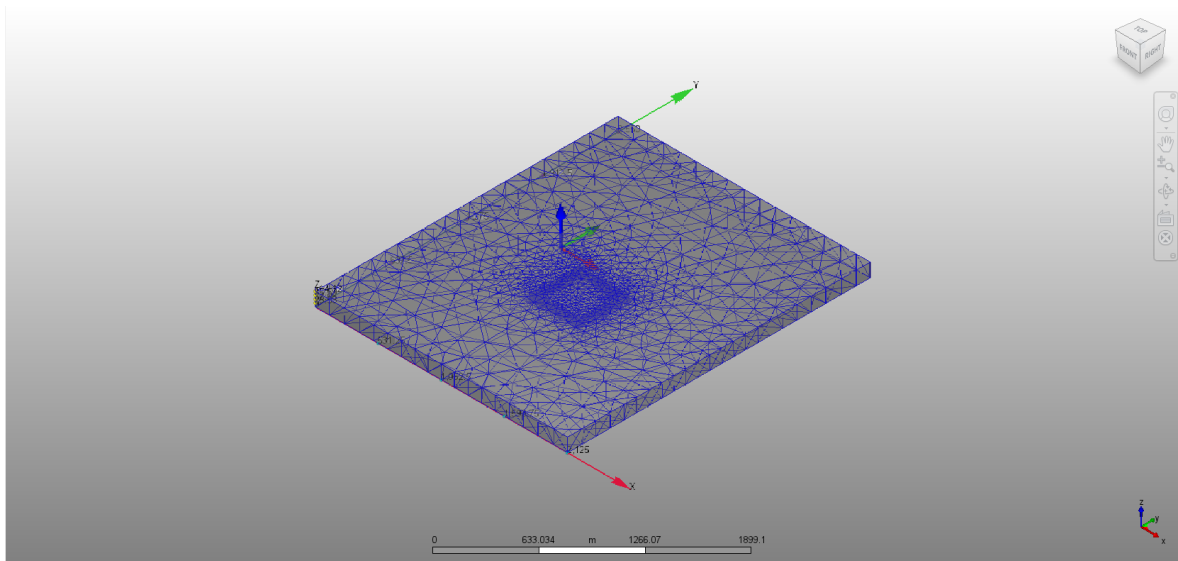
Figure 5.23. Mesh of the first alternative's domain.

At this point, there are few applications are left for completing the model. To begin with, the turbulence model for the simulation should be chosen. There are various turbulence models that can be used in the CFD simulations, yet most of them are not convenient for the wind flow studies as in this thesis. For instance, SST $k - \omega$ model is predicted the flow pattern wrong in a wind flow study [59]. This model is recommended to use in external aerodynamics studies and requires a very fine mesh [60].

Furthermore, Low Reynolds number $k - \varepsilon$ turbulence model can be used for the low speed turbulent flows which have Reynolds number from 1500 to 5000. However, this model is not stable as the Standard $k - \varepsilon$ model and also needs more iterations to converge, which increases the computational cost [60, 61].

On the other hand, RNG turbulence model is also used in the wind flow studies with the notion of getting more accurate results when compared to Standard $k - \varepsilon$ model despite its computational costs. Nevertheless, it is found that the RNG turbulence model predicts wrong wind flow patterns in streets, where the Standard $k - \varepsilon$ turbulence model predicts accurate wind flows [50].

With these in mind, Standard $k - \varepsilon$ turbulence model is used in the study in the thesis. This model is considered as the default turbulent model and works well in most of the CFD simulations [60]. Selection of the turbulence model in solve tab of the Autodesk CFD 2019 is shown at the Figure 5.24.
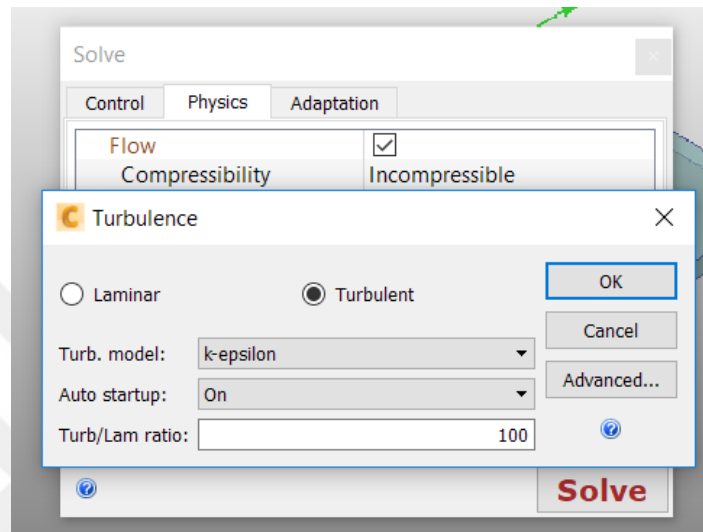
Figure 5.24. Selection of the turbulence model.

Also the selection of incompressible flow for the simulation owing to the lower Mach number than 0.3 can also be seen at the Figure 5.24 [62].

At the end, defining number of iterations to run is the last option before running the CFD simulation. In the Autodesk CFD 2019, 750 is the maximum number of the iterations that can be run at a time. The simulation stops at the end of 750 iterations or when the solution converges, whichever happens first [55]. Thus, the simulations for the study in this thesis is run for 750 iterations in the program, yet all of them converged before reaching the maximum iteration number and definition in the program can be seen at the Figure 5.25.
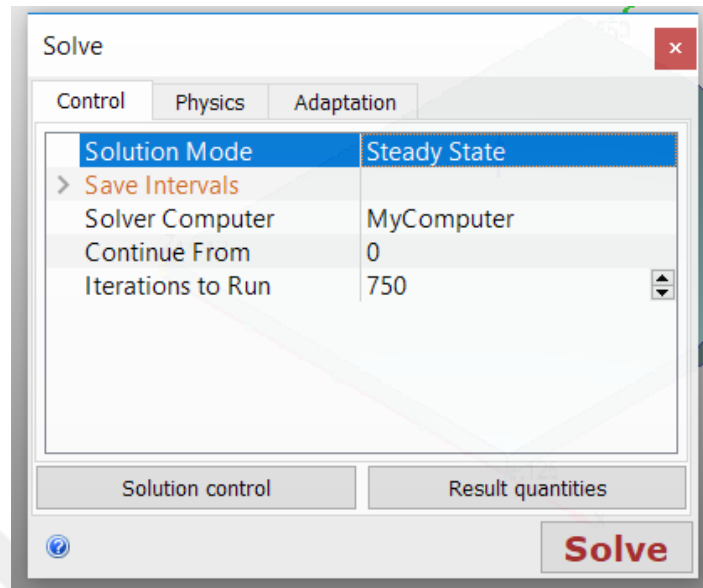
Figure 5.25. Definition of number of iterations to run.

5.5. Calculation of Average Wind Speed

Average wind speed calculations are based on the results of CFD simulations. These calculations are used to get apparent temperatures for the study in this thesis.

Average wind speeds for models are calculated by the way of result planes of Autodesk CFD 2019, which can be created at any level of the model's domain. The result planes can be used to visualize the results of CFD simulations and also can be used to export wind speed results of CFD simulations at any desired level in the domain. Three result planes are created at 2 meters, 10 meters and 50 meters above the ground for each model in this study. An example for result planes can be seen at the Figure 5.26.

For calculating the average wind speed, wind speed results of each point on the desired result plane are exported. However, the buildings are disabled in the result planes before exporting the node results to avoid zero values. In addition, side parts of the building area on the result plane at long direction also neglected in calculations
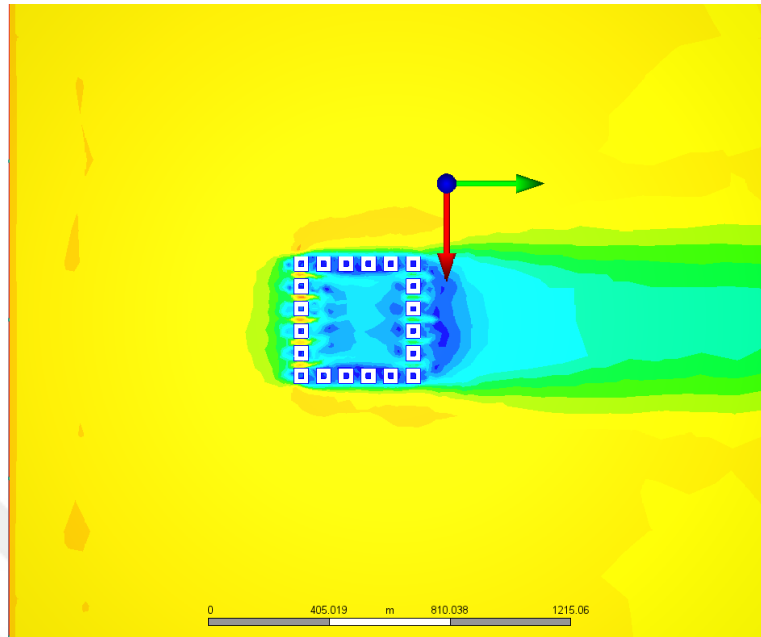
Figure 5.26. An example to result planes from first alternative.

because these parts have similar values. After that, average wind speed calculations are conducted at remained region on the result planes, where the buildings' effect on wind flow is the most. An example to the areas that used at average wind speed calculations on the result planes illustrated between black lines in the Figure 5.27. Calculated average wind speed is the average of wind speed results of exported nodes in this area.

5.6. Calculation of Apparent Temperature

Apparent temperature is the perceived temperature, which is derived from the combination of temperature, relative humidity, radiation and wind speed [63, 64]. The phenomenon was invented in the late 1970s and sun and wind effects also included to calculations in 1980s [65].

In the study of this thesis, focus is the cooling effect of wind for thermal comfort. Thus the calculation of apparent temperature is based on the combination of
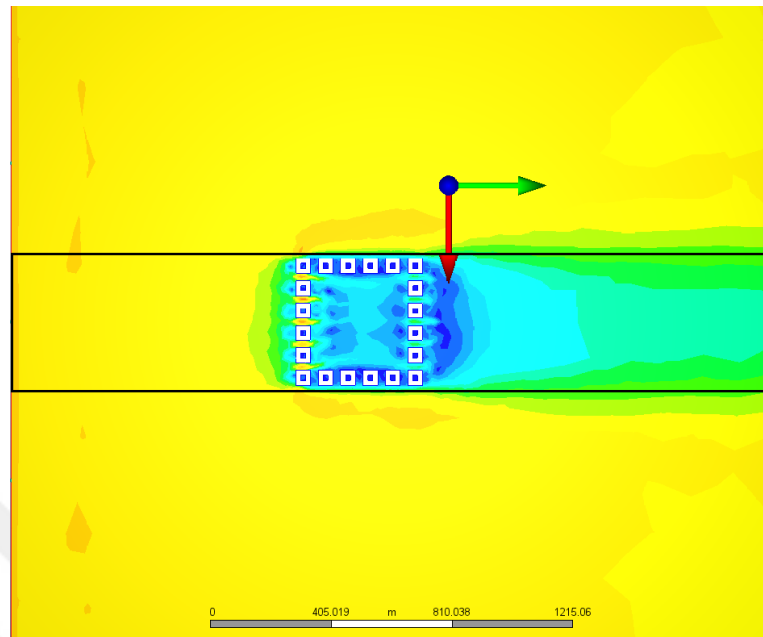
Figure 5.27. An example to the areas that used at average wind speed calculations on result planes.

temperature and wind speed, hence apparent temperature has become a measure of wind chill [65]. Wind chill can be described as cooling effect of the wind on the skin. This cooling effect occurs due to air motion. The air motion increases the heat loss from skin to atmosphere by the means of convection [66].

There are various approaches to wind chill calculation, yet most of them are designed for cold temperatures. For instance, a model that named as Wind Chill Index was used in the North America until the year of 2001. In this model, wind chill temperature and apparent temperature is considered equal for the wind speeds between 0 and 4 mph, hence the wind speeds less than 5 mph creates a warming effect and the model creates misconceptions on people's minds [67, 68]. Furthermore, North American wind chill model, which implemented in the year of 2001 by United States, Canada and United Kingdom is only defined for the temperature of 50 °F or 10 °C and below. Also, the wind speed should be more than 3 mph for using the model [69, 70]. Aim of these kind of models are preventing people from frostbite.

On the other hand, Steadman published an apparent temperature model in 1994, which can be used in hot and cold temperatures. The variables in the Steadman apparent temperature model are, temperature, humidity, wind speed and external solar radiation. Furthermore, in subsequent publication of Steadman in the year of 1998, wind chill calculation is separated from the apparent temperature model and variables are reduced to two, temperature and wind speed. This new equation is named as Steadman wind chill. When the complex Steadman apparent temperature and Steadman wind chill are compared, rounded difference between the results of equations is not more than 1 °C [68]. The Steadman wind chill equation used in this thesis can be written in metric units as following Equation 5.14. Where, V is wind speed in m/s and T is air temperature in Celsius.

$$Wind\ Chill_{SC} = 1.41 - 1.162V + 0.980T + 0.0124V^2 + 0.185(VT) \qquad (5.14)$$

6. RESULTS

6.1. Wind Simulation Results When Wind Blows from North Direction

In this section, wind simulation results of Mecidiyeköy and five alternatives can be found when the wind blows from north. With the help of result planes, simulation results are illustrated by the way of figures for each model at two meters for pedetsrian level, 10 meters for height of an ordinary flat and 50 meters for representing the situation above the buildings. Furthermore, average wind speeds at these three elevations are summarized in tables for alternatives. At all figures, wind flows through left hand side to right hand side. Legends on top left corner of each figure indicates the velocity of the result plane by colors. Velocity increases from dark blue to red.

6.1.1. Results of Mecidiyeköy at Northern Wind
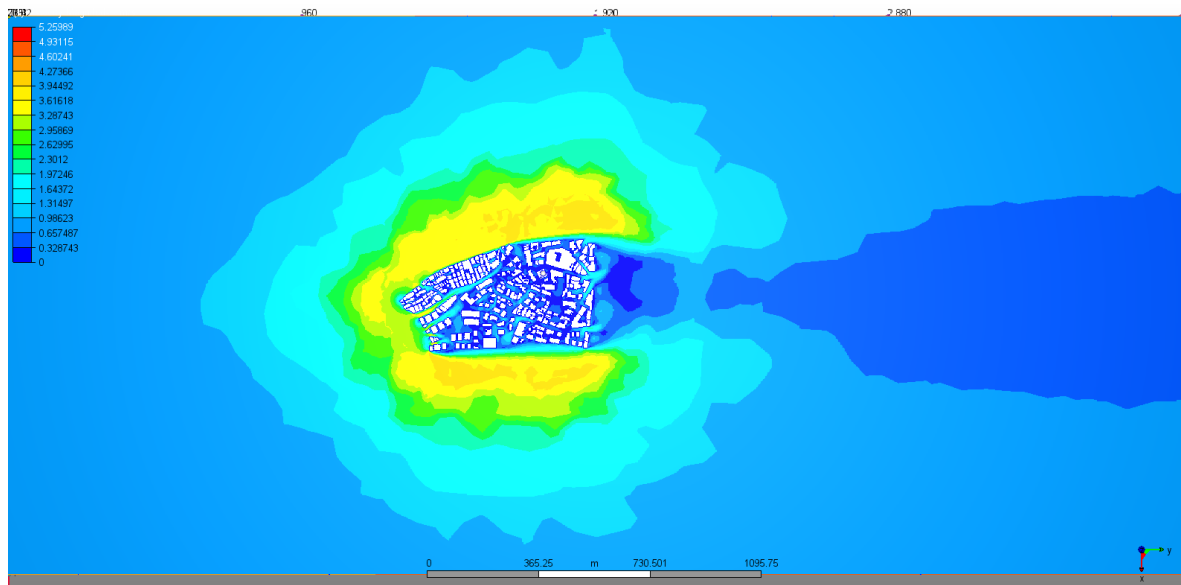
Figure 6.1. Result plane of Mecidiyeköy, 2 meters above the ground at northern wind.
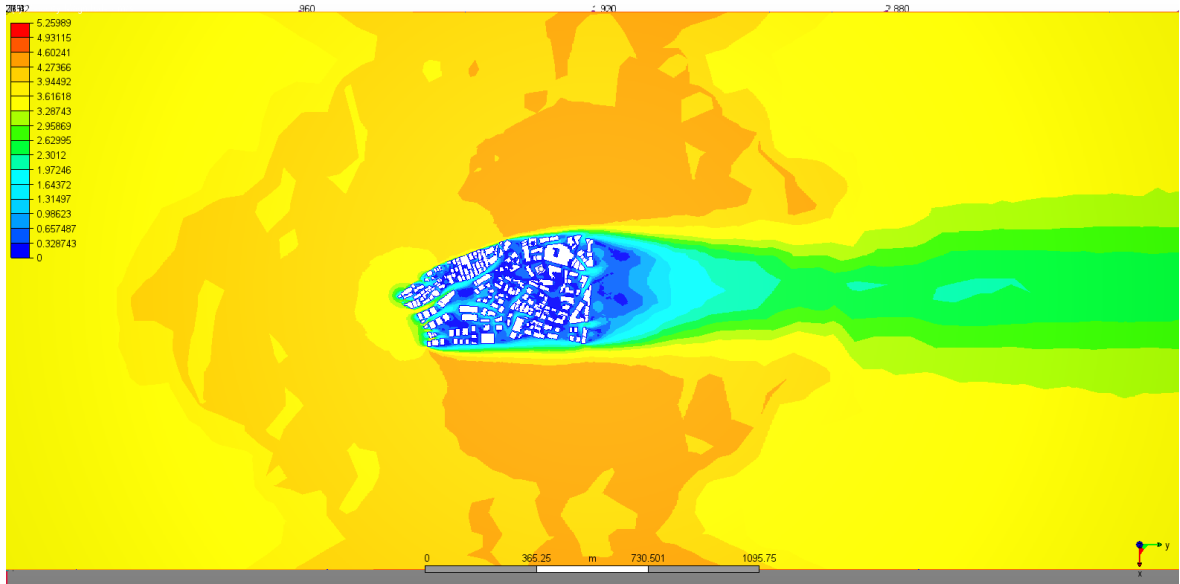
Figure 6.2. Result plane of Mecidiyeköy, 10 meters above the ground at northern wind.

Figure 6.3. Result plane of Mecidiyeköy, 50 meters above the ground at northern wind.

Table 6.1. Average wind speeds of Mecidiyeköy at northern wind.

	At 2 m.	**At 10 m.**	**At 50 m.**
Average Wind Speed (m/s)	0.96	2.82	4.00

When the wind blows from north, it is obvious that the wind flow is restricted among buildings and streets. The situation is even more drastic at the pedestrian level. When the result plane at two meters is taken into account, it can be seen that most of the street canyons are in the tones of dark blue which indicates almost zero velocity. As a result of irregular urbanization, streets cannot ventilate themselves by wind. After stepping to the result plane at 10 meters above the ground, the situation of inner streets mostly do not change. Still the wind velocity at the streets are close to zero. However, due to the absence of buildings less than 10 meters, some regions experience less restricted wind flow. Moreover, the result plane at 50 meters shows that effect of the buildings on wind flow continues even they do not reach that height.

6.1.2. Results of First Alternative at Northern Wind

Figure 6.4. Result plane of first alternative, 2 meters above the ground at northern wind.

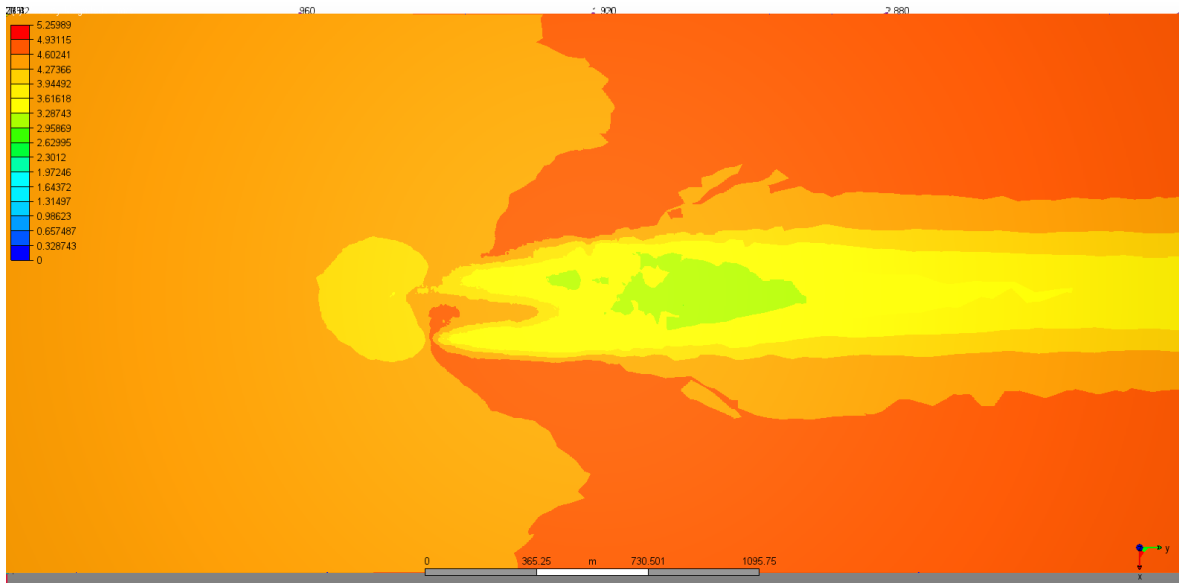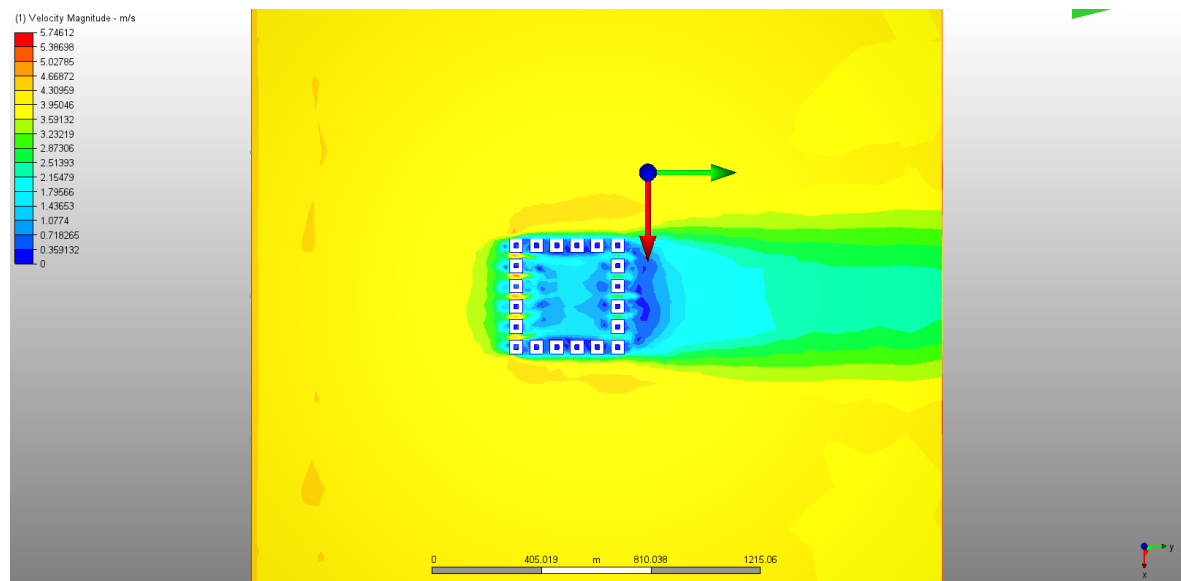Figure 6.5. Result plane of first alternative, 10 meters above the ground at northern wind.

Figure 6.6. Result plane of first alternative, 50 meters above the ground at northern wind.

Table 6.2. Average wind speeds of first alternative at northern wind.

	At 2 m.	At 10 m.	At 50 m.
Average Wind Speed (m/s)	2.74	3.03	3.81

This model has two distinguishing features that differs it from the other alternatives. First, the courtyards in the middle of each building. Second, the biggest park among the alternatives that surrounded by the buildings. When looking to the result plane at two meters above the ground, the big difference from the Mecidiyeköy can be seen at first glance. Furthermore, the quantative difference between two models is also big. Average wind speed of the first alternative is almost triple of the Mecidiyeköy at pedestrian level. Due to the design of this model low wind velocity in the courtyards and between the buildings perpendicular to the wind flow is expected, yet the result of these regions are still not bad as the streets of the Mecidiyeköy. On the other hand, reduced wind velocity at the park is also an expected fact as a result of Venturi effect. However, the wind velocity trend at the park is around 1.5 to 2 (m/s). When the second result plane at 10 meters is taken into account, increasing wind velocity at the courtyards and between the buildings perpendicular to the wind flow can be seen. Moreover, at the last result plane at 50 meters above the ground, there are no buildings cutting the plane. Thus, the effect of the buildings after their height also continues, yet this time it is not as sharp as the Mecidiyeköy's model.

6.1.3. Results of Second Alternative at Northern Wind

Figure 6.7. Result plane of second alternative, 2 meters above the ground at northern wind.
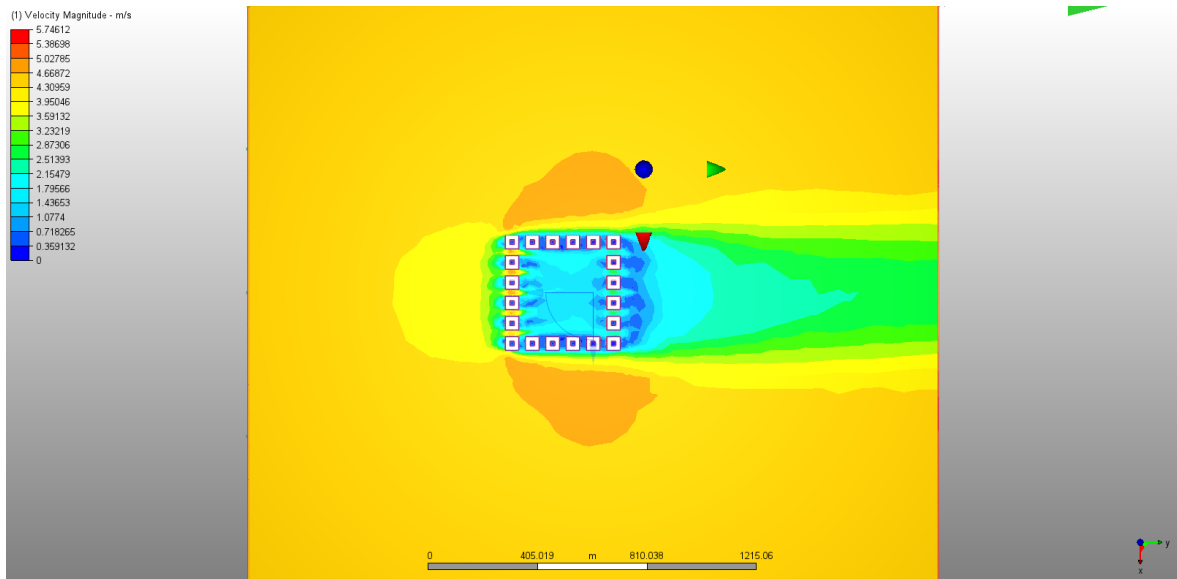

Figure 6.8. Result plane of second alternative, 10 meters above the ground at northern wind.
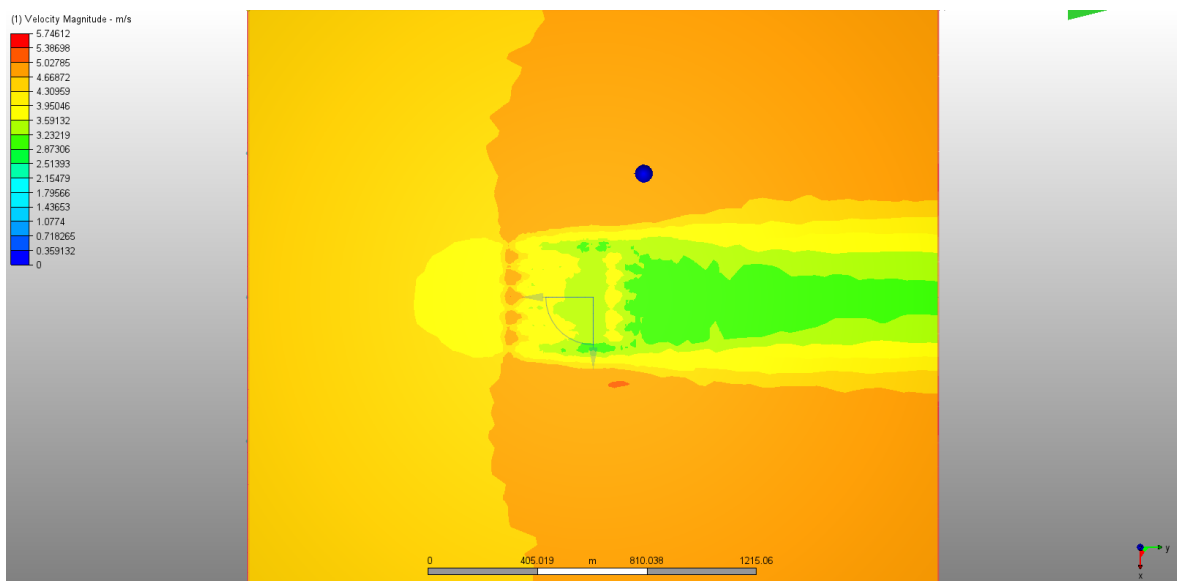
Figure 6.9. Result plane of second alternative, 50 meters above the ground at northern wind.

Table 6.3. Average wind speeds of second alternative at northern wind.

	At 2 m.	At 10 m.	At 50 m.
Average Wind Speed (m/s)	1.60	2.94	3.79

This alternative is similar to the first alternative. As the first one this model also have a park that surrounded by the buildings. However, number of the buildings are more than the first alternative. At the result plane at two meters of second alternative, it is obvious that the wind velocity is lower than the first alternative. Velocities at the park, between the buildings perpendicular to the wind flow and streets between the building rows are low. However, the average wind velocity of the model is still noticeably better than the Mecidiyeköy at pedestrian level. When looking at the plane at 10 meters, it can be seen that the wind velocitiy increases at the park, betwenn buildings perpendicular to the wind flow and, streets between the building rows. Moreover, the plane at 50 meters shows that the effect of buildings after their height and it is more than the first alternative, yet similar to the Mecidiyeköy due to number of buildings.

6.1.4. Results of Third Alternative at Northern Wind
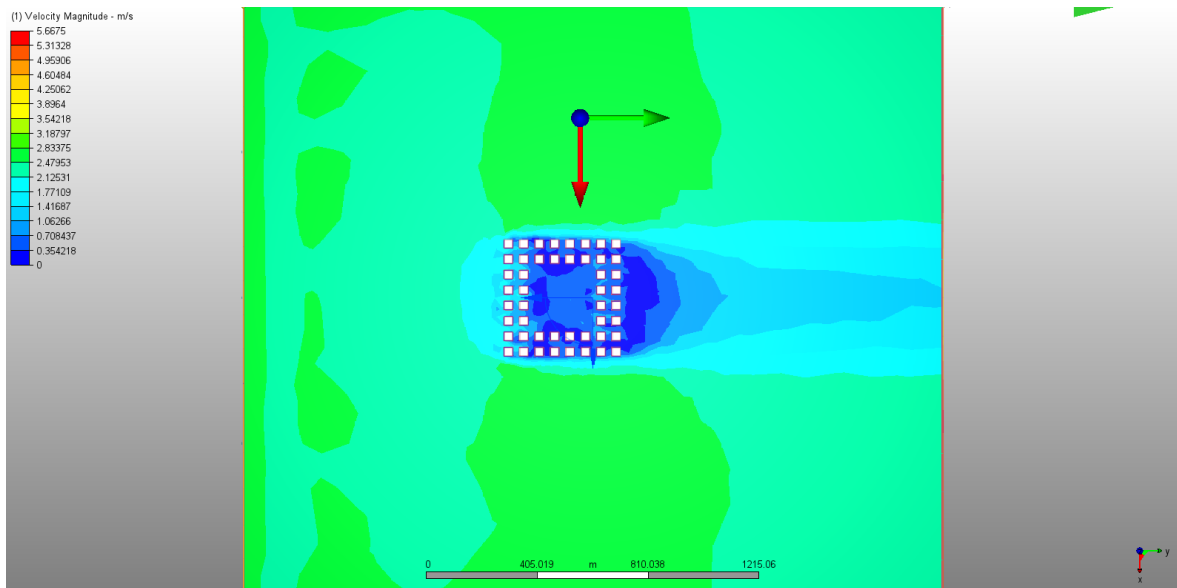

Figure 6.10. Result plane of third alternative, 2 meters above the ground at northern wind.
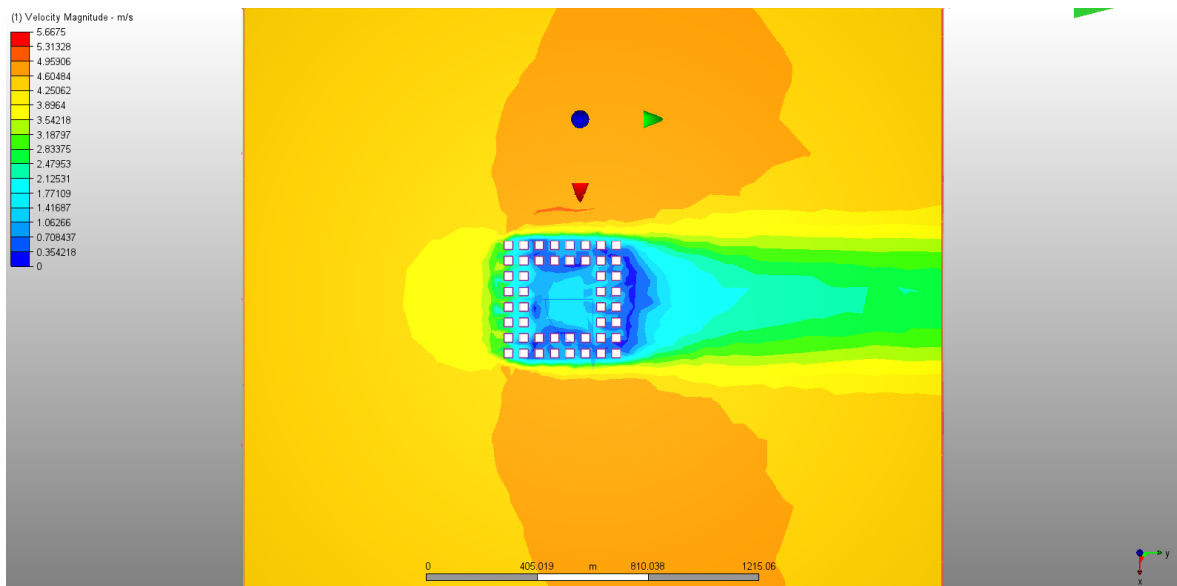

Figure 6.11. Result plane of third alternative, 10 meters above the ground at northern wind.

Figure 6.12. Result plane of third alternative, 50 meters above the ground at northern wind.

Table 6.4. Average wind speeds of third alternative at northern wind.

	At 2 m.	At 10 m.	At 50 m.
Average Wind Speed (m/s)	1.96	3.12	3.89

Third alternative shares the same buildings with the previous alternative, yet because of the increasing building number the height of buildings are lowered. When looking the result plane at two meters, a slow wind velocity trend among the buildings can be seen. After two building rows perpendicular to the wind flow, streets are started to get darker tones of blue. However, continuous long street canyons parallel to the wind flow do not slow the wind velocity like the previous model's park. As a result of that, average velocity of this model at pedestrian height is a bit higher than the second alternative. Furthermore, at the result plane at 10 meters, the increasing wind velocity among the buildings has ended up with better ventilation. The plane at 50 meters shows again the buildings effect on the wind flow is related with the building number and density.

6.1.5. Results of Fourth Alternative at Northern Wind

Figure 6.13. Result plane of fourth alternative, 2 meters above the ground at northern wind.

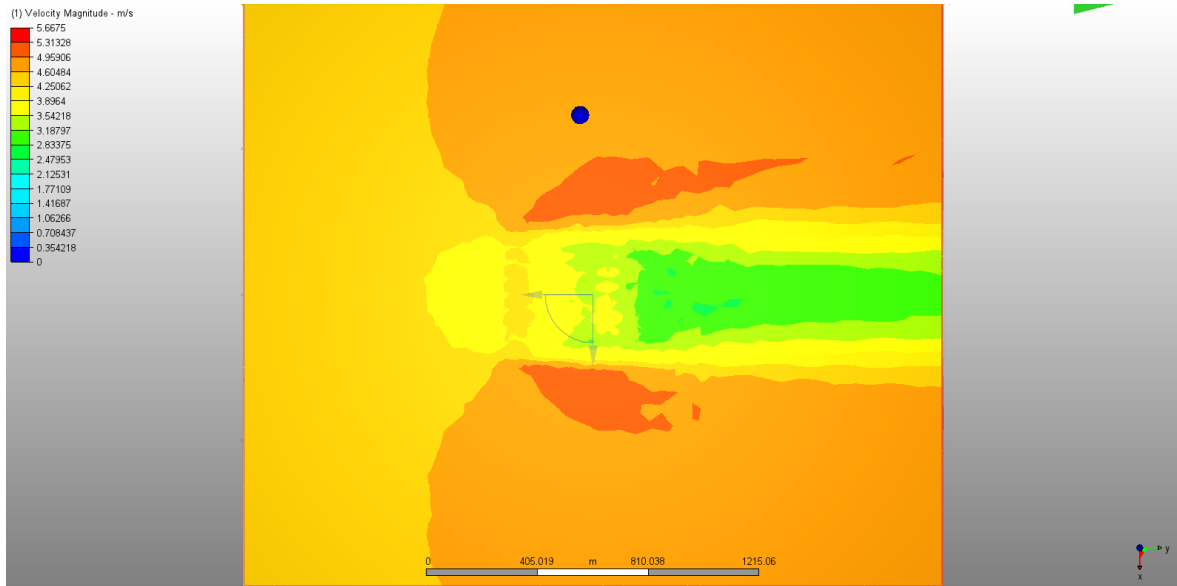Figure 6.14. Result plane of fourth alternative, 10 meters above the ground at northern wind.
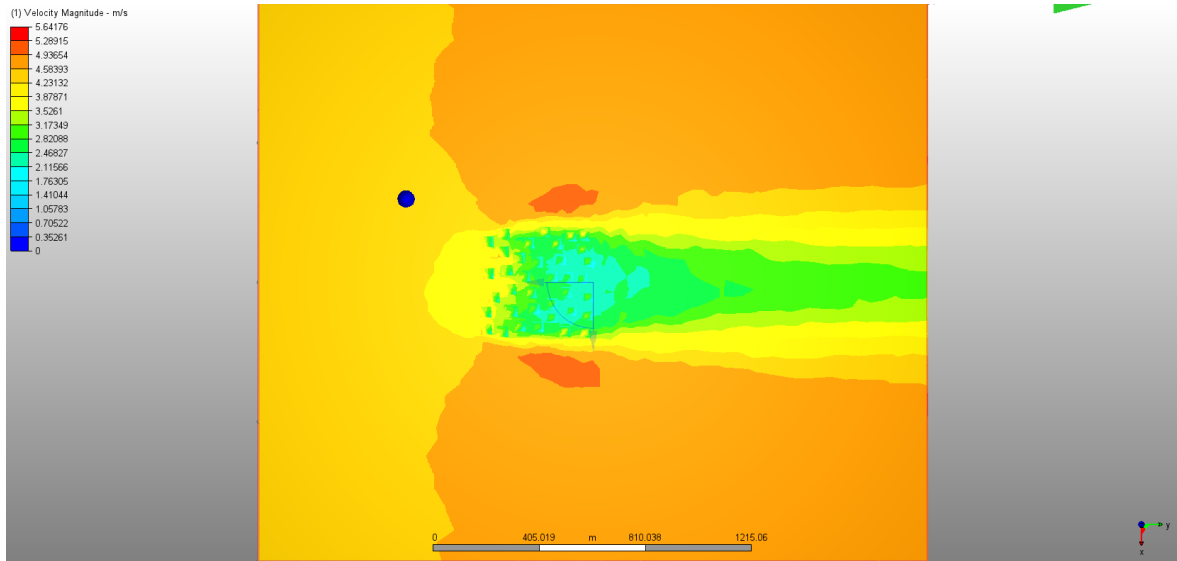
Figure 6.15. Result plane of fourth alternative, 50 meters above the ground at northern wind.

Table 6.5. Average wind speeds of fourth alternative at northern wind.

	At 2 m.	At 10 m.	At 50 m.
Average Wind Speed (m/s)	1.61	2.97	3.57

Settlements of the buildings in fourth alternative can be considered similar to the Mecidiyeköy. The buildings at this model are randomly scattered and result of this situation can be seen at the result plane of pedestrian level. Like Mecidiyeköy's model it is hard for wind flow to move among the buildings, hence the ventilation is also become a problem. When looking closer to the plane, it is apparent that the wind velocity is very low. Furthermore, it can be said that the situation is better at the other planes at higher levels but the problem is still there. Also, reduction at number of buildings increased the height. Owing to that, the flow trend among the buildings continues at the last result plane.

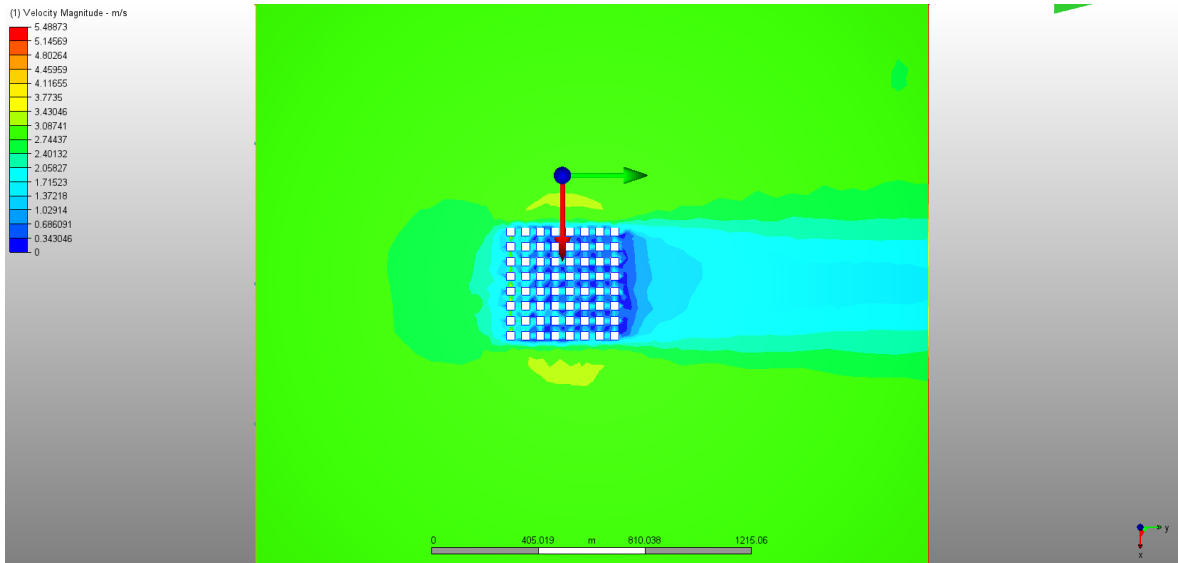### 6.1.6. Results of Fifth Alternative at Northern Wind
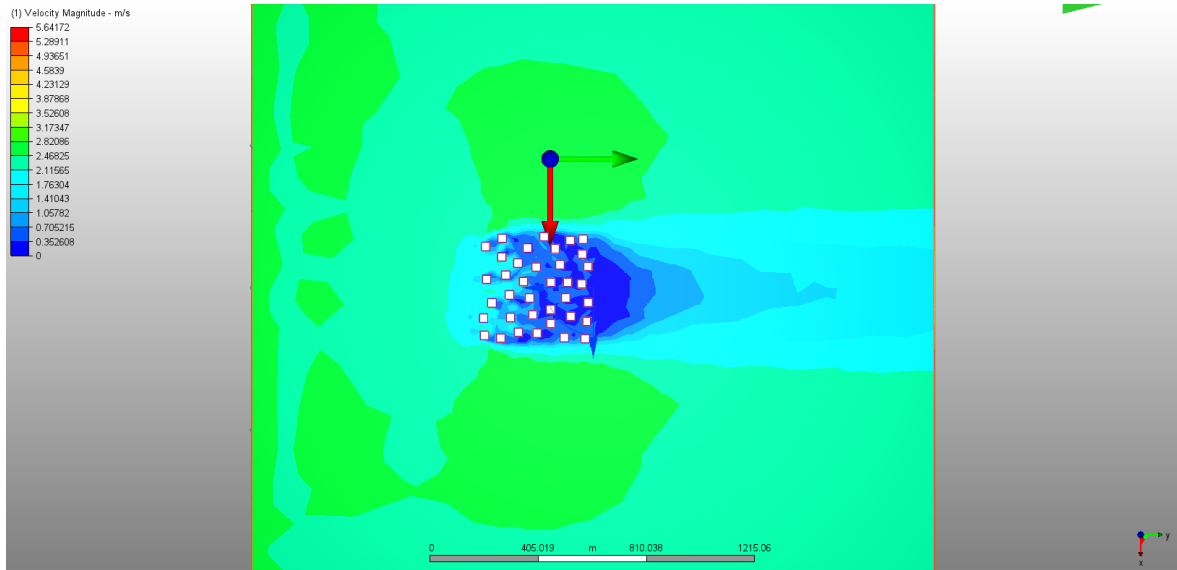
Figure 6.16. Result plane of fifth alternative, 2 meters above the ground at northern wind.
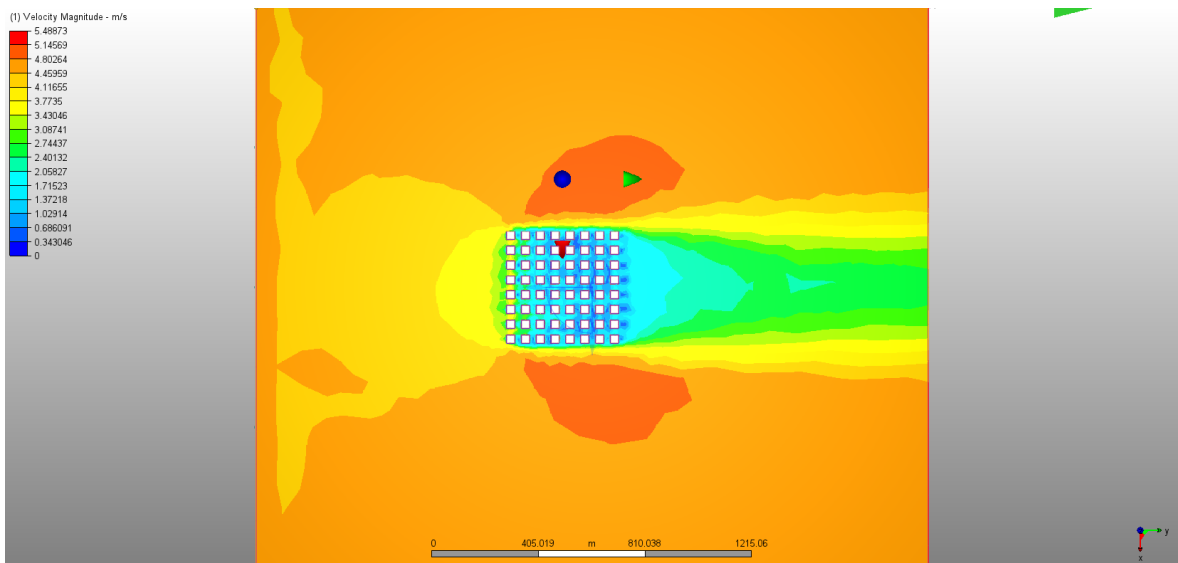

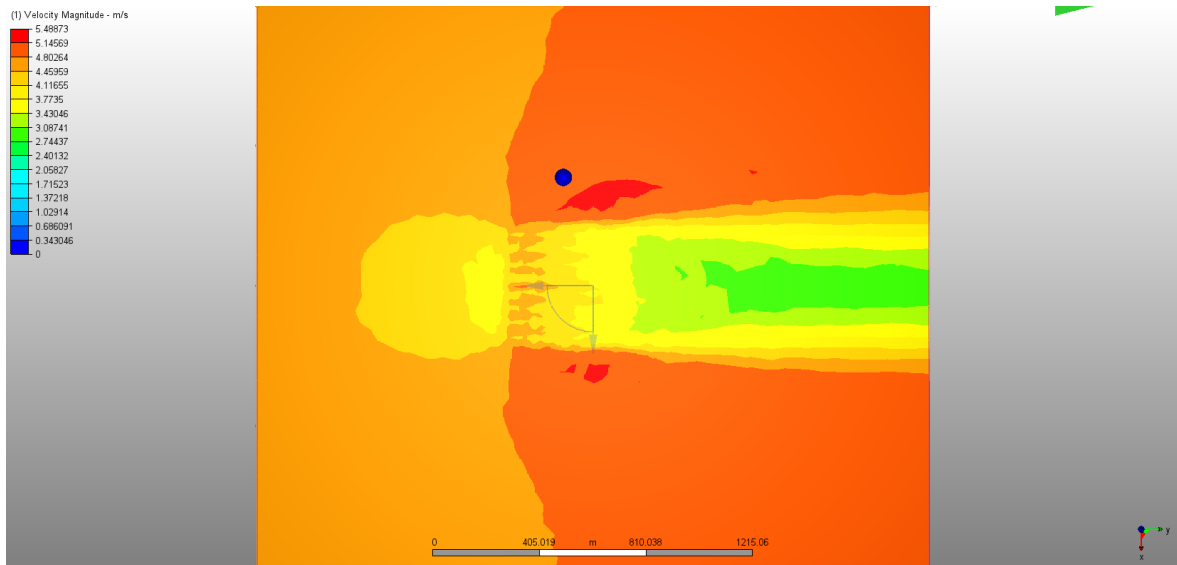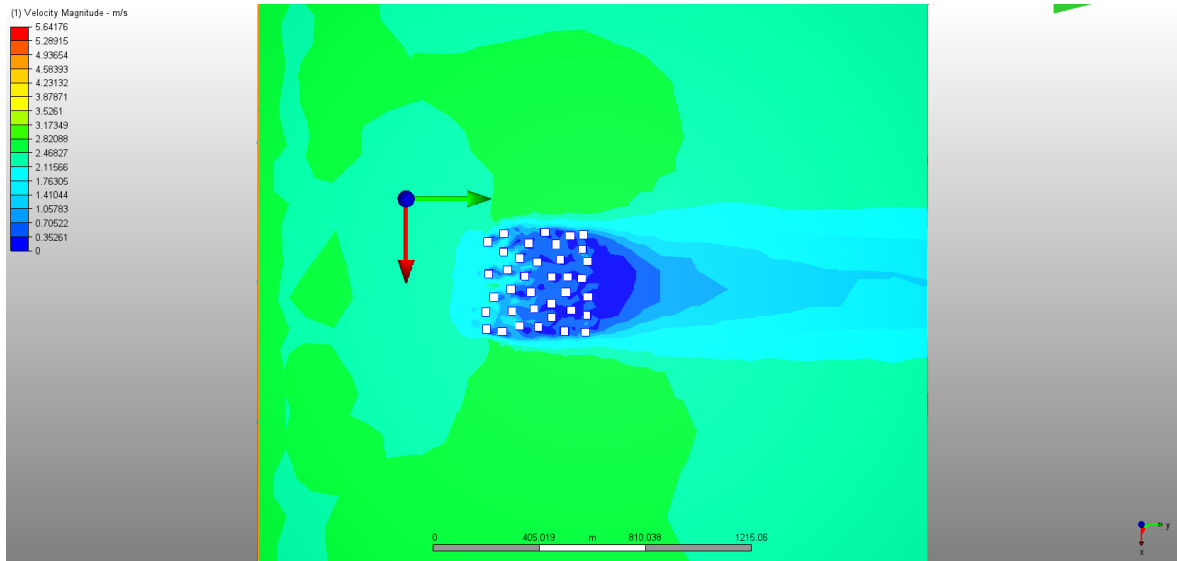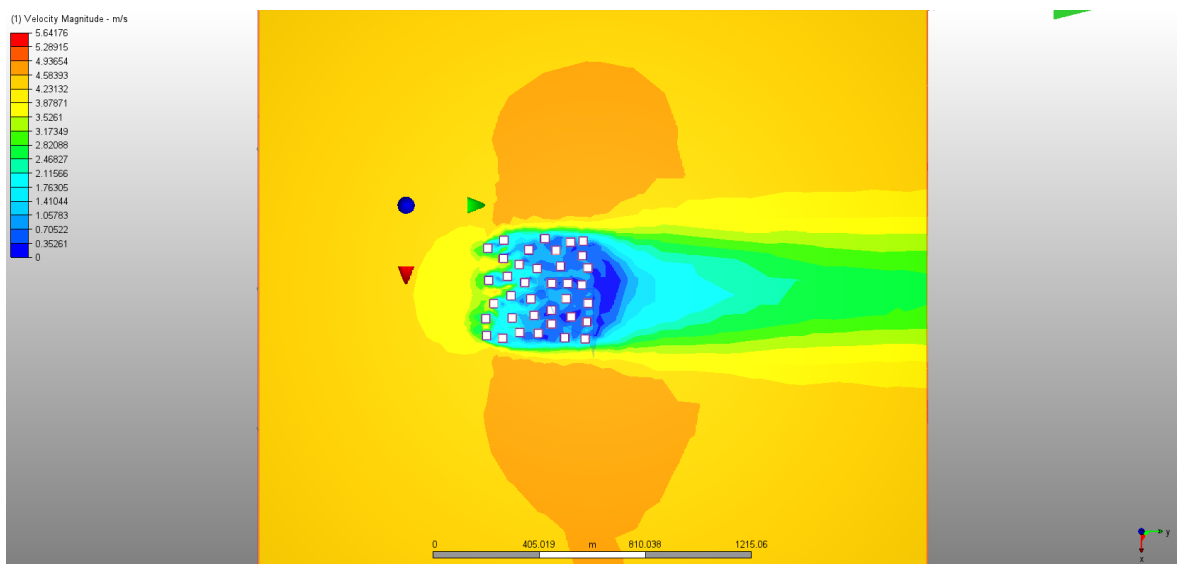Figure 6.17. Result plane of fifth alternative, 10 meters above the ground at northern wind.

Figure 6.18. Result plane of fifth alternative, 50 meters above the ground at northern wind.

Table 6.6. Average wind speeds of fifth alternative at northern wind.

	At 2 m.	At 10 m.	At 50 m.
Average Wind Speed (m/s)	1.64	3.03	3.55

The fifth alternative is similar to the fourth alternative except building heights. Results of this alternative is very close to the fourth one. The differences in results occur due to the various building heights of the model. For instance, results planes at two meters and 10 meters are very close to each other. However the last planes of the models at 50 meters above the ground is different. Fifth model, is the only one in all models that have buildings more than 50 meters of height. The buildings that cut the plane affect the wind flow and make it slower at this level, hence the average velocity at 50 meters is slightly dropped.

6.2. Wind Simulation Results When Wind Blows from Northeast Direction

In this section, wind simulation results of Mecidiyeköy and five alternatives can be found when the wind blows from northeast direction. In the CFD simulation program, models are rotated 45° in the domain, hence at all figures, wind flows through left hand side to right hand side. With the help of result planes, simulation results are illustrated by the way of figures for each model at 2 meters for pedestrian level, 10 meters for height of an ordinary flat and 50 meters for representing the situation above the buildings. Furthermore, also average wind speeds at these three elevations are summarized in tables for each alternative. Also, legends on top left corner of each figure indicates the velocity of the result plane by colors. Velocity increases from dark blue to red as seen at the legend.

6.2.1. Results of Mecidiyeköy at Northeastern Wind
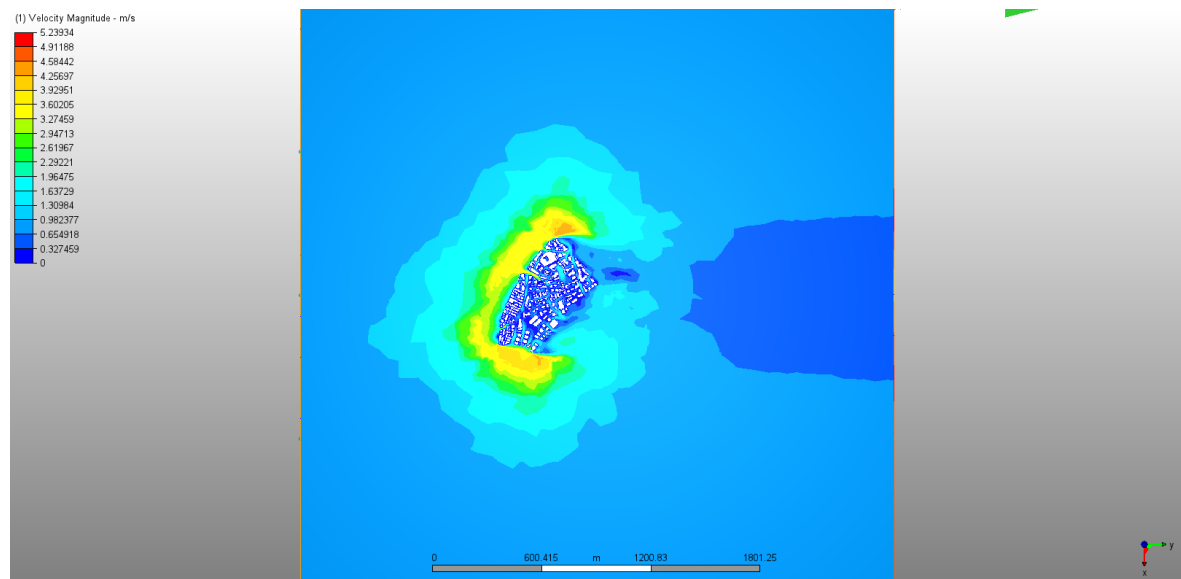
Figure 6.19. Result plane of Mecidiyeköy, 2 meters above the ground at northeastern wind.
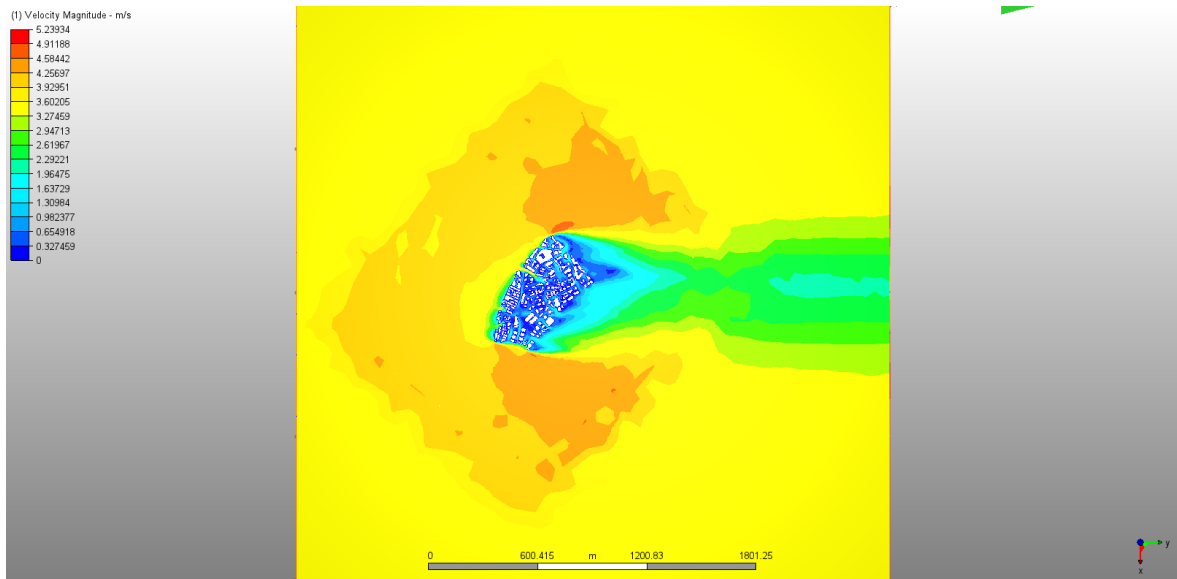
Figure 6.20. Result plane of Mecidiyeköy, 10 meters above the ground at northeastern wind.

Figure 6.21. Result plane of Mecidiyeköy, 50 meters above the ground at northeastern wind.

Table 6.7. Average wind speeds of Mecidiyeköy at northeastern wind.

	At 2 m.	At 10 m.	At 50 m.
Average Wind Speed (m/s)	1.00	2.94	4.04

When the wind flow blows from northeast, results do not change much for Mecidiyeköy. Wind flow is restricted among the buildings and streets. Most of the model still experience wind velocity close to zero, except some gaps between buildings or streets that parallel to wind flow. It can be said that, lack of natural ventilation at pedestrian level is a general problem for Mecidiyeköy independent of wind flow direction. The second result plane at 10 meters above the ground also shows that, inner part of the model continue to experience lack of appropriate wind flow like when the wind flow comes from north. Moreover, result plane at 50 meters also under effect of the buildings at the model and wind flow gets faster.

6.2.2. Results of First Alternative at Northeastern Wind

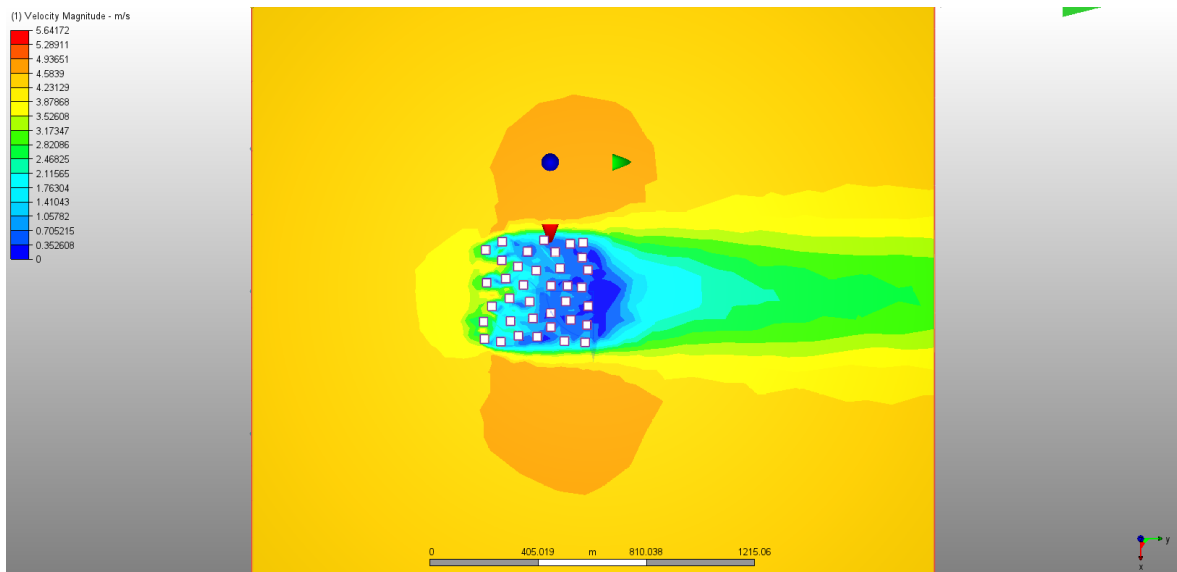Figure 6.22. Result plane of first alternative, 2 meters above the ground at northeastern wind.

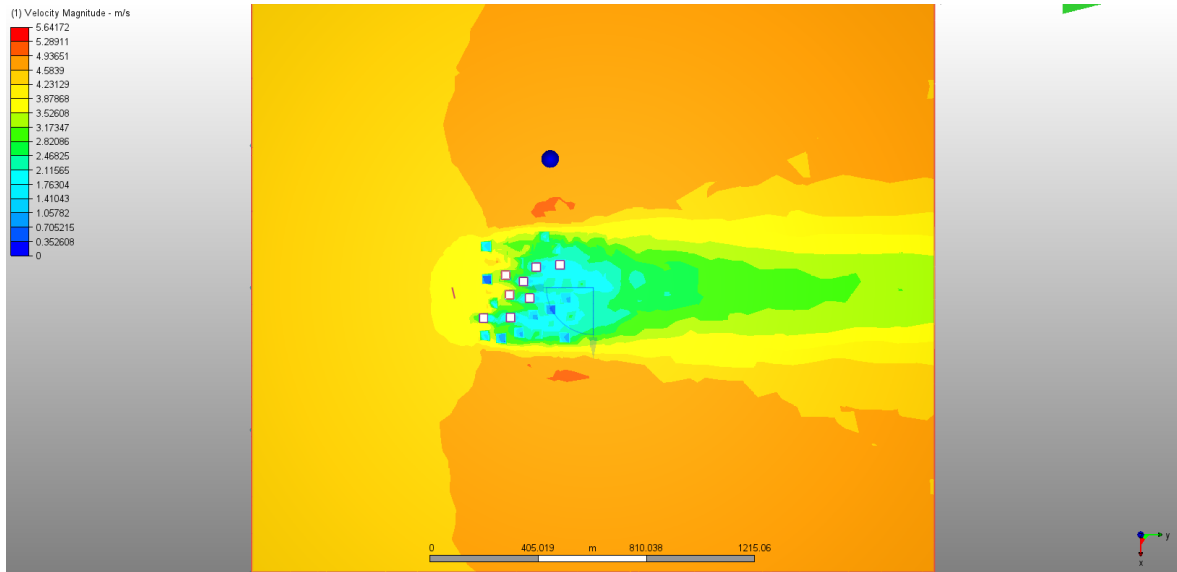Figure 6.23. Result plane of first alternative, 10 meters above the ground at northeastern wind.

Figure 6.24. Result plane of first alternative, 50 meters above the ground at northeastern wind.

Table 6.8. Average wind speeds of first alternative at northeastern wind.

	At 2 m.	At 10 m.	At 50 m.
Average Wind Speed (m/s)	2.19	3.27	3.86

When the direction of wind flow is changed from north to northeast, first alternative experience slower wind flow between the buildings that oriented to the wind flow and at the park. Especially, at the edges of the of the park. However, the model is still better than the Mecidiyeköy. For instance, the park, where is the region that gets the slower wind velocity did not experience bad ventilation as Mecidiyeköy in all scenarios. Furthermore, the average wind velocity of the model is decreased a little when its compared to the results of same model, when the wind flow comes from north direction. However, average wind velocity of the model is still more than double of Mecidiyeköy's average at pedestrian level. As expected, wind flow gets faster at 10 meters and result plane shows the situation. Thus, regions between the buildings and the park gets lighter tones. However, the model makes the wind flow faster even after the height of the buildings. The result of this can be seen at the plane of 50 meters.

6.2.3. Results of Second Alternative at Northeastern Wind

Figure 6.25. Result plane of second alternative, 2 meters above the ground at northeastern wind.

Figure 6.26. Result plane of second alternative, 10 meters above the ground at northeastern wind.
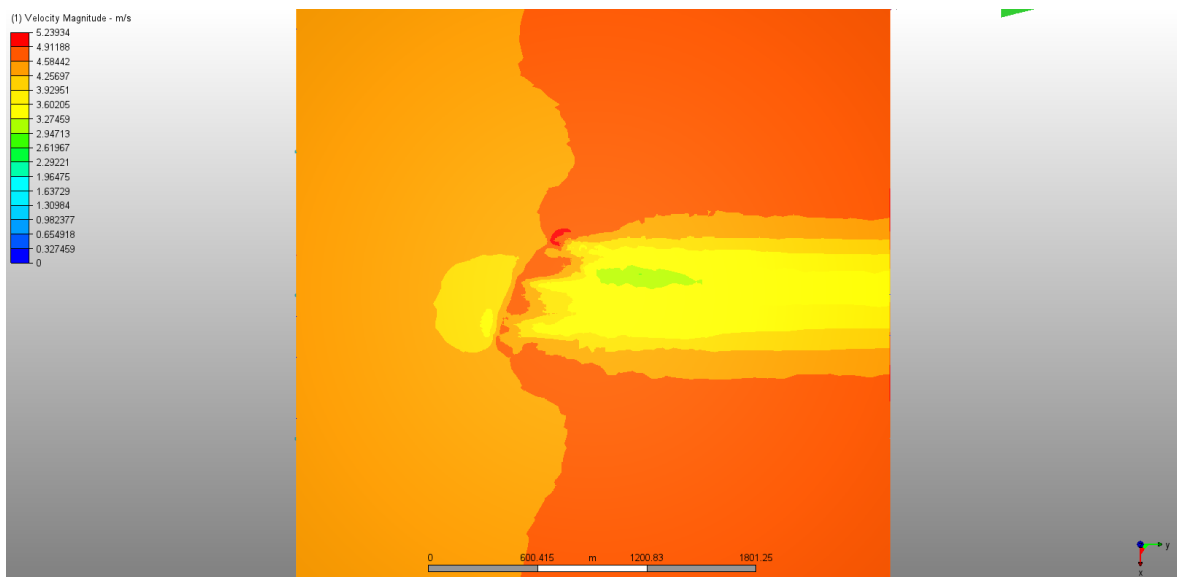
Figure 6.27. Result plane of second alternative, 50 meters above the ground at northeastern wind.

Table 6.9. Average wind speeds of second alternative at northeastern wind.

	At 2 m.	At 10 m.	At 50 m.
Average Wind Speed (m/s)	1.75	3.21	3.79

Second alternative is similar to the first alternative in some ways. However, the results of both alternatives are different. When the wind blows from northeast direction, second alternative end up with better results than its results at northern wind flow. It can be seen that the result plane at the pedestrian level shows the better ventilation of the park that surrounded by buildings. The park is almost dark blue at the previous scenario of the same model. Also, average wind speed of the model at pedestrian level increased this time. Furthermore, other results planes can also be considered better in comparison to the northern wind flow results of the alternative.

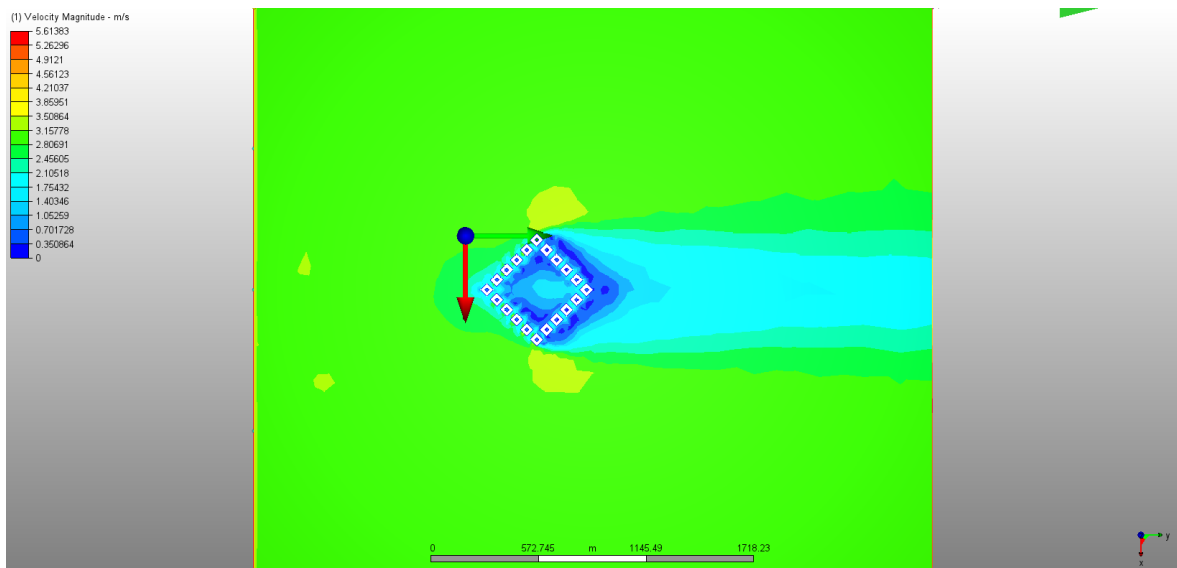### 6.2.4. Results of Third Alternative at Northeastern Wind

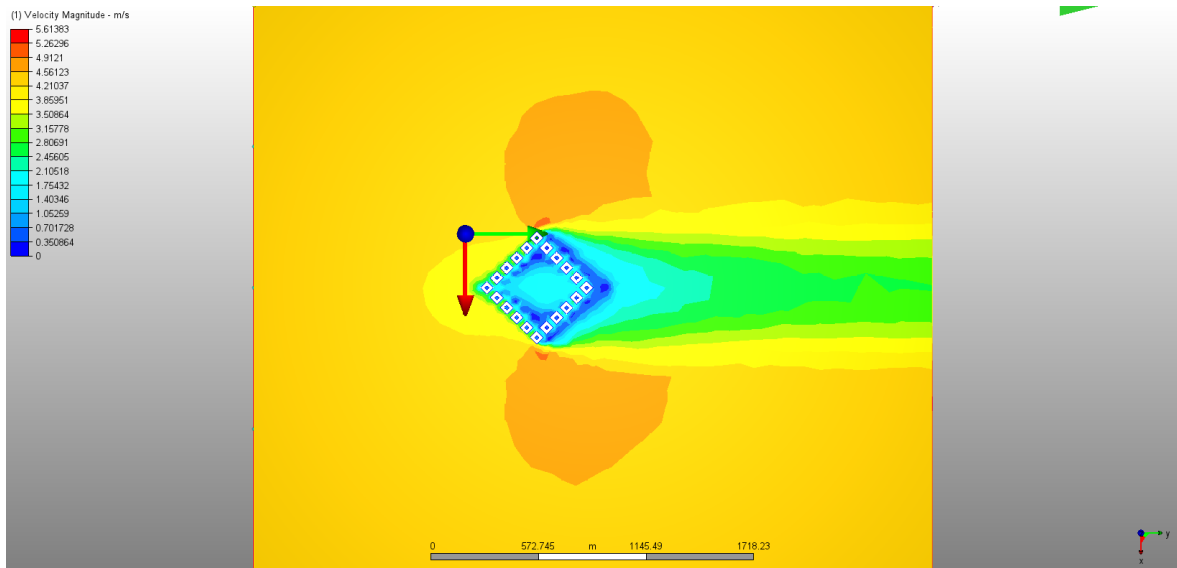Figure 6.28. Result plane of third alternative, 2 meters above the ground at northeastern wind.

Figure 6.29. Result plane of third alternative, 10 meters above the ground at northeastern wind.
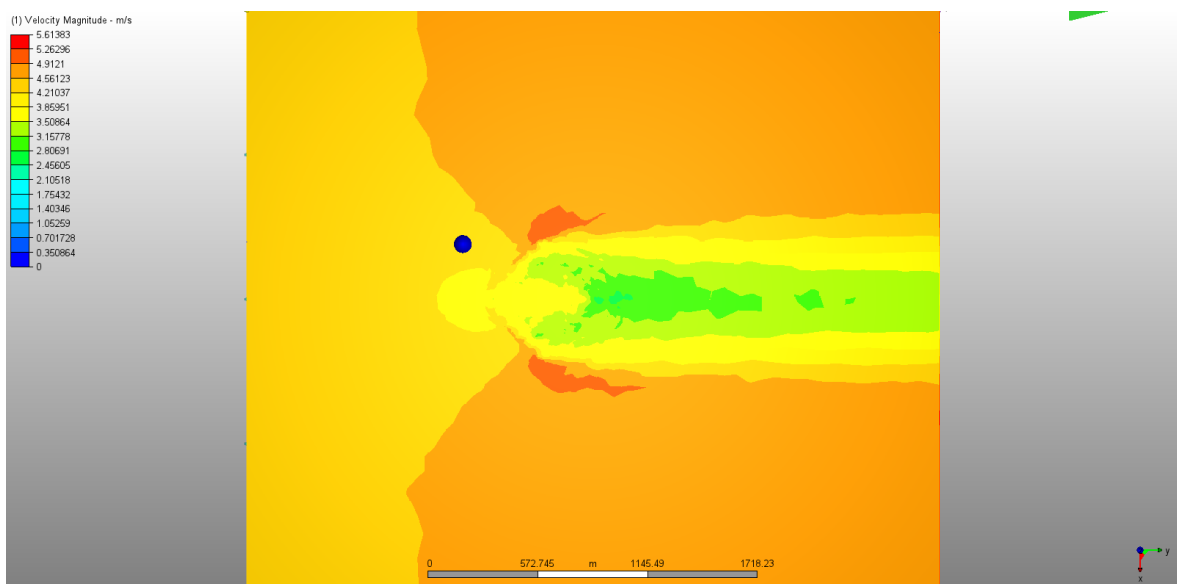
Figure 6.30. Result plane of third alternative, 50 meters above the ground at northeastern wind.

Table 6.10. Average wind speeds of third alternative at northeastern wind.

	At 2 m.	At 10 m.	At 50 m.
Average Wind Speed (m/s)	2.06	3.28	3.88

Third alternative is the second best after the first alternative at the northeastern wind flow scenario. It can be said that it is not hard for wind flow to go through large streets even it is not parallel to the street canyons. Third alternative has the advantage of continuous streets instead of a park which make wind flow slower. Like the second alternative, third alternative's pedestrian level average wind speed also increased. Furthermore, result plane at 10 meters shows that ventilation among the buildings is become better with increasing flow velocity. The last result plane of the alternative at 50 meters above the ground is not very different than the same plane at northern wind flow scenario.

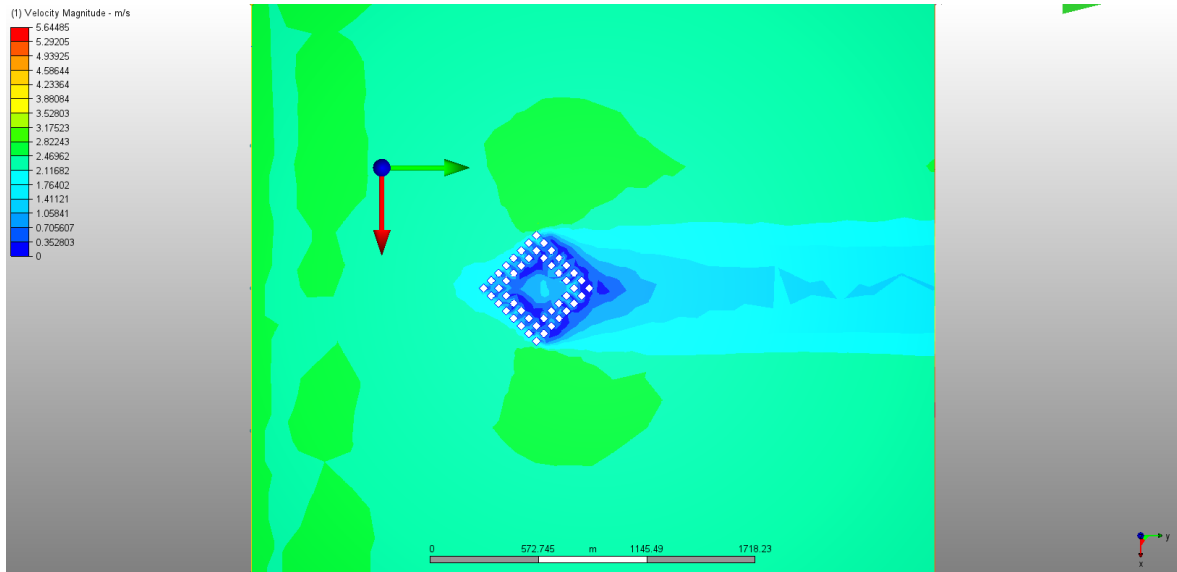## 6.2.5. Results of Fourth Alternative at Northeastern Wind
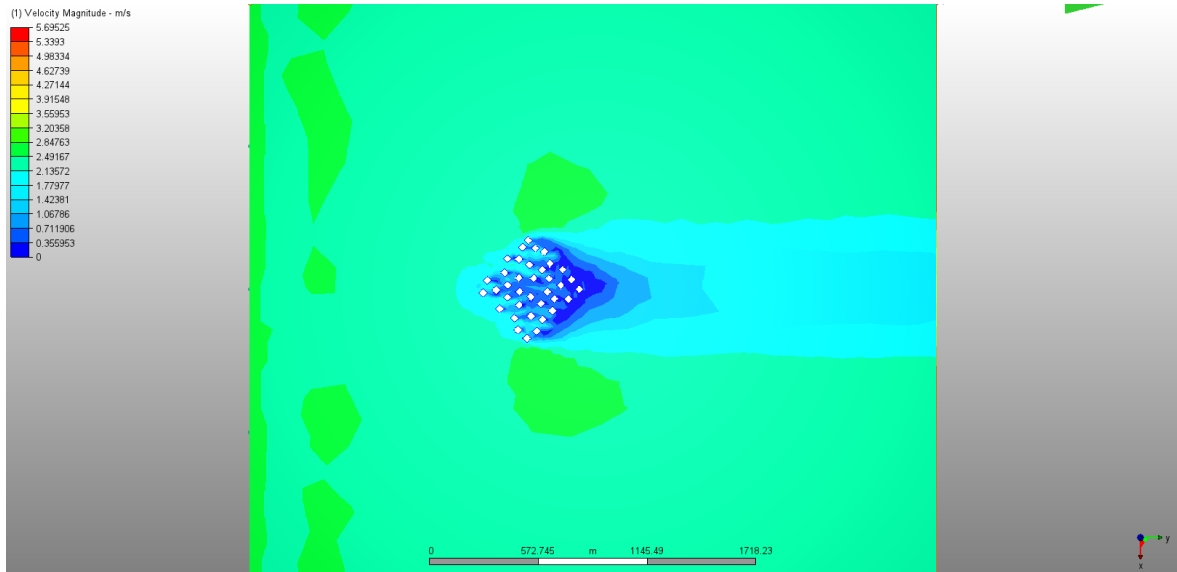
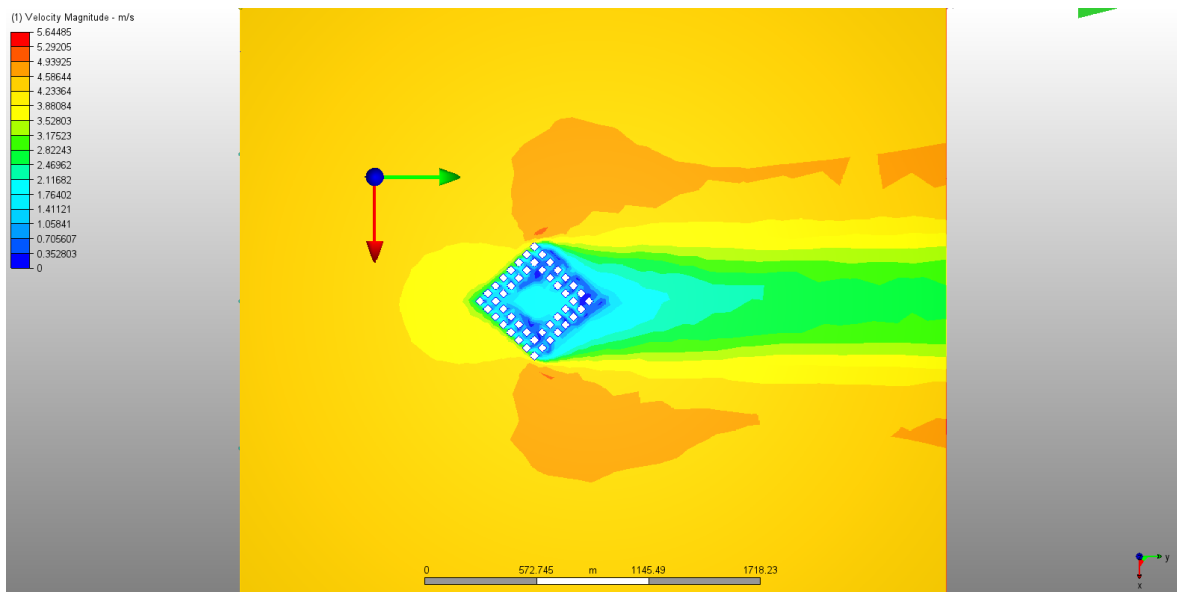Figure 6.31. Result plane of fourth alternative, 2 meters above the ground at northeastern wind.
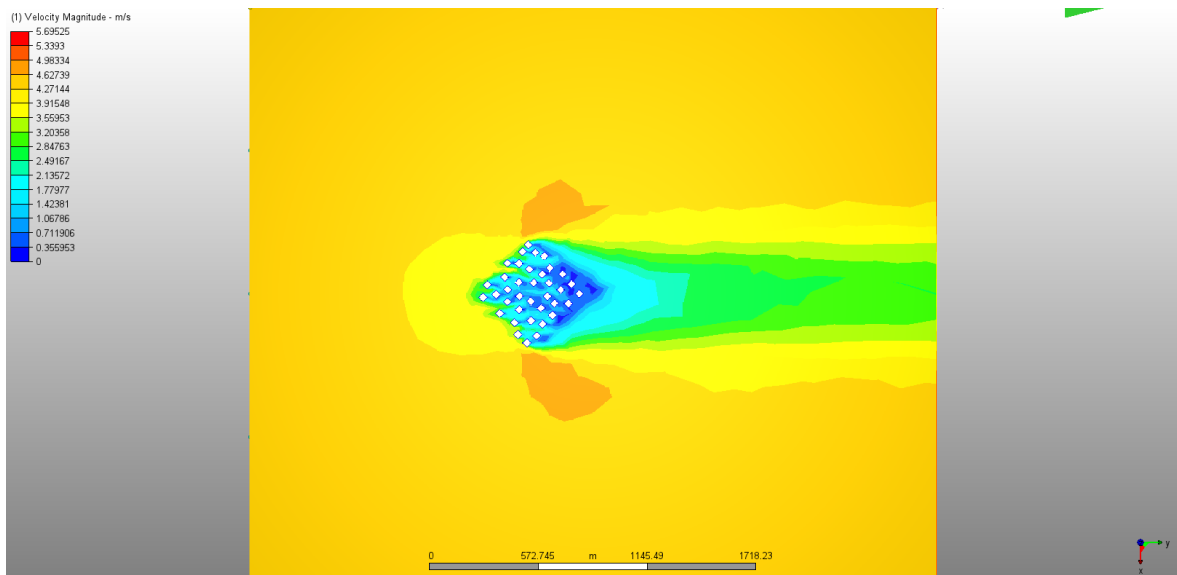
Figure 6.32. Result plane of fourth alternative, 10 meters above the ground at northeastern wind.
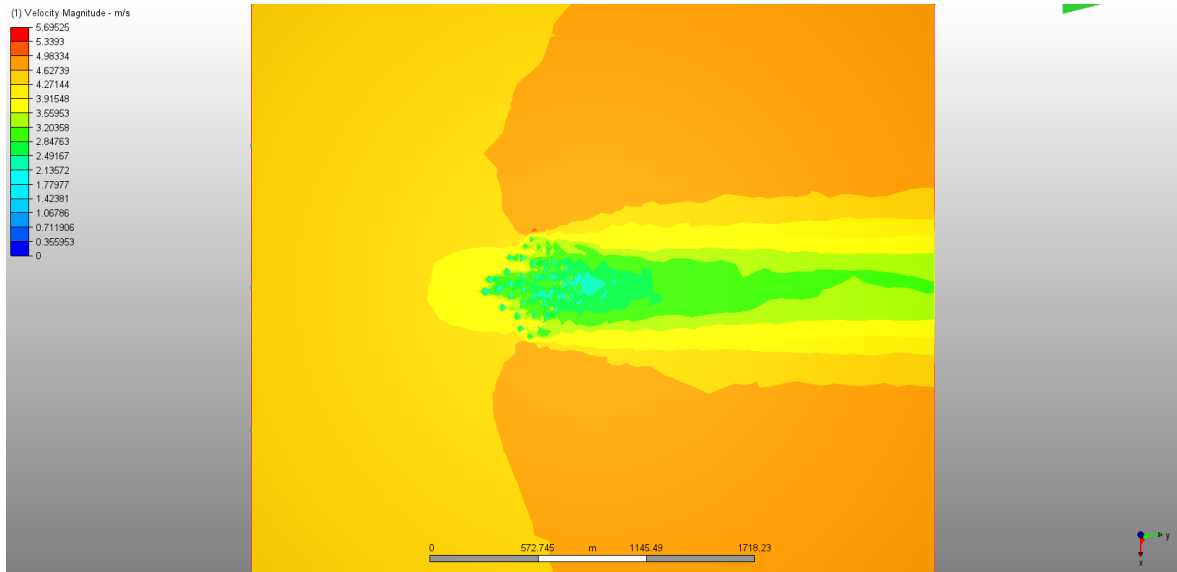
Figure 6.33. Result plane of fourth alternative, 50 meters above the ground at northeastern wind.

Table 6.11. Average wind speeds of fourth alternative at northeastern wind.

	At 2 m.	At 10 m.	At 50 m.
Average Wind Speed (m/s)	1.79	3.27	3.73

Results for fourth alternative do not change very much dependent on the wind flow direction. Arbitrary placed buildings still struggle to handle needs of natural ventilation like Mecidiyeköy. Buildings mostly restrict the wind flow, hence every building has become an obstacle for the one at its behind by the means of ventilation. The situation is apparent at the plane at pedestrian level. At following result plane at 10 meters shows that wind flow reached to the streets and buildings at the backwards easier. The last result plane at 50 meters do not change significantly when compared to the northern wind flow.

6.2.6. Results of Fifth Alternative at Northeastern Wind
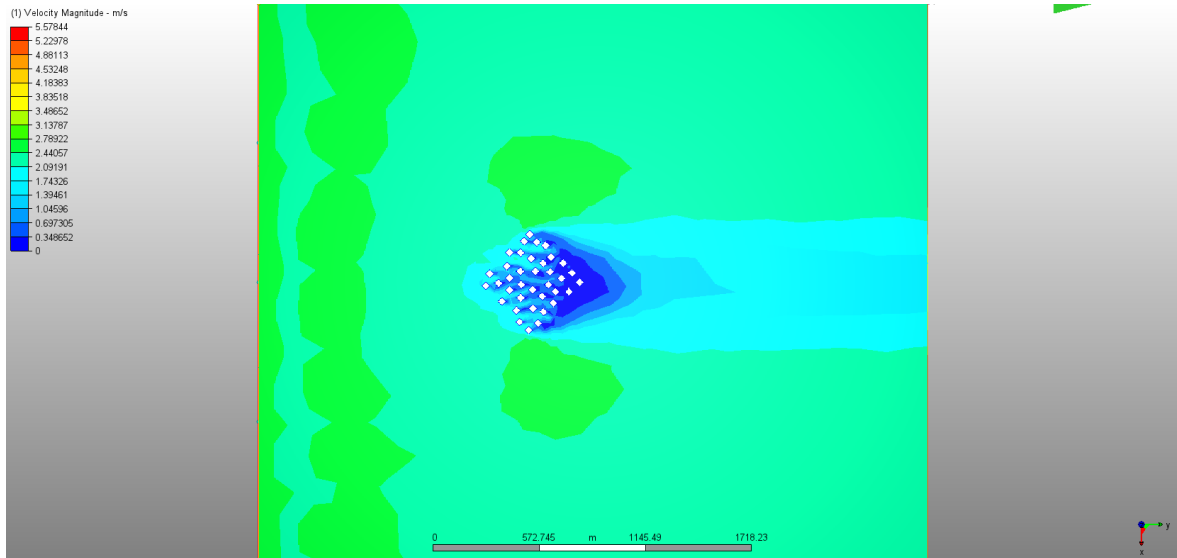
Figure 6.34. Result plane of fifth alternative, 2 meters above the ground at northeastern wind.
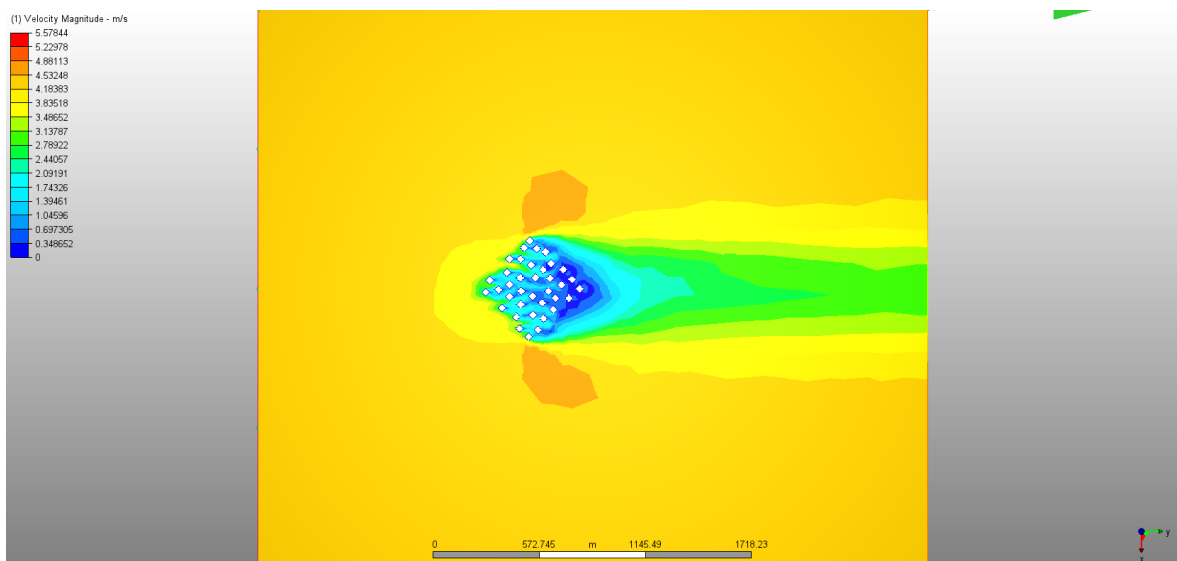
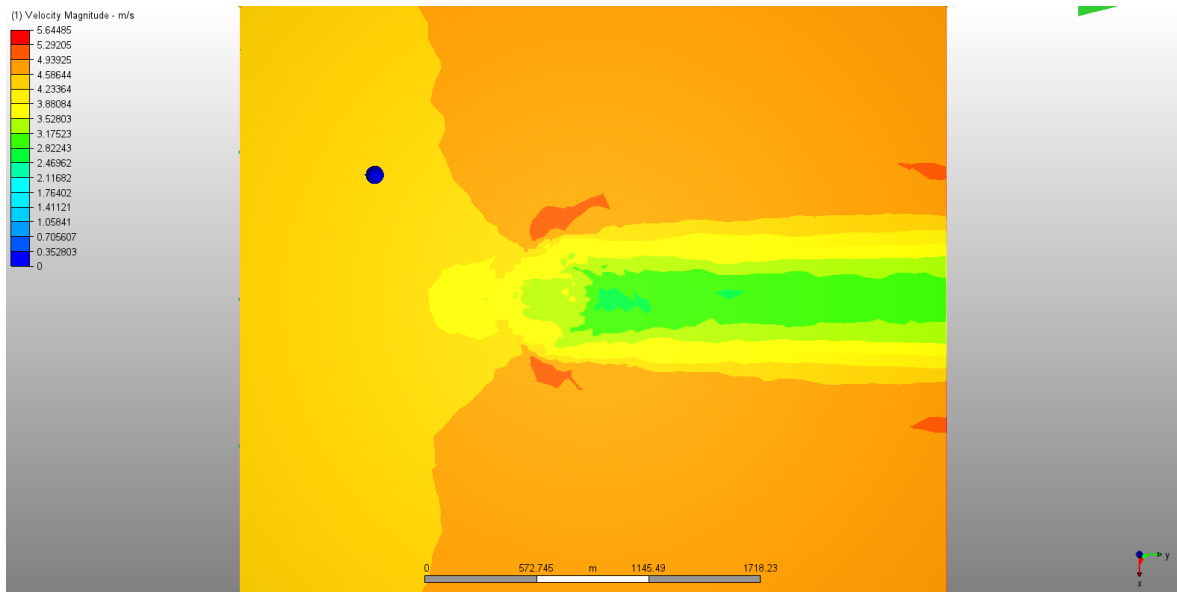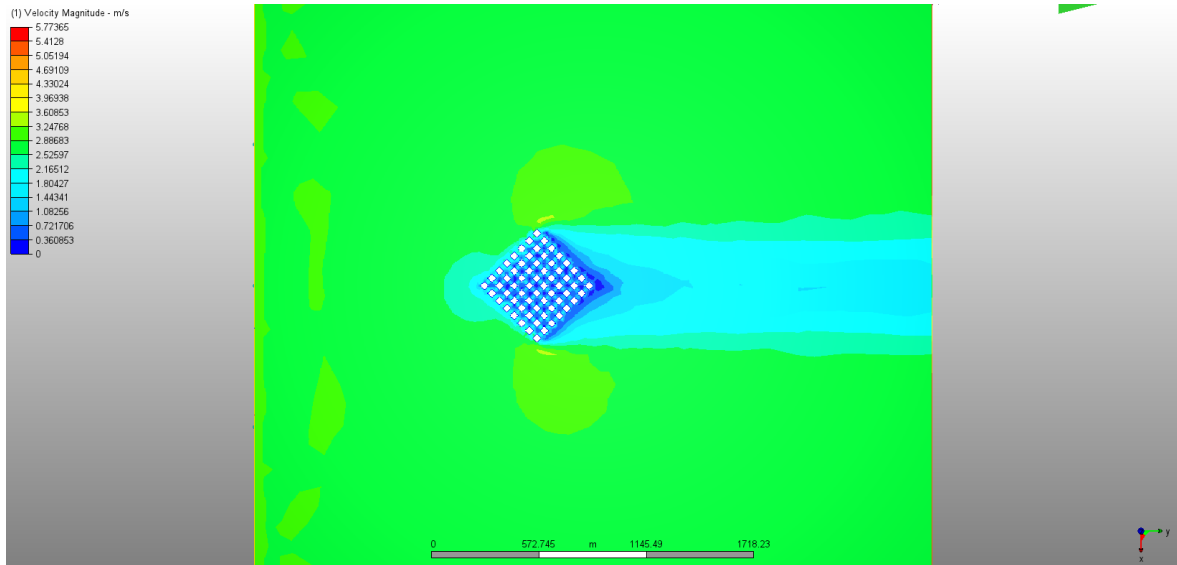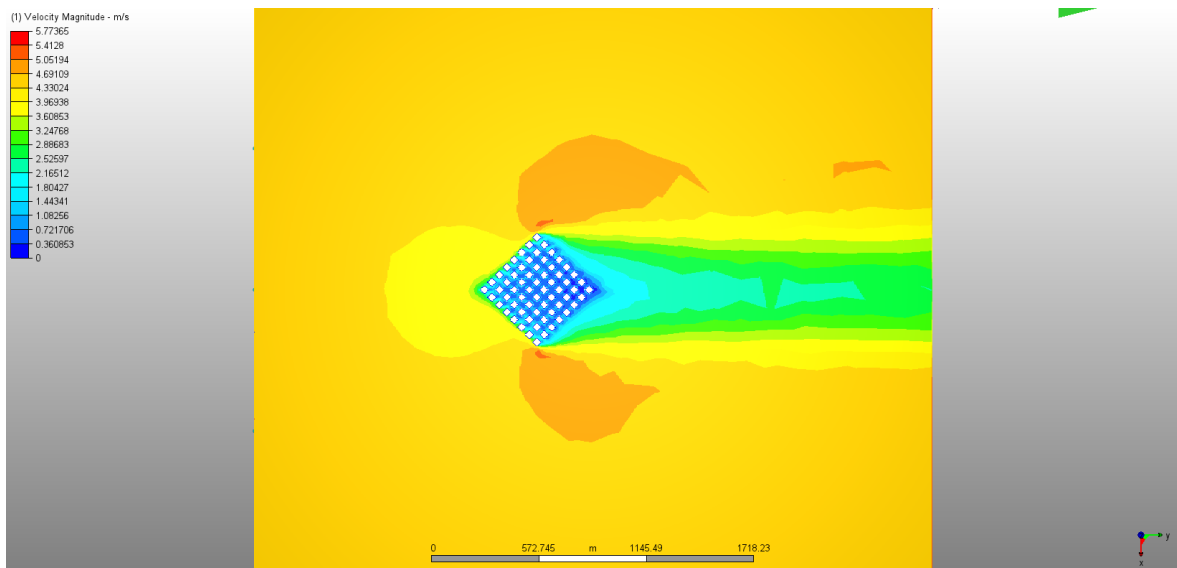Figure 6.35. Result plane of fifth alternative, 10 meters above the ground at northeastern wind.
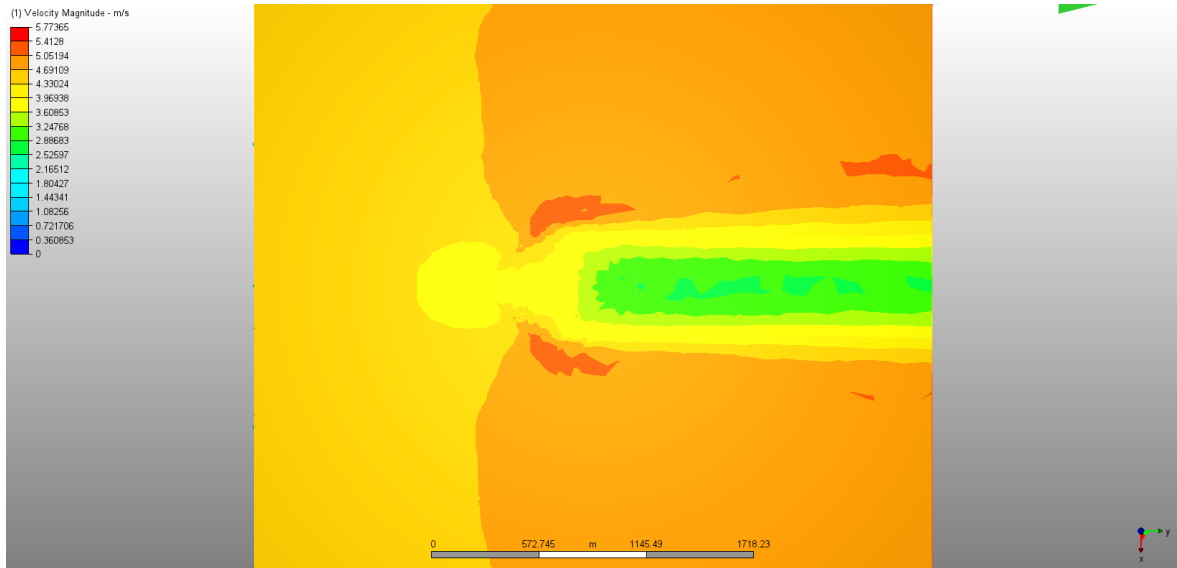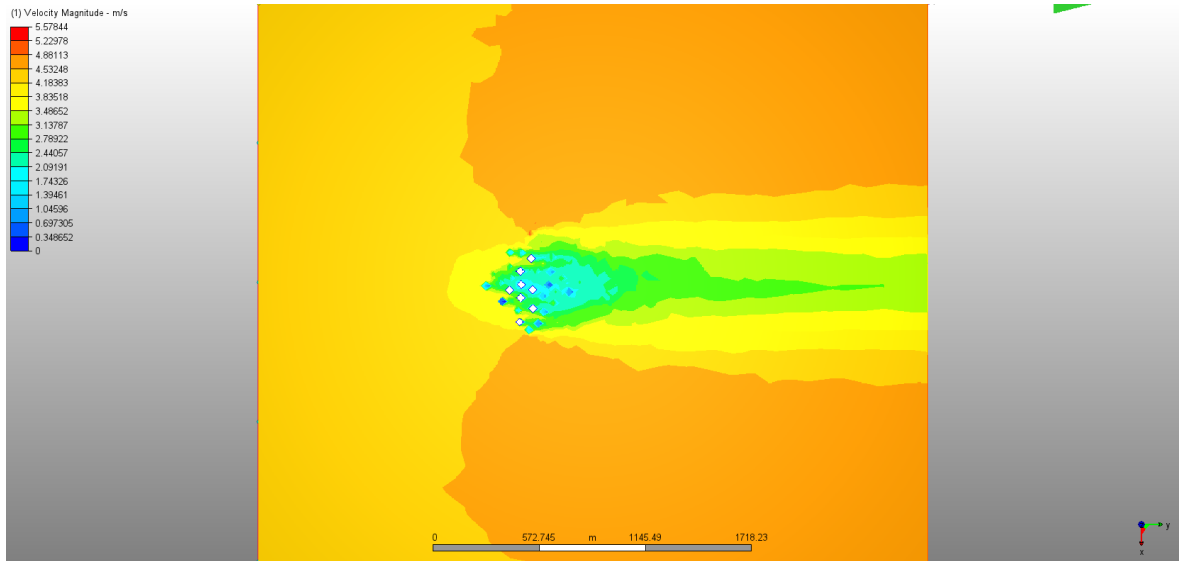
Figure 6.36. Result plane of fifth alternative, 50 meters above the ground at northeastern wind.

Table 6.12. Average wind speeds of fifth alternative at northeastern wind.

	At 2 m.	At 10 m.	At 50 m.
Average Wind Speed (m/s)	1.77	3.26	3.68

Results of the fifth alternative are almost identical to the fourth alternative's results. Slight differences arise because of changing building heights. To illustrate the situation, one can take a look at the result planes of the both alternatives at two and 10 meters. Nevertheless, result planes of the alternatives at 50 meters above the ground differ. Some of the buildings of the fifth alternative cut this plane and slow down the velocity of the wind flow.

6.3. Results of Apparent Temperature Calculations

In this section, results of apparent temperature calculations via average wind speeds are summarized in tables for 25 °C, 30 °C and 35 °C for north and northeast winds. Also results at tables are shown in column charts to ease comparison of models.

6.3.1. Apparent Temperature When the Wind Blows from North

Table 6.13. Apparent temperature at 25 °C air temperature and northern wind.

	At 2 m.	At 10 m.	At 50 m.
1. Alternative	24.086 °C	23.904 °C	23.425 °C
2. Alternative	24.823 °C	23.961 °C	23.437 °C
3. Alternative	24.587 °C	23.848 °C	23.377 °C
4. Alternative	24.816 °C	23.942 °C	23.571 °C
5. Alternative	24.796 °C	23.904 °C	23.583 °C
Mecidiyeköy	No cooling effect.	24.036 °C	23.310 °C
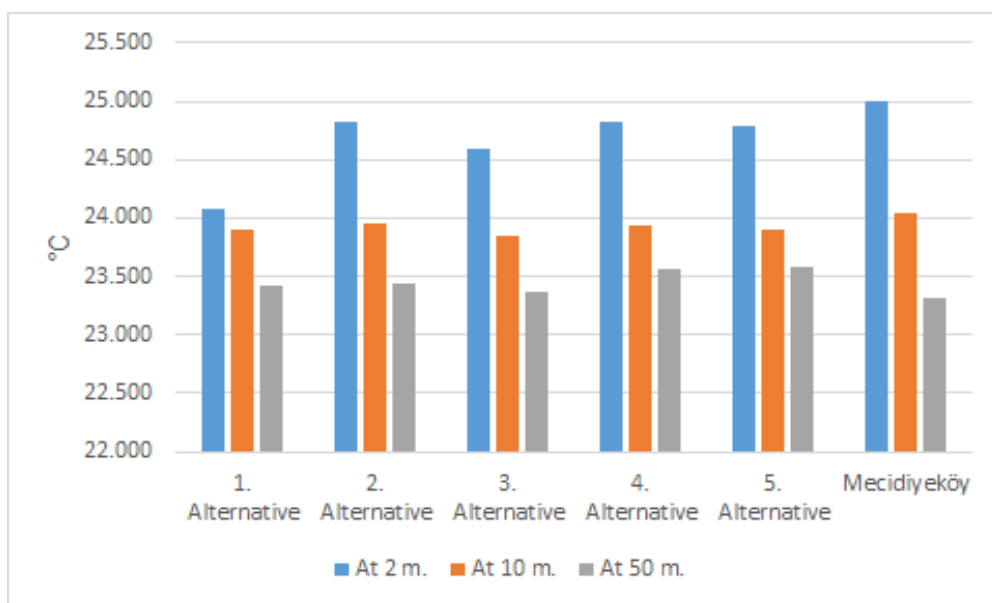
Figure 6.37. Chart of apparent temperature results at 25 °C and northern wind.

Table 6.14. Apparent temperature at 30 °C air temperature and northern wind.

	At 2 m.	At 10 m.	At 50 m.
1. Alternative	29.240 °C	29.085 °C	28.677 °C
2. Alternative	29.871 °C	29.133 °C	28.688 °C
3. Alternative	29.668 °C	29.037 °C	28.636 °C
4. Alternative	29.865 °C	29.117 °C	28.801 °C
5. Alternative	29.848 °C	29.085 °C	28.811 °C
Mecidiyeköy	No cooling effect.	29.197 °C	28.580 °C

Figure 6.38. Chart of apparent temperature results at 30 °C and northern wind.

Table 6.15. Apparent temperature at 35 °C air temperature and northern wind.

	At 2 m.	At 10 m.	At 50 m.
1. Alternative	34.393 °C	34.265 °C	33.930 °C
2. Alternative	34.919 °C	34.305 °C	33.938 °C
3. Alternative	34.749 °C	34.225 °C	33.896 °C
4. Alternative	34.914 °C	34.291 °C	34.031 °C
5. Alternative	34.900 °C	34.265 °C	34.040 °C
Mecidiyeköy	No cooling effect.	34.358 °C	33.850 °C
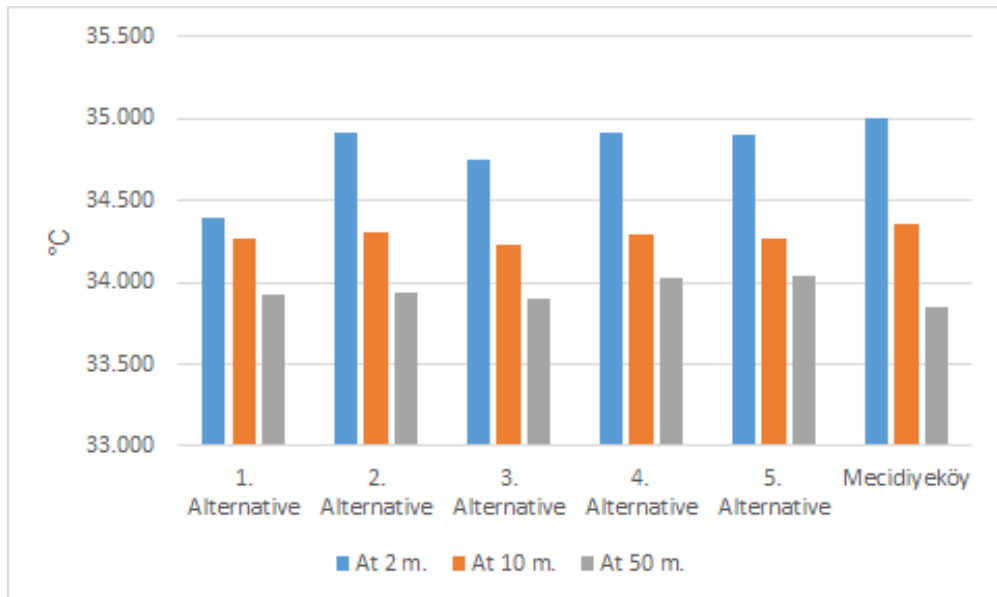
Figure 6.39. Chart of apparent temperature results at 35 °C and northern wind.

Apparent temperature is a very important issue for thermal comfort of human. Furthermore, the issue also has become more significant at pedestrian level. As can be seen at the tables and charts, current building situation of Mecidiyeköy cannot provide necessary conditions for benefiting cooling effect of northern wind flow.

When looking to the apparent temperature results at 25 °C air temperature, first alternative has the coolest apparent temperature at pedestrian level, which is almost one degree Celsius below the air temperature. However, Mecidiyeköy has not ended up with any cooling effect. At level of 10 meters above the ground, results of the models are closer, yet Mecidiyeköy's apparent temperature is slightly hotter than the other alternatives. At 50 meters above the ground, third and fourth alternatives are hotter than the other alternatives' similar results.

Under the conditions of 30 °C air temperature, first alternative again has the coolest apparent temperature at pedestrian level, and followed by other alternatives. Mecidiyeköy still cannot provide any cooling effect at pedestrian level at 30 °C air temperature too. At 10 meters, third alternative has the coolest apparent temperature and followed by first alternative, yet the difference between results of alternatives is not significant and Mecidiyeköy's result is slightly hotter than the other alternatives. At 50 meters above the ground results of the models are closer. In addition, the trend for third and fourth alternatives is same at this level.

At 35 °C air temperature, first alternative is still the coolest model at pedestrian level and followed by other alternatives. Moreover, nothing has changed for model of Mecidiyeköy again at pedestrian level at 35 °C too. When the calculation level is increased to 10 meters, results of the models are close to each other. Furthermore, at 50 meters above the ground models end up with almost same results. Again, third and fourth alternatives are a little hotter than the others.

All in all, under the effect of northern wind flow, first alternative is the best model by the means of cooling in apparent temperature results at pedestrian level, where

Mecidiyeköy is the worst. At calculations of 10 meters, Mecidiyeköy end up with the warmest result, yet all models gives similar results at 10 and 50 meters. Moreover, as it can be seen from results that the cooling effect of the wind flow decreases with the increasing air temperature.

6.3.2. Apparent Temperature When the Wind Blows from Northeast

Table 6.16. Apparent temperature at 25 °C air temperature and northeastern wind.

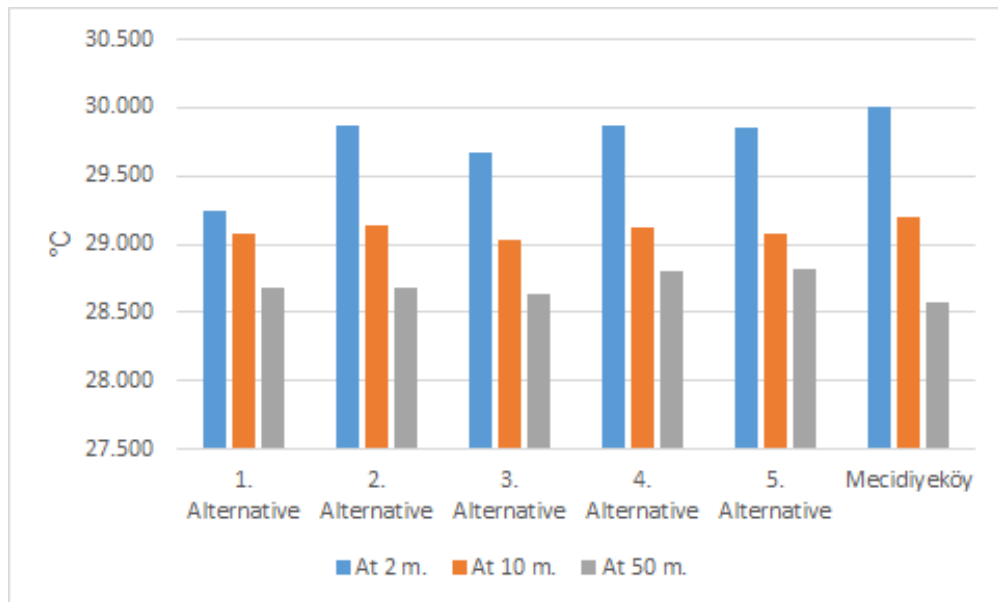|	At 2 m.	At 10 m.	At 50 m.
1. Alternative	24.438 °C	23.755 °C	23.395 °C
2. Alternative	24.724 °C	23.792 °C	23.437 °C
3. Alternative	24.522 °C	23.749 °C	23.383 °C
4. Alternative	24.698 °C	23.755 °C	23.473 °C
5. Alternative	24.711 °C	23.761 °C	23.504 °C
Mecidiyeköy	No cooling effect.	23.961 °C	23.286 °C
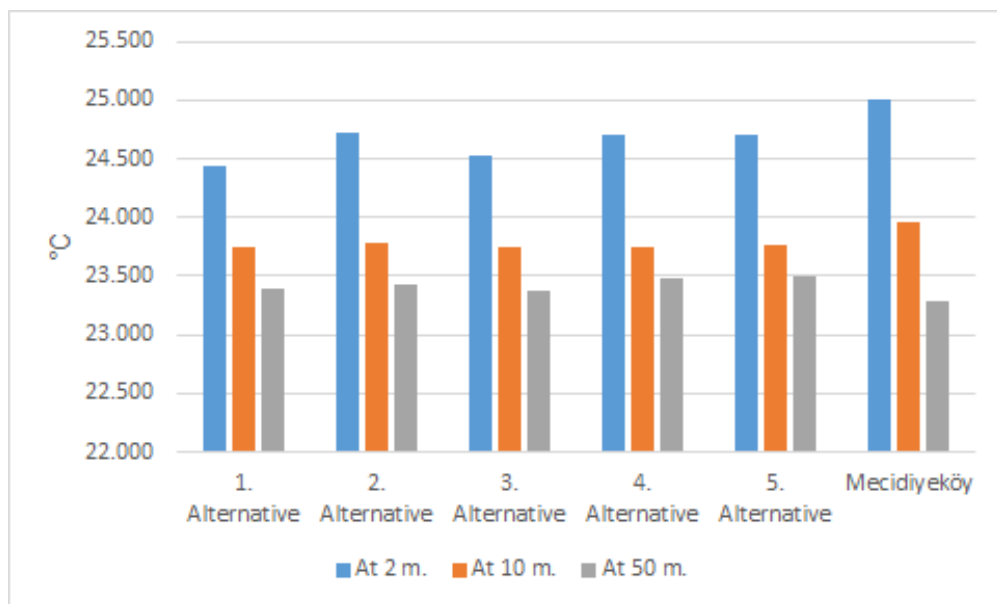
Figure 6.40. Chart of apparent temperature results at 25 °C and northeastern wind.

Table 6.17. Apparent temperature at 30 °C air temperature and northeastern wind.

	At 2 m.	**At 10 m.**	**At 50 m.**
1. Alternative	29.540 °C	28.958 °C	28.652 °C
2. Alternative	29.786 °C	28.989 °C	28.688 °C
3. Alternative	29.612 °C	28.952 °C	28.642 °C
4. Alternative	29.763 °C	28.958 °C	28.718 °C
5. Alternative	29.774 °C	28.963 °C	28.744 °C
Mecidiyeköy	No cooling effect.	29.133 °C	28.560 °C
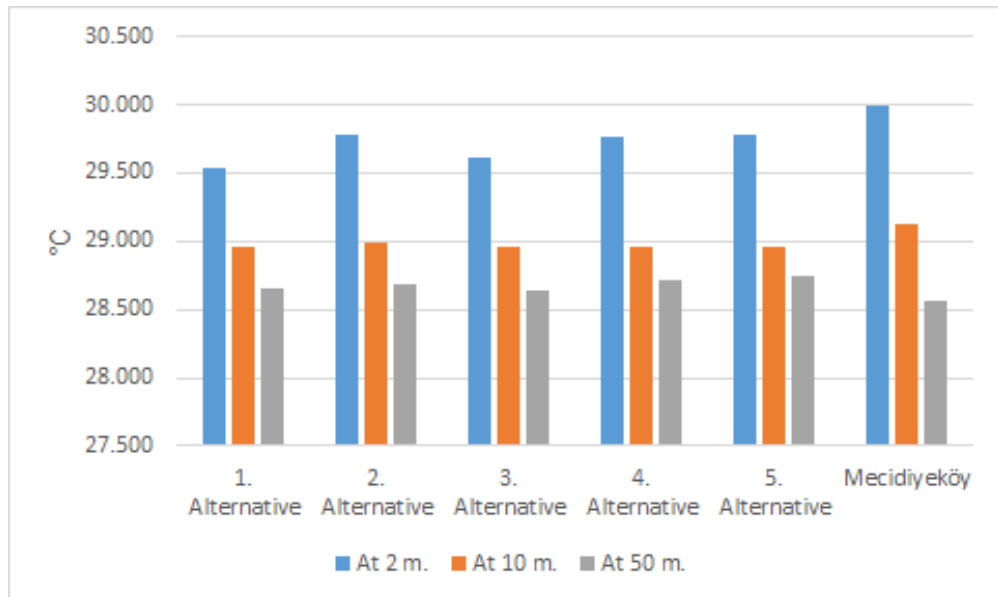
Figure 6.41. Chart of apparent temperature results at 30 °C and northeastern wind.

Table 6.18. Apparent temperature at 35 °C air temperature and northeastern wind.

	At 2 m.	**At 10 m.**	**At 50 m.**
1. Alternative	34.643 °C	34.160 °C	33.909 °C
2. Alternative	34.848 °C	34.186 °C	33.938 °C
3. Alternative	34.703 °C	34.156 °C	33.900 °C
4. Alternative	34.829 °C	34.160 °C	33.963 °C
5. Alternative	34.838 °C	34.165 °C	33.985 °C
Mecidiyeköy	No cooling effect.	34.305 °C	33.834 °C
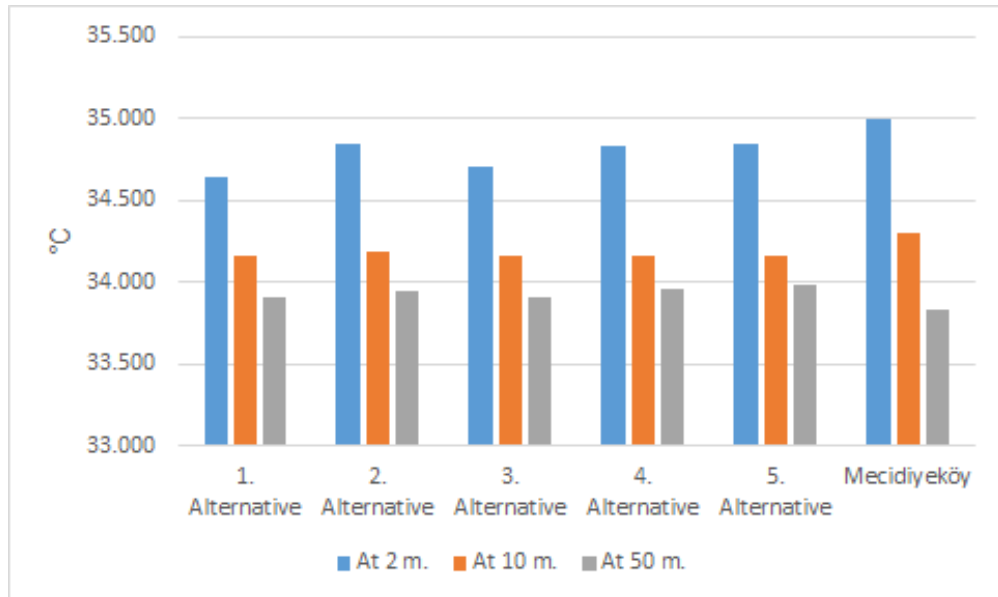
Figure 6.42. Chart of apparent temperature results at 35 °C and northeastern wind.

Like the northern, under the effect of northeastern wind Mecidiyeköy cannot take benefits of cooling effect of wind flow. The situation is more apparent especially at pedestrian level. Thus, it is understood that direction of wind flow do not alleviate ventilation problem of the Mecidiyeköy.

When looking to the results at pedestrian level at 25 °C air temperature, first alternative has the coolest apparent temperature and followed by the third alternative. Under these conditions, Mecidiyeköy cannot provide any cooling by the way of wind flow as northern wind. At 10 meters above the ground, results of all models are very close, yet Mecidiyeköy is slightly hotter than other five alternative. At 50 meters, apparent temperature results of the models are nearly same. However, third and fourth alternatives are a little bit hotter.

At the air temperature of 30 °C, the coolest apparent temperature belongs to the first alternative at two meters and closely followed by the third alternative where Mecidiyeköy has not any cooling effect. At 10 meters above, apparent temperature results of the models are get closer, yet the model of Mecidiyeköy is the worst, which has the hotter apparent temperature. At 50 meters above the ground results are almost same except the trend of third and fourth alternatives.

With the increase of air temperature to 35 °C, result trends do not change. At the pedestrian level, first alternative provide the coolest apparent temperature and Mecidiyeköy still cannot show any cooling sign at the results of the calculations. After stepping to the 10 meters above the ground, apparent temperature results of models are not very different, yet the model of Mecidiyeköy again has the worst result. Furthermore, at 50 meters above the ground, models end up with close results to each other.

At the end, under the conditions of northeastern wind flow, first alternative can be considered as the best model by the means of cooling at pedestrian level as it is

at northern wind flow. Also Mecidiyeköy is again the worst one too. At the results of 10 and 50 meters all models produce similar results at calculations. Moreover, like the calculations of northern wind flow, cooling results of northeastern wind flow calculations are decreased by the increasing air temperature as well.

7. CONCLUSION

Recently, people's complaints about hot weather conditions in summer seasons are parts of daily life. The focus of complaints is increase of current weather conditions when they are compared to previous years. The complaints are not nonsense and reason of them is climate change. However, there are also other factors which enhance effects of climate change, hence increase discomfort of people. One of these factors are densely built urban areas.

Istanbul is Turkey's one and only megacity. Moreover, the population of city has been beyond its limits for years. This excessive population has destroyed city's texture and demography over the years. As a result of this, arbitrary built urban areas are emerged around every corner of the city. The study area of this thesis, Mecidiyeköy is a great example for this areas.

Arbitrarily built urban areas, restrict the wind flow in streets. Thus, wind has become slower. This kind of unplanned urbanization prevents urban areas from taking benefits of natural ventilation and cooling effect of wind.

In this thesis, a part of Mecidiyeköy is 3D modeled and compared to five other alternatives in same conditions. The comparison is based on wind flow in urban area and apparent temperature. When the study is conducted, it is seen that an arbitrary built urban area, Mecidiyeköy cannot reap the benefits of cooling effect of wind. However, other alternatives take the benefits of wind's cooling effect. Thus, in all five alternatives, apparent temperature is decreased to some extend and the situation is especially more significant at pedestrian level calculations. Mecidiyeköy's model can be considered as the worst at this point. Even arbitrary scattered buildings end up with better results.

To sum up, it is clear that thermal comfort of people can be better in well designed urban areas. This also would decrease the use of energy by the way of cooling systems. On the other hand, proper natural ventilation move the pollutants to out of urban areas without any external effect, hence air pollution would be decreased. In conclusion, governments must handle these issues with proper regulations for the sake of future generations.

REFERENCES

1. Terzi, F. and F. Bolen, "Urban sprawl measurement of Istanbul", *European Planning Studies*, Vol. 17, No. 10, pp. 1559–1570, 2009.

2. Yaman Galantini, Z. D. and A. Tezer, "Resilient urban planning process in question: Istanbul case", *International Journal of Disaster Resilience in the Built Environment*, Vol. 9, No. 1, pp. 48–57, 2018.

3. The Editors of Encyclopaedia Britannica, *Urbanization*, 2017, `https://www.britannica.com/topic/urbanization`, accessed at October 2018.

4. Davis, K., "The urbanization of the human population", *Scientific American*, Vol. 213, No. 3, pp. 40–53, 1965.

5. United Nations Department of Economic and Social Affairs Population Division (2018), *World Urbanization Prospects: The 2018 Revision, Online Edition*, 2018, `https://population.un.org/wup/Publications/`, accessed at October 2018.

6. UN, *World Urbanization Prospects: The 2014 Revision-Highlights*, UN, 2014.

7. United Nations Population Division, *World Urbanization Prospects 2018*, 2018, `https://population.un.org/wup/DataQuery/`, accessed at October 2018.

8. United Nations Population Division, *The World's Cities in 2016*, 2016, `http://www.un.org/en/development/desa/population/theme/urbanization/index.shtml`, accessed at October 2018.

9. Turkish Statistical Institute, *Population and Demography*, 2018, `http://www.turkstat.gov.tr/UstMenu.do?metod=temelist`, accessed at

October 2018.

10. European Environment Agency, *Urban sprawl in Europe - The ignored challenge*, 2006, `https://www.eea.europa.eu/publications/eea_report_2006_10`, accessed at October 2018.

11. Garreau, J., *Edge city: Life on the new frontier*, Anchor, 1992.

12. Burchell, R., A. Downs, B. McCann and S. Mukherji, *Sprawl costs: Economic impacts of unchecked development*, Island Press, 2005.

13. Wikipedia Contributors, *Suburbanization*, 2018, `https://en.wikipedia.org/w/index.php?title=Suburbanization&oldid=856264944`, accessed at October 2018.

14. Wikipedia Contributors, *Levittown New York*, 2018, `https://en.wikipedia.org/w/index.php?title=Levittown,_New_York&oldid=861919694`, accessed at October 2018.

15. Galyeans, C. N., *Levittown The Imperfect Rise of the American Suburbs*, 2015, `http://ushistoryscene.com/article/levittown/`, accessed at October 2018.

16. Bannon, M., S. Thomas and A. Cassidy, "The Role of Dublin in Europe, a Research Paper Prepared for the National Spatial Strategy Team", *DOELG, Dublin*, 2000.

17. Gkartzios, M. and M. Scott, *Countryside, here I come: urban rural migration in the Dublin city-region*, University College Dublin, Department of Planning and Environmental Policy, 2005.

18. European Environmental Agency, *Dublin 1990 and modelled scenario for 2025*, 2012, `https://www.eea.europa.eu/data-and-maps/figures/dublin-1990-and-modelled-scenario-for-2025#tab-hard-copy`, accessed at October 2018.

19. Turkish Statistical Institute, *Population Censuses*, 2018, `https://biruni.tuik.gov.tr/nufus80app/idari.zul?yil=1965`, accessed at October 2018.

20. İnceoglu, A. and I. Yurekli, "Urban transformation in Istanbul: potential for a better city", *Enhr Conference*, pp. 5–8, 2011.

21. Dökmeci, V. and L. Berköz, "Transformation of Istanbul from a monocentric to a polycentric city", *European Planning Studies*, Vol. 2, No. 2, pp. 193–205, 1994.

22. Gall, C., *Displaced Turks, Promised New Homes, Can Only Protest on an Empty Lot*, 2018, `https://www.nytimes.com/2018/09/30/business/turkey-economy-development-protests.html`, accessed at October 2018.

23. Turkish Statistical Institute, *Population Censuses*, 2018, `https://biruni.tuik.gov.tr/nufus80app/idari.zul`, accessed at October 2018.

24. Torus, B. and N. A. Yönet, "URBAN TRANSFORMATION in ISTANBUL", *Archi-Cultural Interactions through the Silk Road*, 2016.

25. Tunç, G., *Istanbul Chaos*, 2013, `https://www.deviantart.com/gokcentunc/art/Istanbul-Chaos-435441251`, accessed at October 2018.

26. Ergun, N., "Gentrification in Istanbul", *Cities*, Vol. 21, No. 5, pp. 391–405, 2004.

27. Çağdaş, G. and L. Berköz, "Dynamic behavior of the city center in Istanbul", *Computers, environment and urban systems*, Vol. 20, No. 3, pp. 153–164, 1996.

28. Saatci, A. M., "Solving water problems of a metropolis", *Journal of Water Resource and Protection*, Vol. 5, No. 04, p. 7, 2013.

29. European Environmental Agency, *Istanbul 2000 and 2020*, 2012, `https://www.eea.europa.eu/data-and-maps/figures/istanbul-2000-and-2020`,

accessed at October 2018.

30. Ayazli, I. E., F. Batuk and B. Kleinschmit, "Simulating landuse changes driven by a 3rd Bosphorus Bridge", *ASPRS/CaGIS 2010 Fall Specialty Conference, Orlando, Florida*, pp. 15–19, 2010.

31. Landsberg, H. E., *The urban climate*, Vol. 28, Academic press, 1981.

32. Ng, E., I. Tam, A. Ng, B. Givoni, L. Katzschner, K. Kwok and V. Cheng, "Feasibility study for establishment of air ventilation assessment system–final report", *Hong Kong: Department of Architecture, Chinese University of Hong Kong*, Vol. 16, 2005.

33. Ng, E., "Policies and technical guidelines for urban planning of high-density cities–air ventilation assessment (AVA) of Hong Kong", *Building and environment*, Vol. 44, No. 7, pp. 1478–1488, 2009.

34. Hang, J., Y. Li, M. Sandberg, R. Buccolieri and S. Di Sabatino, "The influence of building height variability on pollutant dispersion and pedestrian ventilation in idealized high-rise urban areas", *Building and Environment*, Vol. 56, pp. 346–360, 2012.

35. Chew, L. W., N. Nazarian and L. Norford, "Pedestrian-level urban wind flow enhancement with wind catchers", *Atmosphere*, Vol. 8, No. 9, p. 159, 2017.

36. Nazarian, N., J. Fan, T. Sin, L. Norford and J. Kleissl, "Predicting outdoor thermal comfort in urban environments: A 3D numerical model for standard effective temperature", *Urban climate*, Vol. 20, pp. 251–267, 2017.

37. Martin, J., *The European environment: state and outlook 2010: synthesis*, European Environment Agency, 2010.

38. Tang, W., B. Knutson, A. Mahalov and R. Dimitrova, "The geometry of iner-

tial particle mixing in urban flows, from deterministic and random displacement models", *Physics of Fluids*, Vol. 24, No. 6, p. 063302, 2012.

39. Di Sabatino, S., R. Buccolieri and P. Salizzoni, "Recent advancements in numerical modelling of flow and dispersion in urban areas: a short review", *International Journal of Environment and Pollution 7*, Vol. 52, No. 3-4, pp. 172–191, 2013.

40. Wikipedia Contributors, *Mecidiyeköy, Şişli*, 2018, `https://tr.wikipedia.org/wiki/Mecidiyeköy,_Şişli`, accessed at November 2018.

41. Google, *Mecidiyeköy Neighborhood*, 2017, `https://bit.ly/2OrPCyh`, accessed at November 2018.

42. Tezcanoğlu, S., *News From Social Media*, 2018, `https://www.cnnturk.com/sosyal-medya/65-yas-ustu-otobuse-bedava-biniyorsa-ogrenciler-de-binsin?page=1`, accessed at November 2018.

43. Şişli Municipality, *Şişli Tarihçesi*, 2018, `https://www.sisli.bel.tr/icerik/sisli-tarihcesi`, accessed at November 2018.

44. Google, *Google Street View*, 2018, `https://goo.gl/maps/vhjzLQty1BR2`, accessed at November 2018.

45. Şişli Municipality, *City Guide*, 2018, `http://kentrehberi.sisli.bel.tr/`, accessed at November 2018.

46. Wikipedia Contributors, *SketchUp — Wikipedia, The Free Encyclopedia*, 2018, `https://en.wikipedia.org/wiki/SketchUp`, accessed at November 2018.

47. Blocken, B. and J. Carmeliet, "Pedestrian wind environment around buildings: Literature review and practical examples", *Journal of Thermal Envelope and Building*

Science, Vol. 28, No. 2, pp. 107–159, 2004.

48. Oke, T. R., *Boundary layer climates*, Routledge, 2002.

49. Oke, T. R., "Street design and urban canopy layer climate", *Energy and buildings*, Vol. 11, No. 1-3, pp. 103–113, 1988.

50. Wen, H., *The Effect of Urban Geometries and Roof Shapes on Airflow and Pollutant Dispersion: A CFD Investigation*, Ph.D. Thesis, UCL (University College London), 2017.

51. Carpentieri, M., A. G. Robins and S. Baldi, "Three-dimensional mapping of air flow at an urban canyon intersection", *Boundary-Layer Meteorology*, Vol. 133, No. 2, pp. 277–296, 2009.

52. Autodesk Knowledge Network, *General Fluid Flow and Heat Transfer Equations*, 2018, `https://knowledge.autodesk.com/support/cfd/learn-explore/caas/CloudHelp/cloudhelp/2019/ENU/SimCFD-Learning/files/GUID-83A92AE5-0E9E-4E2D-B61F-64B3696E5F66-htm.html`, accessed at November 2018.

53. Autodesk Knowledge Network, *Turbulent Flow*, 2018, `https://knowledge.autodesk.com/support/cfd/learn-explore/caas/CloudHelp/cloudhelp/2014/ENU/SimCFD/files/GUID-BBA4E008-8346-465B-9FD3-D193CF108AF0-htm.html`, accessed at November 2018.

54. Autodesk Knowledge Network, *Two Equation Turbulence Models (TKE & TED)*, 2018, `https://knowledge.autodesk.com/support/cfd/learn-explore/caas/CloudHelp/cloudhelp/2017/ENU/SimCFD-Learning/files/GUID-61C4EB55-362C-48A0-8B22-20F9148D190D-htm.html`, accessed at November 2018.

55. Autodesk Knowledge Network, *Autodesk CFD 2019, Wind Loading)*, 2018, `http://help.autodesk.com/view/SCDSE/2019/ENU/?guid=GUID-2BF3C8A5-6D70-4F6A-A792-95A27C605E3D`, accessed at December 2018.

56. Weather Online, *(Istanbul, Climate Robot)*, 2018, `https://www.weatheronline.co.uk`, accessed at December 2018.

57. Autodesk Knowledge Network, *Flow Boundary Conditions*, 2018, `http://help.autodesk.com/view/SCDSE/2019/ENU/?guid=GUID-9C1E28D5-B32E -4546-8620-7F428982184A`, accessed at December 2018.

58. Autodesk Knowledge Network, *Automatic Meshing of CAD Models*, 2018, `http://help.autodesk.com/view/SCDSE/2019/ENU/?guid=GUID-AA5E9A73-6088 -476A-88E5-CADE9951A1A2`, accessed at December 2018.

59. Borsani, A., S. Maltagliati, F. Martelli and L. Procino, "Test Case Optimization of an Urban Section", *BBAA VI International Colloquium on: Bluff Bodies Aerodynamics & Applications*, Citeseer, 2008.

60. Autodesk Knowledge Network, *Autodesk CFD 2019, Turbulence*, 2018, `http://help.autodesk.com/view/SCDSE/2019/ENU/?guid=GUID-E9E8ACA1-8D49 -4A49-8A35-52DB1A2C3E5F`, accessed at December 2018.

61. Allegrini, J., V. Dorer, T. Defraeye and J. Carmeliet, "An adaptive temperature wall function for mixed convective flows at exterior surfaces of buildings in street canyons", *Building and Environment*, Vol. 49, pp. 55–66, 2012.

62. Autodesk Knowledge Network, *Compressible vs. Incompressible flow in Autodesk CFD*, 2018, `https://knowledge.autodesk.com/support/cfd/troubleshooting/caas/ sfdcarticles/sfdcarticles/How-to-decide-whether-to-run- incompressible-or-compressible.html`, accessed at December 2018.

63. National Weather Service, *National Digital Forecast Database Definitions*, 2018, `https://digital.weather.gov/staticpages/definitions.php`, accessed at January 2019.

64. Wikipedia Contributors, *Apparent temperature — Wikipedia, The Free Encyclopedia*, 2018, `https://en.wikipedia.org/wiki/Apparent_temperature`, accessed at January 2019.

65. Australian Government Bureau of Meteorology, *Thermal Comfort observations*, 2010, `http://www.bom.gov.au/info/thermal_stress/#apparent`, accessed at January 2019.

66. American Meteorological Society, *Wind Chill*, 2012, `http://glossary.ametsoc.org/wiki/Wind_chill`, accessed at January 2019.

67. Kessler, E., "Wind chill errors", *Bulletin of the American Meteorological Society*, Vol. 74, No. 9, pp. 1743–1744, 1993.

68. Quayle, R. G. and R. G. Steadman, "The Steadman wind chill: An improvement over present scales", *Weather and Forecasting*, Vol. 13, No. 4, pp. 1187–1193, 1998.

69. National Weather Service, *Wind Chill Chart*, 2018, `https://www.weather.gov/safety/cold-wind-chill-chart`, accessed at January 2019.

70. Wikipedia Contributors, *Wind chill — Wikipedia, The Free Encyclopedia*, 2019, `https://en.wikipedia.org/wiki/Wind_chill`, accessed at January 2019.